

Late Stage Functionalization of 1,2-Azaborines for Application in Biomedical Research:

Author: Jeremy Richard Armand

Persistent link: <http://hdl.handle.net/2345/bc-ir:108646>

This work is posted on [eScholarship@BC](#),
Boston College University Libraries.

Boston College Electronic Thesis or Dissertation, 2019

Copyright is held by the author. This work is licensed under a Creative Commons Attribution-NoDerivatives 4.0 International License (<http://creativecommons.org/licenses/by-nd/4.0>).

Boston College
Graduate School of the Morrissey College of Arts and Sciences
Department of Chemistry

LATE STAGE FUNCTIONALIZATION OF 1,2-AZABORINES FOR APPLICATION
IN BIOMEDICAL RESEARCH

A thesis

by

JEREMY RICHARD ARMAND

submitted in partial fulfillment of the requirements

for the degree of

Master of Science

October 2019

Late Stage Functionalization of 1,2-Azaborines for Application in Biomedical Research

by

JEREMY RICHARD ARMAND

Thesis Advisor:

Professor Shih-Yuan Liu, Ph.D.

Abstract

Chapter 1. Use of boron as a pharmacophore is as growing but still underdeveloped strategy for expanding chemical space in biomedical research. In addition to more established methods of incorporating boron in drug development, an attractive and emerging method of introducing boron into biologically active compounds is through boron-nitrogen containing heterocycles. In particular, the Liu group has focused on exploring the interactions of monocyclic 1,2-azaborines in biological space. In order to install complicated chemical functionality needed for further studies, methods for late stage functionalization of 1,2-azaborines must be developed. Described herein is a method for functionalizing 1,2-azaborine at the C3- and C5-positions, with bromine and iodine handles, respectively.

Chapter 2. Described is the application of the turbo Grignard reaction to 1,2-azaborines bearing a B–Cl bond. The reaction utilizes *i*PrMgCl·LiCl to form aryl carbon nucleophiles and is tolerant of sensitive functional groups such as nitriles and esters. Development of the reaction obviates the need to use toxic organotin reagents to install aryl groups at the B-position that bear sensitive, electrophilic functionalities.

For Seymour

Table of Contents

Table of Contents	v
List of Figures	vii
List of Schemes	viii
List of Tables	x
List of Abbreviations	xi

Chapter 1: Towards a Tetra-Orthogonally Reactive Azaborine: Functionalizing the C3- and C5-Positions of 1,2-Azaborines with Chemically Distinct Handles

1.1 Introduction.....	1
1.1.1 Boron Containing Compounds in Medicinal Chemistry	1
1.1.2 BN/CC Isosterism and Azaborines.....	10
1.2 Background.....	14
1.2.1 BN/CC Isosterism in Biological Space	14
1.2.2 Late Stage Functionalization of 1,2-Azaborines	24
1.3 Towards the Synthesis of a Tetra-Orthogonally Reactive 1,2-Azaborine	31
1.3.1 Identifying 3,5-Dibromo- <i>N</i> -TBS- <i>B</i> -Cl-1,2-azaborine as a Synthetic Target ..31	
1.3.2 Synthesis and Evaluation of 3,5-Dibromo- <i>N</i> -TBS- <i>B</i> -Cl-1,2-azaborine.....	32
1.3.3 Synthesis of 3-Bromo-5-iodo- <i>N</i> -TBS- <i>B</i> -Cl-1,2-azaborine	33
1.4 Conclusions.....	38
1.5 Experimental.....	39
1.5.1 General Considerations	39
1.5.2 Synthesis of 1,2-Azaborines.....	40
1.5.3 Attempts to Regenerate <i>N</i> -TBS- <i>B</i> -OMe-3-bromo-5-iodo-1,2-azaborine.....	45
1.5.4 Spectral Data	46

Chapter 2: Development of a Functional Group Tolerant Grignard-Type Reaction for Addition to the B-Position of 1,2-Azaborines

2.1 Introduction: The Turbo Grignard Reagent	58
2.1.1 Limitations of the Traditional Grignard Reaction	58
2.1.2 Use of <i>i</i> PrMgCl·LiCl to Achieve Broad Functional Group Tolerance	63
2.2 Late Stage Functionalization of 1,2-Azaborines at the B-Position.....	69

2.2.1 Nucleophilic Addition to the B-Position	69
2.2.2 Non-Nucleophilic Activation of the B–R and B–Cl Bond	71
2.3 Development of a Functional Group Tolerant B–Aryl Nucleophilic Substitution Method	75
2.3.1 Biaryl Molecules as a Privileged Class in Medicinal Chemistry	75
2.3.2 Adapting the Turbo Grignard Reaction to 1,2-Azaborines	76
2.4 Conclusions	79
2.5 Experimental	80
2.5.1 General Considerations	80
2.5.2 Addition of Turbo Grignard Reagents to 1,2-Azaborines	81
2.5.3 Spectral Data	86

List of Figures

Figure 1.1 Boromycin

Figure 1.2 Boron Containing Drugs Approved for Sale by the FDA

Figure 1.3 Diborane and Six Common Carboranes

Figure 1.4 Select Carborane Containing Molecules that Have Been Investigated for Biological Activity

Figure 1.5 BN Isosteres of Ethene and Benzene

Figure 1.6 BN Isosteres of Phenanthrene and Naphthalene Synthesized by Dewar for BNCT Studies

Figure 1.7 A Substituted Thienodiazaborine

Figure 1.8 BN-Tryptophan

Figure 1.9 Binding Study Substrates

Figure 1.10 Effects of BN/CC Isosterism of BN/CC Isosterism on Biological Activity and Solubility

Figure 1.11 Resonance Structures and Electrostatic Potential Map of 1,2-Dihydro-1,2-azaborine

Figure 2.1 Difference in Electronegativity between Carbon and Various Metals Using the Allred-Rochow Electronegativity Scale

List of Schemes

- Scheme 1.1** Inhibition of West Nile Virus Protease by a Boronic Acid Flavavirus Protease Inhibitor
- Scheme 1.2** Late Stage Functionalization of 1,2-Azaborines at the C3-Position
- Scheme 1.3** Late Stage Functionalization of 1,2-Azaborines at the C6-Position
- Scheme 1.4** Borylation and Chemical Resolution of 1,2-Azaborines at the C4- and C5-Positions
- Scheme 1.5** Selective Functionalization of 1,2-Azaborine at the C5-Position
- Scheme 1.6** Synthesis and Evaluation of 3,5-Dibromo-1,2-azaborine
- Scheme 1.7** Synthesis and Attempted Purification of 3-Br-5-I-1,2-azaborine
- Scheme 1.8** Synthesis and Purification of 3-Br-5-I-B-OH-1,2-azaborine
- Scheme 1.9** Attempt to Regenerate **1.52** by Reaction with a Methyl Electrophile
- Scheme 2.1** The Grignard Reaction as Originally Proposed by Victor Grignard
- Scheme 2.2** Use of Alkyl–Magnesium Reagents as Originally Described by Prevost
- Scheme 2.3** Selected Examples of the Functional Group Tolerance of the Turbo Grignard Reagent
- Scheme 2.4** Boron Electrophiles as Substrates in the Turbo Grignard Reaction
- Scheme 2.5** Nucleophilic Attack by *in situ* Generated Nucleophile
- Scheme 2.6** Nucleophilic Addition to B–OR Substituted 1,2-Azaborines via a B–Cl Intermediate
- Scheme 2.7** Selected Product of Rh-Catalyzed Arylation of B–Cl Substituted 1,2-Azaborines
- Scheme 2.8** Rh-Catalyzed B–H Activation of 1,2-Azaborines

Scheme 2.9 Copper Catalyzed Oxidation of B–C Bonds of 1,2-Azaborines

Scheme 2.10 Turbo Grignard Reaction with *N*-TBS-*B*-Cl-1,2-Azaborine

Scheme 2.11 Turbo Grignard Reaction with 3-Br-*N*-TBS-*B*-Cl-1,2-Azaborine

Scheme 2.12 Attempts to Adapt Turbo Grignard Reaction to 3-Br-5-I-*N*-TBS-*B*-Cl-1,2-Azaborine

Scheme 2.13 Turbo Grignard Reaction with 3-Br-*N*-TBS-*B*-OMe-1,2-Azaborine

List of Tables

Table 1.1 Atomic Abundance of the Elements

Table 1.2 PDE10A Inhibition Potency, Lipophilicity, and Metabolic Stability of Quinolinylnyl-, Borazaronaphthyl-, and Naphthyl-Compounds

Table 1.3 Physicochemical and *in vitro* ADME Properties of **1.28** and **1.29** Compared to Those of Propranolol

Table 1.4 Relative Calculated Energy Levels for Radical and Carbocation Formation

Table 1.5 Pharmacokinetic Parameters of **1.33** and **1.34** after Administration to Rats

Table 1.6 Screening of Conditions for Iodination of 3-Br-*N*-TBS-*B*-Cl-1,2-azaborine

Table 1.7 Screening of Conditions for Iodination of 3-Br-*N*-TBS-*B*-Cl-1,2-azaborine (continued)

Table 1.8 Attempts to Regenerate **1.52** by Nucleophilic Displacement of –OH by Methanol

Table 2.1 Scope of Functional Group Tolerance for the Grignard Reaction Using Activated Magnesium

Table 2.2 New Functional Group Tolerance Displayed by Mg-I Exchange Using Alkyl–Magnesium Reagents

Table 2.3 Addition of LiCl Allows for Magnesium-Bromine Exchange of Unactivated C–Br Bonds

Table 2.4 Substrate Scope of Knochel’s Initial Study of *i*PrMgCl·LiCl Mediated Grignard Reaction

Table 2.5 Nucleophilic Attack on B–Cl Bond of 1,2-Azaborines

Table 2.6 Nucleophilic Attack on B–H Bond of 1,2-Azaborines

List of Abbreviations

5HT1A	serotonin 1A receptor
Å	angstrom
Ac	acetyl
ADME	absorption, distribution, metabolism, and excretion
ADMET	absorption, distribution, metabolism, excretion, and toxicity
Ala	alanine
Ar	aryl
AUC _{po}	area under the curve after oral treatment
AUC _{iv}	area under the curve after intravenous treatment
bp	boiling point
BDE	bond dissociation energy
BIHEP	2,2'-bis(diphenylphosphino)biphenyl
Bn	benzyl
B ₂ pin ₂	bis-Pinacolatodiboron
Bu	butyl
C _{max}	concentration
cAMP	cyclic adenosine monophosphate
CDK2	cyclin-dependent kinase 2
CHO	Chinese hamster ovary cells
Cl _{int}	intrinsic clearance
CNS	central nervous system
cod	1,5-cyclooctadiene
D	debye
<i>D</i>	distribution coefficient
d	doublet
dd	doublet of doublets
DART	direct analysis in real time
dppf	1,1'-bis(diphenylphosphino)ferrocene
DTBP	Di-tert-butyl peroxide
dtbpy	4,4'-di-tert-butyl-2,2'-dipyridyl
E	electrophile
EC ₂₀	20% maximal effective concentration
equiv	equivalent(s)
Et	ethyl
F	bioavailability
FDA	Food and Drug Administration
FG	functional group
FTIR	Fourier-transform infrared spectroscopy
Gln	glutamine
h	hour(s)
(Het)	hetero
HIV	human immunodeficiency virus
HRMS	high resolution mass spectrometry
<i>i</i>	<i>iso</i>

IC ₅₀	half maximal inhibitory concentration
Ile	isoleucine
inh	inhibition
i.v.	intravenous
K _i	inhibition constant
Leu	leucine
LTC	lowest toxic concentration
M	molar
m	multiplet
Me	methyl
Mes	mesityl
Met	methionine
min	minute
MTBE	methyl <i>tert</i> -butyl ether
<i>n</i>	normal
nbd	norbornadiene
NMO	N-Methylmorpholine N-oxide
NMR	nuclear magnetic resonance spectroscopy
Nu	nucleophile
<i>P</i>	partition coefficient
PDE10A	Phosphodiesterase 10A
Ph	phenyl
pin	pinacolato
PPAR	peroxisome proliferator-activated receptor
Pr	propyl
PTFE	polytetrafluoroethylene
RSE	resonance stabilization energy
s	singlet
Sol	solubility
t	triplet
<i>t</i>	<i>tert</i>
<i>t</i> _{max}	time
TBAF	tetra-butylammonium fluoride
TBS	<i>tert</i> -butyldimethylsilyl
THF	tetrahydrofuran
TMS	trimethylsilyl
TMSE	(trimethylsilyl)ethyl
USFDA	United States Food and Drug Administration
v	volume
WNV	West Nile virus

CHAPTER 1

Towards a Tetra-Orthogonally Reactive Azaborine: Functionalizing the C3- and C5-Positions of 1,2-Azaborines with Chemically Distinct Handles

1.1 Introduction

1.1.1 Boron Containing Compounds in Medicinal Chemistry

Boron is the fifth element on the periodic table, and it occupies a place immediately before carbon, nitrogen, and oxygen. Unlike its ubiquitous neighbors, however, boron is not widely found in the chemical framework of biology. In fact, boron is relatively rare not just on earth but in the universe at large (**Table 1.1**). While carbon, nitrogen, oxygen, and neon have an estimated fractional atomic abundance of 9.3×10^{-4} by number, lithium, beryllium, and boron only have an abundance of 3.3×10^{-9} by number. The relative scarcity of these lighter elements, a difference of five orders of magnitude, can be understood as a direct result of their unique manner of formation and their instability at the high temperatures of stellar environments.¹

Table 1.1 Atomic Abundance of the Elements (Si = 1×10^6)^{1a-b}

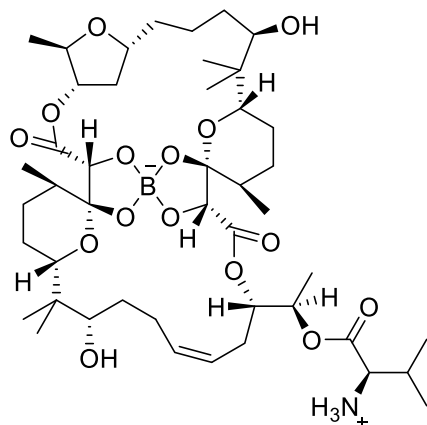
Element	Abundance by Number
H	4.00×10^{10}
He	3.08×10^9
Li	100
Be	20
B	24
C	3.5×10^6
N	6.6×10^6
O	2.15×10^7
Ne	8.6×10^6

¹ (a) Suess, H. E.; Urey, H. C. Abundances of the Elements. *Rev. Mod. Phys.* **1956**, *28*, 53–74. (b) Suess, H. E. V. M. Goldschmidt and Origin of the Universe. *Appl. Geochem.* **1988**, *3*, 385–391. (c) Burbidge, E. M.; Burbidge, G. R.; Fowler, W. A.; Hoyle, F. Synthesis of the Elements in the Stars. *Rev. Mod. Phys.* **1957**, *29*, 547–650. (d) Anderson, D. L. Chemical Composition of the Mantle in *Theory of the Earth*; Blackwell Scientific Publications: Boston, **1989**, 147–177.

While most elements lighter than iron are formed in the high temperature environment immediately following the big bang or in the interior of stars, more fragile elements, such as boron, are not able to survive such environments.^{2a} It is believed that boron, in addition to beryllium and lithium, is formed by cosmic ray interactions in the interstellar medium. This process, known as “cosmic ray spallation,” produces lithium, beryllium, and boron *via* energetic collisions between carbon, nitrogen, or oxygen and protons, alpha particles, or helium nuclei.² These interactions are of lower energy and at lower density than stellar nucleosynthesis, and as a result are far less prolific. Consequently, the abundance of these three elements in the universe is much lower than the elements directly succeeding them.

Understandably, boron is not widely found in biological systems. While boron as

Figure 1.1 Boromycin



boric acid is essential in trace amounts to the health of plants, its incorporation into natural products is fairly rare.³ The first natural product known to contain boron, boromycin (**Figure 1.1**), was discovered in 1967 and characterized in 1971.^{3b,4} As in boromycin, all boron-containing

² (a) Prantzos, N.; Casse, M.; Vangioni-Flam, E. Production and Evolution of LiBeB Isotopes in the Galaxy. *ApJ*. **1993**, *403*, 630–643. (b) Ramaty, R.; Kozlovsky, B.; Lingenfelter, R. E.; Reeves, H. Light Elements and Cosmic Rays in the Early Galaxy. *ApJ*. **1997**, *488*, 730–748. (c) Reeves, H.; Fowler, W. A.; Hoyle, F. Galactic Cosmic Ray Origin of Li, Be, and B in Stars. *Nature* **1970**, *226*, 727–729.

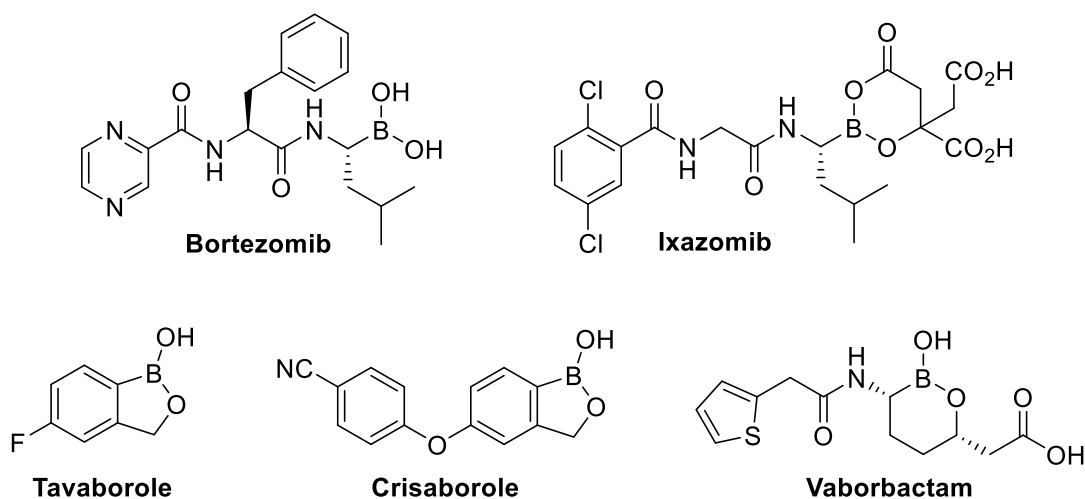
³ (a) Yoshinari, A.; Takano, J. Insights into the Mechanisms Underlying Boron Homeostasis in Plants. *Front. Plant Sci.* **2017**, *8*, 1951 (b) Uluisik, I.; Karakaya, H. C.; Koc, A. The Importance of Boron in Biological Systems. *J. Trace Elem. Med. Biol.* **2018**, *45*, 156–162. (c) Miwa, K.; Fujiwara, T. Boron Transport in Plants: Co-ordinated Regulation of Transporters. *Annals of Botany* **2010**, *105*, 1103–108.

⁴ (a) Dunitz, J. D.; Hawley, D. M.; Miklos, D.; White, D. N. J.; Berlin, Y.; Marusic, R.; Prelog, V. Structure of Boromycin. *Helvetica Chimica Acta* **1971**, *54*, 1709–1713. (b) Chen, T. S. S.; Chang, C.-J.; Floss, H. G. On the Biosynthesis of Boromycin. *J. Org. Chem.* **1981**, *46*, 2661–2665.

natural products feature boron bound exclusively to oxygen; no known natural products contain boron–carbon bonds.⁵

In part due to its relative absence in natural products, boron-containing drugs have not been widely used in medicinal chemistry. To date, only five drugs containing boron have been approved for commercial use by the USFDA (**Figure 1.2**): Bortezomib was the first boron containing drug (2003) and is a serine protease inhibitor approved for treatment of multiple myeloma.⁶ Following bortezomib's approval, it was another ten years before tavaborole was approved as a topical antifungal treatment.⁷

Figure 1.2 Boron Containing Drugs Approved for Sale by the FDA



In 2015, ixazomib was approved for treatment of multiple myeloma as well. Like bortezomib, it also acts as a protease inhibitor. Unlike bortezomib, ixazomib can be orally administered, which is due to the hydrophilic boronic ester formed with citric acid.⁸ Crisaborole was approved as a topical phosphodiesterase inhibitor for treatment of atopic

⁵ Diaz, D. B.; Yudin, A. K; The Versatility of Boron in Biological Target Engagement. *Nat. Chem.* **2017**, *9*, 731–742.

⁶ Paramore, A.; Frantz, S. Bortezomib. *Nat. Rev. Drug Discov.* **2003**, *2*, 611–612.

⁷ Markham, A. Tavaborole: First Global Approval. *Drugs* **2014**, *74*, 1555–1558.

⁸ Shirley, M.; Ixazomib: First Global Approval. *Drugs* **2016**, *76*, 405–411.

dermatitis in 2016.⁹ The following year vaborbactam, a β -lactamase inhibitor, was approved in combination with the carbapenem antibiotic meropenem as a treatment against carbapenem-resistant bacteria.¹⁰

In recent years the use of boron in the development of drugs and biologically-active molecules has increased dramatically.^{5,11} Because of its unique electronic properties and versatile molecular geometry, which arise from a vacant *p*-orbital, boron possesses unique reactivity that is not found elsewhere in the arsenal of medicinal chemistry. Because of its absence in biology, there are few sources of natural inspiration from which drug design approaches can be drawn, and novel methods of incorporating boron into biologically-active compounds must be explored.

The ability of boron to exist as both tri-substituted, charge neutral species and tetra-substituted, negatively charged species is essential to the unique target engagement of boronic acid-containing compounds.⁵ For many of these compounds, serine proteases are the most common target of inhibition.⁵ Natural protease substrates can be used as inspiration for their inhibitors; for most boronic acid inhibitors, the most significant change is the replacement of a scissile amide bond with a boronic acid moiety.^{5,11}

Boronic acids first gained attention as potential enzymatic inhibitors in the late 1960s and early 1970s. Several early studies found that boronic acids acted as inhibitors of subtilisin and chymotrypsin proteolytic enzymes, and the structure of the inhibitor-

⁹ Paton, D. M. Crisaborole: Phosphodiesterase Inhibitor for Treatment of Atopic Dermatitis. *Drugs Today* **2017**, *53*, 239–245.

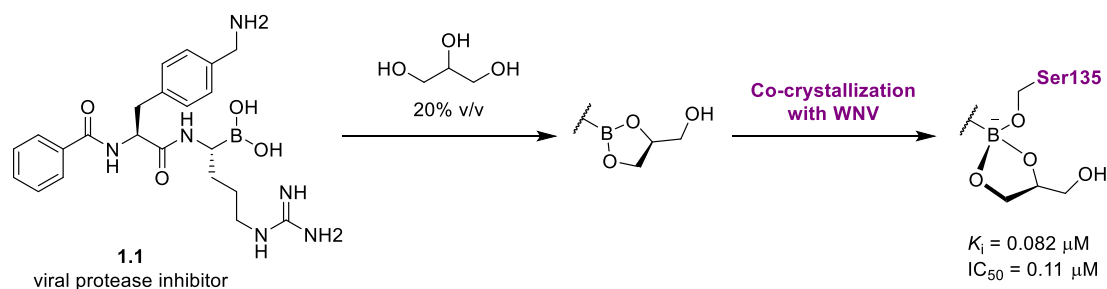
¹⁰ Lee, Y.; Kim, J.; Trinh, S. Meropenem–Vaborbactam (VabomereTM): Another Option for Carbapenem-Resistant Enterobacteriaceae. *P. T.* **2019**, *44*, 110–113.

¹¹ Kahlert, J.; Austin, C. J. D.; Kassiou, M.; Rendina, L. M. The Fifth Element in Drug Design: Boron in Medicinal Chemistry. *Aust. J. Chem.* **2013**, *66*, 1118–1123.

enzyme complex was posited to be a tetra-coordinate boronate species.¹² Further crystallographic studies of two boronic acid inhibitors of subtilisin confirmed the presence of a tetra-coordinate boron bound covalently to oxygen of a serine residue in the enzyme active site.¹³

An example of typical inhibition of proteases by boronic acid containing compounds has been provided in **Scheme 1.1**. In this case, the boronic acid forms a cyclic diester with glycerol, which was present in enzyme preparation. After association with the inhibitor, the catalytic serine residue covalently captures the boron electrophile. The boron undergoes a transition from the tri-coordinate boronic ester to a tetra-coordinate borate species. While the tetrahedral transition state of the natural enzyme substrate is unstable and leads to amide scission, the stability of this anionic boron species arrests the mechanism of the enzyme, leading to target inhibition.^{5,14}

Scheme 1.1 Inhibition of West Nile Virus Protease by a Boronic Acid Flavivirus Protease Inhibitor^{5,14}



¹² (a) Antonov, V. K.; Ivanina, T. V. *n*-Alkylboronic Acids as Bifunctional Reversible Inhibitors of α -Chymotrypsin. *FEBS Lett.* **1970**, *7*, 23–25. (b) Koehler, K. A.; Lienhard, G. E. 2-Phenylethaneboronic Acid, a Possible Transition State Analog for Chymotrypsin. *Biochemistry* **1971**, *10*, 2477–2483. (c) Philipp, M.; Bender, M. L. Inhibition of Serine Proteases by Arylboronic Acids. *Proc. Natl. Acad. Sci.* **1978**, *68*, 478–480. (d) Lindquist, R. N.; Terry, C. Inhibition of Subtilisin by Boronic Acids, Potential Analogs of Tetrahedral Reaction Intermediates. *Arch. Biochem. Biophys.* **1974**, *160*, 135–144.

¹³ Matthews, D. A.; Alden, R. A.; Birktoff, J. J.; Freer, S. T.; Kraut, J. X-ray Crystallographic Study of Boronic Acid Adducts with Subtilisin BPN^o (Novo). *J. Biol. Chem.* **1975**, *250*, 7120–7126.

¹⁴ (a) Lei, J.; Hansen, G.; Nitsche, C.; Klein, C. D.; Hilgenfeld, R. Crystal Structure of Zika Virus NS2B-NS3 Protease in Complex with a Boronate Inhibitor. *Science* **2016**, *353*, 503–505. (b) Nitsche, C.; Zhang, L.; Weigel, L. F.; Schilz, J.; Graf, D.; Bartenschlager R.; Hilgenfeld, R.; Klein, C. D. Peptide–Boronic Acid Inhibitors of Flaviviral Proteases: Medicinal Chemistry and Structural Biology. *J. Med. Chem.* **2017**, *60*, 511–516.

While most research of boronic acid-containing compounds and medicinal chemistry has focused on their role as protease inhibitors, they have also been utilized as inhibitors of enzymes, such as proteasomes,¹⁵ arginases,¹⁶ and β -lactamases,¹⁷ among others. Like protease inhibitors, many of these boronic acid inhibitors utilize boron's ability to form stable bonds with nucleophilic moieties to arrest enzymatic activity.^{5,14}

Boron's unique electronic properties can also be observed in its ability to form boron clusters.^{18b} Boron can form compounds with stable, three-center two-electron boron–hydrogen–boron bonds, the most simple of which is diborane (**1.2**). Boron and hydrogen can also produce a number of stable three-dimensional boron clusters of the general formula $B_nH_n^{2-}$. Carboranes are a similar class of clusters in which two of the B–H bonds are typically replaced with the isoelectronic C–H⁺ bonds, giving the general formula $C_2B_nH_{n+2}$ (**Figure 1.3**). The most commonly used carboranes in medicinal chemistry are the *closo*- $C_2B_{10}H_{12}$ (**1.3–1.5**) carboranes and the *nido*- $C_2B_9H_{10}^-$ (**1.6–1.8**) carboranes.^{18b} These clusters do not possess classic two-center two-electron bonds, but instead feature electrons delocalized throughout the molecule. As such, carboranes can be described as having three-dimensional aromaticity.^{18a} As a result of this unique mode of bonding, boron and carbon atoms are hexacoordinate, though vertices simply represent

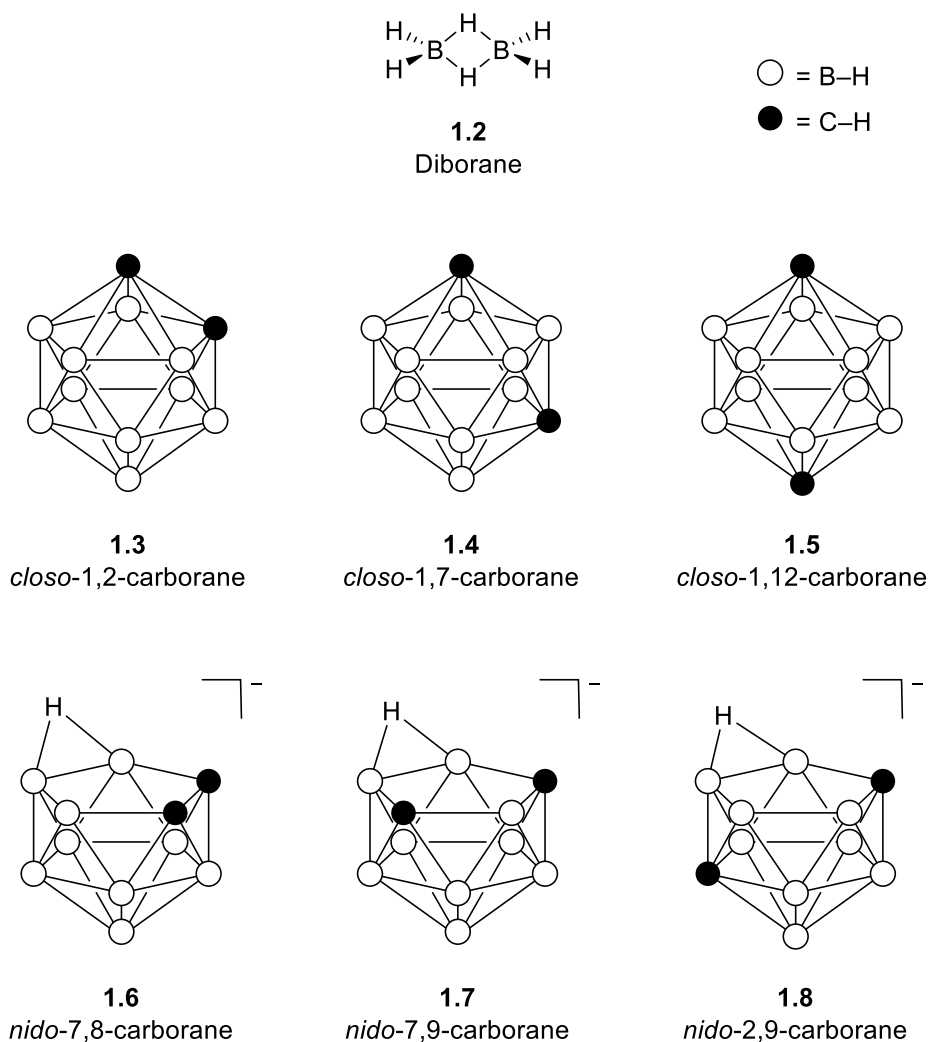
¹⁵ (a) Richardson, P. G.; et al. A Phase 2 Study of Bortezomib in Relapsed, Refractory Myeloma. *N. Engl. J. Med.* **2003**, *348*, 2609–2617. (b) Piva, R.; et al. CEP-18770: A Novel, Orally Active Proteasome Inhibitor with a Tumor-Selective Pharmacological Profile Competitive with Bortezomib. *Blood* **2008**, *111*, 2765–2775. (c) Kumar, S. J.; et al. Safety and Tolerability of Ixazomib, an Oral Protease Inhibitor, in Combination with Lenalidomide and Dexamethasone in Patients with Previously Untreated Multiple Myeloma: An Open Label Phase 1/2 Study. *Lancet* **2014**, *15*, 1503–1512.

¹⁶ (a) Baggio, R.; et al. Inhibition of Mn^{2+} -Arginase by Borates Leads to the Design of a Transition State Analogue Inhibitor, 2(*S*)-Amino-6-boronohexanoic Acid. *J. Am. Chem. Soc.* **1997**, *119*, 8107–8108. (b) Cox, J. D.; Kim, N. N.; Traish, A. M.; Christianson, D. W. Arginase Boronic-acid Complexes Highlights a Physiological Role in Erectile Dysfunction. *Nat. Struct. Biol.* **1999**, *6*, 1043–1047.

¹⁷ (a) Weston, G. S.; Blázquez, J.; Baquero, F.; Shoichet, B. K. Structure-Based Enhancement of Boronic Acid-Based Inhibitors of AmpC β -Lactamase. *J. Med. Chem.* **1998**, *41*, 4577–4586. (b) Hecker, S. J.; et al. Discovery of a Cyclic Boronic Acid β -Lactamase Inhibitor (RPX7009) with Utility vs Class A Serine Carbapenemases. *J. Med. Chem.* **2015**, *58*, 3682–3692.

connections between atoms rather than electron pairs as in traditional bonding convention. Another important distinction between C–H and B–H bonds is in the behavior of bound hydrogen atom: B–H bonds are hydridic in nature while the C–H bonds are protic.¹⁸

Figure 1.3 Diborane and Six Common Carboranes¹⁸



¹⁸ (a) Issa, F.; Kassiou, M.; Rendina, L. M. Boron in Drug Discovery: Carboranes as Unique Pharmacophores in Biologically Active Compounds. *Chem. Rev.* **2011**, *111*, 5701–5722. (b) Leśniowski, S. J. Challenges and Opportunities for the Application of Boron Clusters in Drug Design. *J. Med. Chem.* **2016**, *59*, 7738–7758. (c) Stockmann, P.; Gozzi, M.; Kuhnert, R.; Sárosi, M. B.; Hey-Hawkins, E. New Keys for Old Locks: Carborane-Containing Drugs as Platforms for Mechanism-Based Therapies. *Chem. Soc. Rev.* **2019**, *48*, 3497–3512.

These unique compounds have found widespread use in medicinal chemistry. Their first use as therapeutic agents came in 1968 when Hiroshi Hatanaka used sodium borocaptate (**1.9**) as a boron source for boron-neutron capture therapy (BNCT).¹⁹ Used to treat malignant brain tumors, BNCT requires the accumulation of ¹⁰B in tumor cells. Tumor cells are then bombarded by neutrons, causing the boron to undergo a fission event and produce lithium-7 and high energy alpha particles. Alpha particles have a short lifetime, travelling less than <10 μm, and thus only destroy cells which have ¹⁰B atoms in them.¹⁹ Because of the high concentration of boron per molecule, as well as their stability in biological environments, boron clusters are attractive candidates for this therapy.¹⁸ To increase uptake by tumors and limit concentration in healthy tissue, boron clusters have been attached to a number of different delivery agents for study as boron sources for BNCT. These delivery agents include sugars,²⁰ polypeptides²¹ and nucleosides²² among many others. A more comprehensive list can be found in a recent review by Barth et al.²³

Carboranes have been the subject of increased investigation as a way to introduce new chemical diversity in biologically-active compounds. Incorporation of lipophilic carboranes offers an attractive avenue for modulating the compound's pharmacokinetic properties and increasing efficacy *in vivo*. The utility of carboranes can be illustrated by compound **1.10**. This molecule was tested as a vitamin D receptor agonist with potency

¹⁹ Nedunchezian, K.; Aswath, N.; Thiruppathy, M.; Thirugnanamurthy, S. Boron Neutron Capture Therapy: A Literature Review. *J. Clin. Diagn. Res.* **2016**, *10*, ZE01–ZE04.

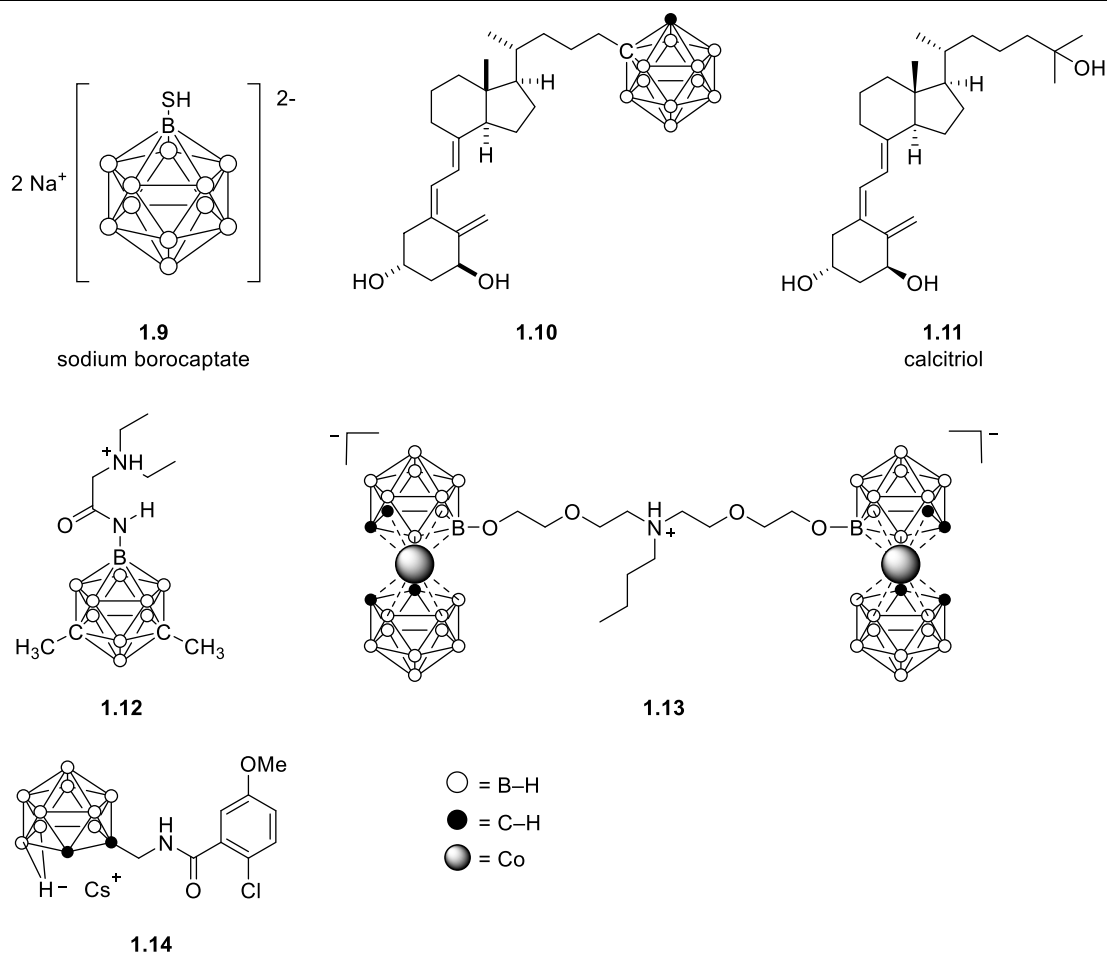
²⁰ Lai, C.-H.; Lin, Y.-C.; Chou, F.-I.; Liang, C.-F.; Lin, E.-W.; Chuang, Y.-J.; Lin, C.-C. Design of Multivalent Galactosyl Carborane as a Targeting Specific Agent for Potential Application to Boron Neutron Capture Therapy. *Chem. Commun.* **2018**, *48*, 612–614.

²¹ Mier, W.; Gabel, D.; Haberkorn, U.; Eisenhut, M. Conjugation of the *closo*-Borane Mercaptoundecahydrododecaborate (BSH) to a Tumor Selective Peptide. *Z. Anorg. Allg. Chem.* **2004**, *630*, 1258–1262.

²² Soloway, A. H.; Zhou, J.-C.; Rong, F.-G.; Lunato, A. J.; Ives, D. H.; Barth, R. F.; Anisuzzaman, A. K. M.; Barth, C. D.; Barnum, B. A. Identification, Development, Synthesis and Evaluation of Boron-Containing Nucleosides for Boron Neutron Capture Therapy. *J. Organomet. Chem.* **1999**, *581*, 150–155.

²³ Barth, R. F.; Mi, P.; Yang, W. Boron Delivery Agents for Boron Neutron Capture Therapy. *Cancer Commun.* **2018**, *38*, <https://doi.org/10.1186/s40880-018-0299-7>

Figure 1.4 Select Carborane Containing Molecules that Have Been Investigated for Biological Activity



comparable to the natural substrate, calcitriol (**1.11**). Interestingly, **1.10** did not exhibit any of the hypercalcemia typically associated with calcitriol.²⁴ Carboranes have also been employed in developing longer lasting lidocaine derivatives (**1.12**),²⁵ as well as developing novel HIV protease inhibitors (**1.13**),²⁶ CNS active antidepressants (**1.14**),²⁷ and other biologically active molecules.¹⁸

²⁴ Otero, R.; Soane, S.; Sigüeiro, R.; Belorusova, A. Y.; Maestro, M. A.; Pérez-Fernández, R.; Rochel, N.; Mouriño, A. Carborane-Based Design of a Potent Vitamin D Receptor Agonist. *Chem Sci.* **2016**, *7*, 1033–1037.

²⁵ Kracke, G. R.; VanGordon, M. R.; Sevryugina, T. V.; Kueffer, P. J.; Kabytayev, K.; Jalisatgi, S. S.; Hawthorne, M. F. Carborane-Derived Local Anesthetics Are Isomer Dependent. *ChemMedChem* **2015**, *10*, 62–67.

²⁶ (a) Kubát, P.; Lang, K.; Cígler, P.; Kožíšek, M.; Matějček, P.; Janda, P.; Zelinger, Z.; Procházka, K.; Král, V. Tetraphenylporphyrin-cobalt(III) Bis(1,2-dicarbollide) Conjugates: From the Solution Characteristics to Inhibition of HIV Protease. *J. Phys. Chem. B.* **2007**, *111*, 4539–4546. (b) Cígler, P.; et al.

In addition to these two more established methods of incorporating boron in drug development, an attractive and emerging method of introducing boron into biologically active compounds is through boron-nitrogen containing heterocycles.⁵ Boron's electron deficient nature, when paired with electron rich nitrogen, allows for the formation of compounds that are isoelectronic and isostructural to carbon-based compounds. This particular use of the unique electronic properties of boron will be discussed thoroughly throughout the remainder of the chapter.

1.1.2 BN/CC Isosterism and Azaborines

The concept of isosterism was first introduced in 1919 by Irving Langmuir who defined the term as molecules that contain the same number of atoms and electrons, different only in the charges on the nuclei of the constituent atoms.²⁸ In his initial publication, Langmuir noted the similarities in physical properties among sets of isosteres, most of which were inorganic compounds. In the 100 years since its initial development, the concept of isosterism has become a practical strategy utilized in organic chemistry.²⁹ In particular, isosteres can be utilized in organic chemistry as a way of introducing chemical diversity as well as modulating chemical properties of molecules while leaving their structural framework largely unchanged.

This concept of isosterism can be illustrated by the concept of BN/CC isosterism, in which a carbon-carbon unit in a molecule is replaced with a boron-nitrogen unit. One of the simplest examples of BN/CC isosterism is the relationship between a carbon-

From Nonpeptide Toward Noncarbon Protease Inhibitors: Metallocarboranes as Specific and Potent Inhibitors of HIV Protease. *PNAS* **2005**, *102*, 15394–15399

²⁷ Wilkinson, S. M.; Gunosewoyo, H.; Barron, M. L.; Boucher, A.; McDonnell, M.; Turner, P.; Morrison, D. E.; Bennett, M. R.; McGregor, I. S.; Rendina, L. M.; Kassiou, M. The First CNS-Active Carborane: A Novel P2X₇ Receptor Agonist with Antidepressant Activity. *ACS Chem. Neurosci.* **2014**, *5*, 335-339.

²⁸ Langmuir, I. Isomorphism, Isosterism, and Covalence. *J. Am. Chem. Soc.* **1919**, *41*, 1543–1559.

²⁹ Lima, L. M.; Barreiro, E. J. Bioisosterism: A Useful Strategy for Molecular Modification and Drug Design. *Curr. Med. Chem.* **2005**, *12*, 23–49.

carbon double bond and nitrogen–boron double bond. Both units contain two atoms and eight valence electrons. In the case of the carbon–carbon double bond, both carbons have four valence electrons and are charge neutral. In the case of the nitrogen–boron double bond, nitrogen possesses five valence electrons while boron possesses three. As a result of this electronic distribution, a nitrogen–boron double bond also has eight valence electrons, but the nitrogen is positively charged while the boron is negatively charged.

While Langmuir was preoccupied with identifying similarities in the properties of isosteres, it is the difference in properties between the CC unit and the BN unit that make BN/CC isosterism noteworthy. Ethene (**1.15**, bp $-104\text{ }^{\circ}\text{C}$) is a volatile gas under standard conditions, and has a bond dissociation energy of $174.1\text{ kcal mol}^{-1}$, $65.0\text{ kcal mol}^{-1}$ of which can be attributed to its π -bond.³⁰ Due to the symmetric nature of the molecule, ethene has no effective dipole moment.³¹ Ethene's BN isostere, aminoborane (**1.16**), lacks the symmetry of ethene. As a result, the properties of aminoborane are markedly different than those of ethene. Aminoborane has a dipole moment of 1.84 D, is generally unstable, and prefers to form cyclic oligomers and polymers.³² Additionally, the π contribution to the bond strength of amino borane is less than that of ethene at only $29.9\text{ kcal mol}^{-1}$ while the σ contribution is comparable at $109.8\text{ kcal mol}^{-1}$.³³

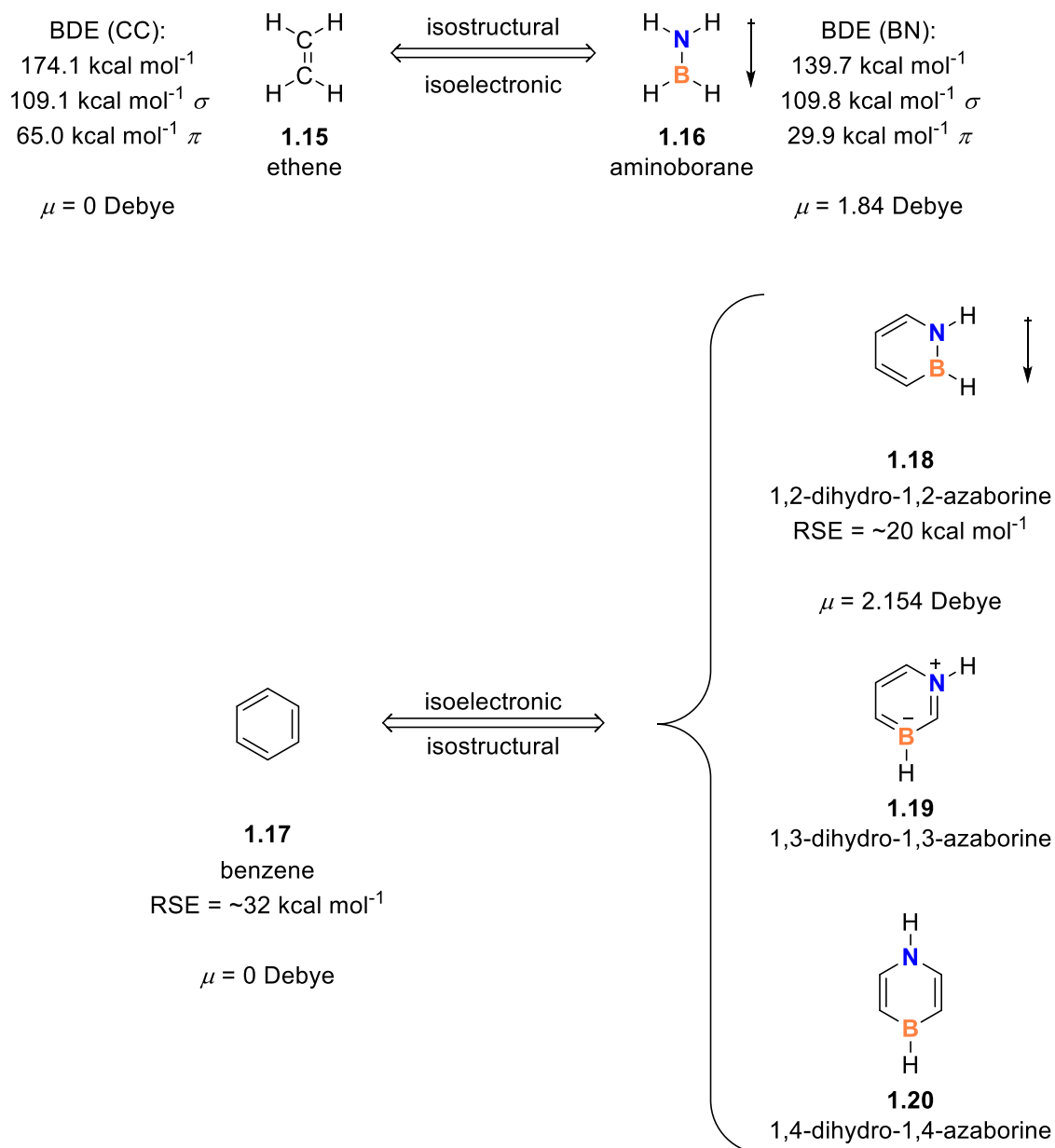
³⁰ Blanksby, S. J.; Ellison, G. B. Bond Dissociation Energies of Organic Molecules. *Acc. Chem. Res.* **2003**, *36*, 255–263.

³¹ Pritchard, R. H; Kern, C. W. Bond Moments in the Two-Carbon Series Ethane, Ethylene, and Acetylene. *J. Am. Chem. Soc.* **1969**, *91*, 1631–1635.

³² Sugie, M.; Takeo, H.; Matsumura, C. Microwave Spectrum of Aminoborane BH_2NH_2 . *Chem. Phys. Lett.* **1979**, *64*, 573–575.

³³ Grant, D. J.; Dixon, D. A. σ - and π -Bond Strengths in Main Group 3-5 Compounds. *J. Phys. Chem.* **2006**, *110*, 12955–12962.

Figure 1.5 BN Isosteres of Ethene and Benzene



Of the applications of BN/CC isosterism, none have received more attention than the substitution of C–C double bonds with B–N in aromatic systems. A number of BN-arenes have been investigated,³⁴ the simplest amongst them being monocyclic azaborines.

³⁴ For Selected Reviews, see: (a) Boset, M. J. D.; Piers, W. E. B–N as a C–C Substitute in Aromatic Systems. *Can. J. Chem.* **2009**, *87*, 8–29. (b) Abbey, E. R.; Liu, S.-Y. BN Isosteres of Indole. *Org. Biomol. Chem.* **2013**, *11*, 2060–2069. (c) Bélanger-Chabor, G.; Braunschweig, H.; Roy, D. K. Recent Developments in Azaborinine Chemistry. *Eur. J. Inorg. Chem.* **2017**, 4353–4368. (d) Giustra, Z. X.; Liu,

1,2-azaborines are BN isosteres of benzene in which a C–C double bond is replaced with a B–N single bond. While three monocyclic azaborine structural isomers can exist (**1.18**–**1.20**), 1,2-azaborines are the only among them that contain a direct B–N bond. 1,2-dihydro-1,2-azaborine (**1.18**), like its CC counterpart benzene, is aromatic with a calculated resonance stabilization energy of 19.6 kcal mol⁻¹.³⁵ Unlike benzene, 1,2-dihydro-1,2-azaborine has a dipole moment of 2.154 D³⁶ and has a protic N–H³⁷ bond which has been shown to act as a hydrogen bond donor.³⁸

The differences between azaborines and benzene allow for modulation of the properties of chemical structures by incorporating azaborines in place of benzene rings. In particular, the polarity and ability to engage in hydrogen bonding of 1,2-azaborine can be beneficial in medicinal chemistry, as this allows for changes to be made to the solubility and target engagement mechanics of biologically-active compounds. By incorporating azaborines into drug like compounds, these properties can be tuned to affect pharmacokinetic behavior.

S.-Y. The State of the Art in Azaborine Chemistry: New Synthetic Methods and Applications. *J. Am. Chem. Soc.* **2018**, *140*, 1184–1194. (e) McConnell C. R.; Liu, S.-Y. Late-Stage Functionalization of BN-Heterocycles. *Chem. Soc. Rev.* **2019**, *48*, 3436–3453.

³⁵ Campbell, P. G.; Abbey, E. R.; Neiner, D.; Grant, D. J.; Dixon, D. A.; Liu, S.-Y. Resonance Stabilization Energy of 1,2-Azaborines: A Quantitative Experimental Study by Reaction Calorimetry. *J. Am. Chem. Soc.* **2010**, *132*, 18048–18050.

³⁶ Chrostoswka, A.; Xu, S.; Lamm, A. N.; Mazière, A.; Weber, C. D.; Dargelos, A.; Baylère, P.; Graciaa, A.; Liu, S.-Y. UV-Photoelectron Spectroscopy of 1,2- and 1,3-Azaborines: A Combined Experimental and Computational Electronic Structure Analysis. *J. Am. Chem. Soc.* **2012**, *134*, 10279–10285.

³⁷ Marwitz, A. J. V.; Matus, M. H.; Zakharov, L. N.; Dixon, D. A.; Liu, S.-Y. A Hybrid Organic/Inorganic Benzene. *Angew. Chem. Int. Ed.* **2009**, *48*, 973–977.

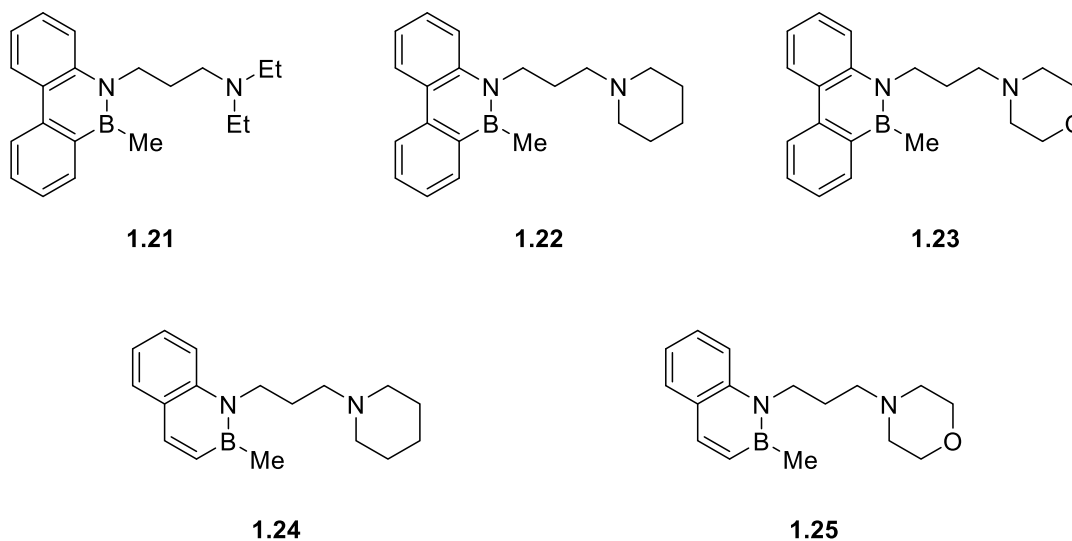
³⁸ Zhao, P.; Nettleton, D. O.; Karki, R. G.; Zécéri, F. J.; Liu, S.-Y. Medicinal Chemistry Profiling of Monocyclic 1,2-Azaborines. *ChemMedChem* **2017**, *12*, 358–361.

1.2 Background

1.2.1 BN/CC Isosterism in Biological Space

Drawing from Langmuir's initial observations that isosteric compounds shared similar properties, the concept of bioisosterism was first expressed in 1951 by Friedman as compounds "that fit the broadest definition for isosteres and have the same type of biological activity."³⁹ Bioisosterism is one approach used by medicinal chemists to change the chemical properties of lead compounds while maintaining desired pharmacological activity.⁴⁰ As will be demonstrated for the case of BN/CC isosterism, replacement of carbonaceous arenes with their BN isosteres can help a medicinal chemist tweak properties such as solubility and lipophilicity or even change the dynamics of binding within the pocket of a target protein.

Figure 1.6 BN Isosteres of Phenanthrene and Naphthalene Synthesized by Dewar for BNCT Studies⁴¹



The first example of BN heterocycles investigated for their biological activity came shortly after Dewar's pioneering synthesis of BN isosteres of polycyclic arenes. In

³⁹ Friedman, H. L. Influence of Isosteric Replacement of Biological Activity. *NASNRS* **1951**, *206*, 295–358.

⁴⁰ Patani, G. A.; LaVoie, E. J. Bioisosterism: A Rational Approach in Drug Design. *Chem. Rev.* **1996**, *96*, 3147–3176.

1964, Dewar prepared a number of polycyclic 10,9-Borazarophenanthrenes (**1.21-1.23**) and 2,1-Borazaronaphthalenes (**1.24-1.25**) as potential candidates for BNCT boron sources (**Figure 1.6**). Though he succeeded in creating BN isosteres that had improved aqueous solubility relative to their carbonaceous counterparts, the compounds showed a preference for concentrating in healthy brain tissue instead of tumors of cancerous mice and killed their hosts immediately upon administration.⁴¹

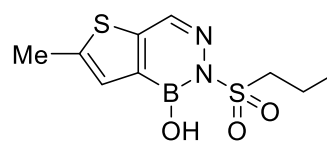
Over a decade after Dewar's initial attempts at using BN heterocycles as BNCT boron sources,

polycyclic diazaborines were studied as antibacterial agents. Diazaborines were found to inhibit biosynthesis of lipopolysaccharide, which is an integral part of the

outer membrane of Gram-negative bacteria.⁴² In 1981, compound **1.26** was found to have antibacterial activity against *E. coli* and *Salmonella typhimurium* with minimum inhibitory concentration values of 1.25 and 2.5 $\mu\text{g/mL}$, respectively.⁴²

Crystallographic analysis inside the binding pocket of *E. coli* enoyl reductase, an enzyme involved in fatty acid biosynthesis, revealed a covalent interaction between the boron of **1.26** and the 2' hydroxyl of a nicotinamide adenine dinucleotide (NAD⁺) ribose present in the enzyme.⁴³ Much like boronic acid containing serine protease inhibitors, this covalent interaction results in a tetracoordinate boron species and provides a clear explanation for the inhibitory properties of diazaborines. Replacement of the BN unit in

Figure 1.7 A Substituted Thienodiazaborine



1.26

⁴¹ Dewar, M. J. S.; Hashmall, J.; Kuba, V. P. New Heterocyclic Boron Compounds. XIX. Water-Soluble Derivatives of 10,9-Borazarophenanthrenes and 2,1-Borazarophenanthrenes as Potential Agents for Neutron Capture Therapy. *J. Org. Chem.* **1964**, *29*, 1755–1757.

⁴² Hogenauer, G.; Woisetschlager, M. A Diazaborine Derivative Inhibits Lipopolysaccharide Biosynthesis. *Nature* **1981**, *293*, 662–664

⁴³ Baldock, C.; Rafferty, J. B.; Sedelnikova, S. E.; Baker, P. J.; Stuitje, A. R.; Slabas A. R.; Hawkes, T. R.; Rice, D. W. A Mechanism of Drug Action Revealed by Structural Studies of Enoyl Reductase. *Science* **1996**, *274*, 2107–2110.

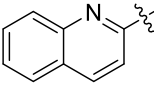
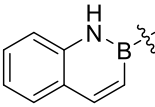
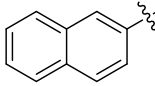
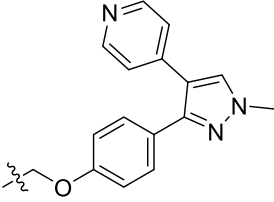
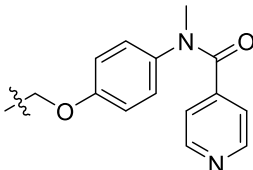
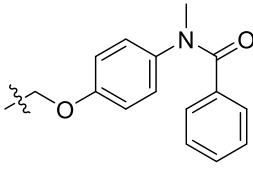
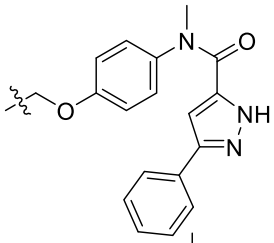
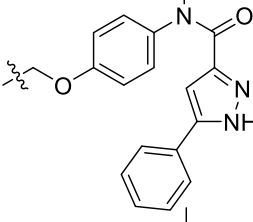
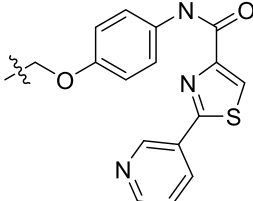
the diazaborine with the isosteric CC unit showed no biological activity, and a number of polycyclic diazaborine compounds have shown similar antibacterial potency.⁴⁴

In 2015, Vlasceanu et al. reported the pharmacokinetic profile of a number of different borazaronaphthyl-containing compounds as PDE10A inhibitors. PDE10A inhibition has gained interest as treatment for Parkinson's Disease, Huntington's Disease, schizophrenia, and obsessive compulsive disorder.⁴⁵ In all cases, the borazaronaphthyl-containing compounds (**1.28a-f**) were more active inhibitors than their carbonaceous counterparts (**1.29a-f**), though the quinolinyl-containing compounds (**1.27a-f**) displayed the greatest potency (**Table 1.2**). The authors noted that borazaronaphthalenes have a polarized B–N bond and a protic NH moiety, which can increase aqueous solubility relative to the naphthalene containing compounds. Direct comparison of the *cLogP* and IC₅₀ values showed correlation between lower lipophilicity and higher inhibitory potency (**Table 1.2**). Trends between lipophilicity and metabolic clearance could not be identified. Co-crystallization of the compounds in the enzyme pocket could not be achieved, and thus the cause of the increased inhibition activity could not be concretely determined.

⁴⁴ Grassberger, M. A.; Turnowsky, F.; Hildebrandt, J. Preparation and Antibacterial Activities of New 1,2,3-Diazaborine Derivatives and Analogues. *J. Med. Chem.* **1984**, *27*, 947–953.

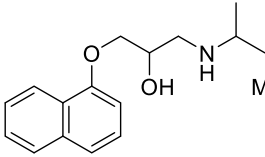
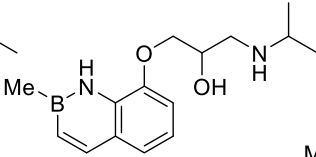
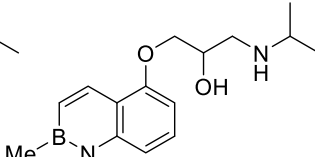
⁴⁵ Vlasceanu, A.; Jessing, M.; Kilburn, J. P. BN/CC Isosterism in Borazaronaphthalenes towards Phosphodiesterase 10A (PDE10A) Inhibitors. *Bioorg. Med. Chem.* **2015**, *23*, 4453–4461.

Table 1.2 PDE10A Inhibition Potency, Lipophilicity, and Metabolic Stability of Quinoliny-, Borazaronaphthyl-, and Naphthyl-Compounds⁴⁵

			
	1.27a IC ₅₀ = 2.6 cLogP = 3.84 Clint = 1.9	1.28a 48% inh. cLogP = 4.44 Clint = 2.5	1.29a 25% inh. cLogP = 5.13 Clint = 5
	1.27b IC ₅₀ = 250 cLogP = 2.85 Clint = 0.9	1.28b 11% inh. cLogP = 3.44 Clint = 6.9	1.29b 2% at 2 μM cLogP = 4.14 Clint = 4.5
	1.27c IC ₅₀ = 31 cLogP = 4.17 Clint = 1.9	1.28c 45% inh. cLogP = 4.76 Clint = 4.4	1.29c 5% inh. cLogP = 5.45 Clint = 2.9
	1.27d IC ₅₀ = 24 cLogP = 4.78 Clint = 1.3	1.28d IC ₅₀ = 1800 cLogP = 5.38 Clint = 0.34	1.29d 3% inh. cLogP = 6.07 Clint = 0.41
	1.27e IC ₅₀ = 12 cLogP = 3.58 Clint = 2.1	1.28e IC ₅₀ = 64 cLogP = 4.18 Clint = 1.5	1.29e 4% inh. cLogP = 4.87 Clint = 1.8
	1.27f IC ₅₀ = 170 cLogP = 2.35 Clint = > 17	1.28f IC ₅₀ = 330 cLogP = 3.95 Clint = > 17	1.29f 2% inh. cLogP = 4.64 Clint = > 17

PDE10A potency measured at 50% inhibitory concentration (IC₅₀) in nM or given as percent inhibition at 10 μM. Lipophilicity given as calculated LogP (cLogP). Metabolic stability given as a measure of microsomal intrinsic clearance (Clint) in L kg⁻¹ h⁻¹

Table 1.3 Physicochemical and *in vitro* ADME Properties of **1.28** and **1.29** Compared to Those of Propranolol⁴⁶

	 1.30 propranolol	 1.31	 1.32
β_2 pIC ₅₀ ^a	7.3	6.3	7.0
β_1 pIC ₅₀ ^a	6.6	6.2	6.7
5HT1A pIC ₅₀ ^a	5.4	<5.3	5.7
log <i>D</i> (pH 7.4) ^b	1.62	2.31	1.81
Clint h ($\mu\text{L min}^{-1} \text{mg}^{-1}$) ^c	28.8	8.7	11.0
Clint m ($\mu\text{L min}^{-1} \text{mg}^{-1}$) ^c	61	>346	175
Clint r ($\mu\text{L min}^{-1} \text{mg}^{-1}$) ^c	>346	289	>346
cytotoxicity (LTC, EC ₂₀ , μM) ^d	>100	18.7	59.0
Ames II positive	no	no	no

^acAMP quantification in h β_2 -CHO cells. ^bDetermined chromatographically. ^c*In vitro* clearance determined by incubation with human (h), mouse (m), or rat (r) liver microsomes, expressed per milligram of protein. ^dBased on an internal analysis of 99 hepatotoxic and non-hepatotoxic compounds, the lowest toxic concentration (LTC) was set at 30 μM .

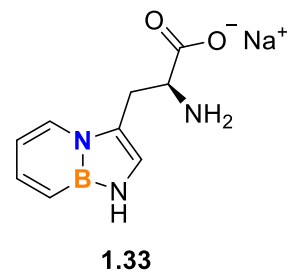
Another study from 2015 compared the pharmacokinetic profiles of two benzazaborinine analogues of propranolol with the carbonaceous version of the molecule (**Table 1.3**).⁴⁶ It was found that compound **1.32** had a comparable pIC₅₀ to propranolol (**1.30**) against the β_2 adrenergic receptor and behaved similarly against β_1 and 5HT1A receptors. Interestingly, experimental log *D* for both **1.31** and **1.32** were higher than **1.30**, indicating that the BN heterocycles are more lipophilic. Both BN containing compounds showed greater metabolic stability than propranolol in human liver microsomes, though all three had high clearance rates in rat and mouse liver microsomes. Cytotoxicity tests,

⁴⁶ Rombouts, F. J. R.; Tovar, F.; Austin, N.; Tresadern, G.; Trabanco A. A. Benzazaborinines as Novel Bioisosteric Replacements of Naphthalene: Propranolol as an Example. *J. Med. Chem.* **2015**, *58*, 9287–9295.

however, showed that **1.31** and **1.32** had higher cytotoxicity than propranolol, which the authors posit might be due to the reduced aromaticity of the ring system. This decreased stability might lead to the formation of toxic metabolites at a higher rate than the more stable propranolol. Ames II tests for all three compounds were negative.

Recently, a BN containing analogue of tryptophan (**Figure 1.8**) was synthesized and incorporated into a superfolder green fluorescent protein (sfGFP).⁴⁷ Boknevitiz et al. were able to demonstrate successful incorporation of the BN-tryptophan into sfGFP by cellular machinery and

Figure 1.8 BN-Tryptophan



that the BN-tryptophan was not toxic to the *E. coli* cells in which they were tested. Additionally, incorporation of BN-tryptophan into the non-fluorescent ketosteroid isomerase (KSI) protein produced a bathochromic shift in absorbance and emission compared to the wild type protein. BN-tryptophan containing KSI had a fluorescence maximum of 372 nm while the wild type KSI maximum was 342 nm. This demonstrates that incorporation of a BN heterocycle can change fluorescent properties of proteins without altering their steric profile.

The first experimental evidence of the interaction of monocyclic 1,2-azaborines with biological systems was provided in 2009.⁴⁸ *N*-ethyl-1,2-azaborine (**1.34**) and the parent 1,2-dihydro-1,2-azaborine (**1.18**) were found to bind in a mutated non-polar cavity of T4 lysozyme. The pocket was formed by the mutation of Leu99→Ala, forming a hydrophobic binding cavity. Binding of benzene in this pocket has been found to stabilize

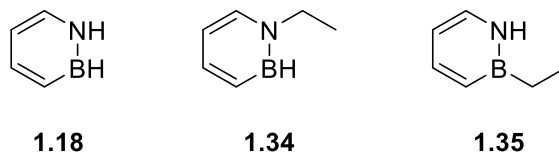
⁴⁷ Boknevitiz, K.; Italia, J. S.; Li, B. Chatterjee, A.; Liu, S.-Y. Synthesis and Characterization of an Unnatural Boron and Nitrogen-Containing Tryptophan Analogue, and Its Incorporation into Proteins. *Chem. Sci.* **2019**, *10*, 4994–4998.

⁴⁸ Liu, L.; Marwitz, A. J. V.; Matthews, B. W.; Liu, S.-Y. Boron Mimetics: 1,2-Dihydro-1,2-azaborines Bind inside a Nonpolar Cavity of T4 Lysozyme. *Angew. Chem. Int. Ed.* **2009**, *48*, 6817–6819.

the protein.⁴⁹ Importantly, it was found that the 1,2-azaborines bound in the pocket in a very similar manner to their carbonaceous isosteres.

Further modification of this pocket by way of Met102→Gln caused the previously hydrophobic pocket to become polar. When **1.18** and *N*-hydro-*B*-ethyl-1,2-azaborine (**1.35**) bind within the pocket, hydrogen bonding between the N–H bond of azaborine and the oxygen of the glutamine residue was observed.⁵⁰ The Gln102=O···H–N hydrogen bond distance was observed via crystal structure to be 3.1 and 3.2 Å for **1.18** and **1.35**, respectively. Additionally, the net free energy of binding was measured to be –0.94 kcal mol⁻¹ for **1.18** and –0.64 kcal mol⁻¹ for **1.35**. Additional studies showed that the strength of this hydrogen bonding decreases in discrete increments as further steric bulk is added to the boron position of the azaborine.⁵¹

Figure 1.9 Binding Study Substrates



In addition to binding in enzymatic pockets, **1.34** and **1.35** have been shown to have similar biological activity to its carbonaceous isostere. Ethylbenzene dehydrogenase (EbdH) is an enzyme with a molybdenum cofactor that catalyzes the hydroxylation of ethyl benzene to (*S*)-1-phenylethanol. Unlike ethylbenzene, which is a substrate of

⁴⁹ Eriksson, A. E.; Baase, W. A.; Wozniak, J. A.; Matthews, B. W. A Cavity-Containing Mutant T4 Lysozyme is Stabilized by Buried Benzene. *Nature* **1992**, *355*, 371–373.

⁵⁰ Lee, H.; Fischer, M.; Shoichet, B. K.; Liu, S.-Y. Hydrogen Bonding of 1,2-Azaborines in the Binding Cavity of T4 Lysozyme Mutants: Structures and Thermodynamics. *J. Am. Chem. Soc.* **2016**, *138*, 12021–12024.

⁵¹ Liu, Y.; Liu, S.-Y. Exploring the Strength of a Hydrogen Bond as a Function of Steric Environment Using 1,2-Azaborine Ligands and Engineered T4 Lysozyme Receptors. *Org. Biomol. Chem.* **2019**, *17*, 7002–7006.

EbDH, both **1.34** and **1.35** were found to act as inhibitors of the enzymatic process.⁵² In particular, **1.34** was found to be a very efficient inhibitor with an IC₅₀ of 2.8 μM. The mechanism of dehydrogenation via EbDH proceeds through both radical and carbocation transition states. Calculated ΔΔG values of the radical and carbocation forming steps on both 1,2-azaborines revealed energy levels substantially higher than that of ethylbenzene (**Table 1.4**). While both 1,2-azaborines can enter the enzymatic pocket of EbDH, their electronic structures prevent them from proceeding as substrates, leading to novel biological activity.

Table 1.4 Relative Calculated Energy Levels for Radical and Carbocation formation⁵²

Compound ^a	ΔΔG radical (kcal mol ⁻¹)	ΔΔG carbocation (kcal mol ⁻¹)
<i>N</i> -ethyl-1,2-azaborine	5.662	2.935
<i>B</i> -ethyl-1,2-azaborine	3.683	5.839
<i>N</i> -ethylimidazole	5.50	9.06
ethylbenzene	0	0
<i>N</i>-ethylpyrrole	4.436	-3.456

^aCompounds in bold act as substrates, other compounds act as inhibitors of EbDH

Finally, in 2017 a series of three azaborine containing isosteres of biologically-active compounds were synthesized and evaluated *in vivo* (**Figure 1.10**).⁵³ Compound **1.41** was evaluated as a dopamine D₃ receptor antagonist. The dopamine D₃ receptor has been tied to cognitive function in both healthy individuals and those with neurological disorders such as schizophrenia, Parkinson's disease, and Alzheimer's disease.⁵⁴ Compound **1.39** was evaluated as a PPAR γ and PPAR δ antagonist. PPAR γ is known to regulate glucose metabolism and insulin sensitization. Activation of PPAR δ enhances

⁵² Knack, D. H.; Marshall, J. L.; Harlow, G. P.; Dudzik, A.; Szalaniec, M.; Liu, S.-Y.; Heider, J. BN/CC Isosteric Compounds as Enzyme Inhibitors: *N*- and *B*-Ethyl-1,2-azaborine Inhibit Ethylbenzene Hydroxylation as Nonconvertible Substrate Analogues. *Angew. Chem. Int. Ed.* **2013**, *52*, 2599–2601.

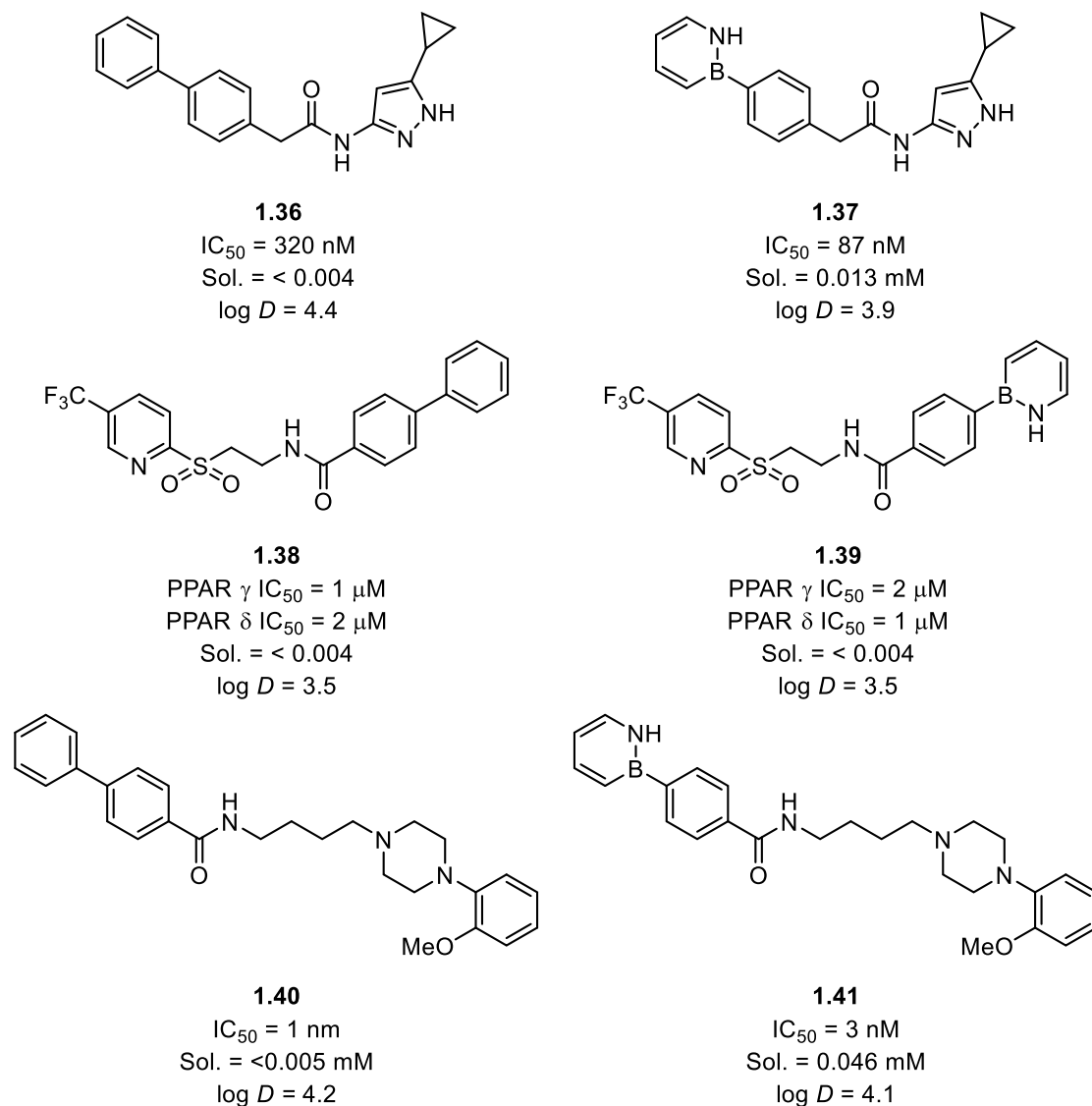
⁵³ Zhao, P.; Nettleton, D. O.; Karki, R. G.; Zécri, F. J.; Liu, S.-Y. Medicinal Chemistry Profiling of Monocyclic 1,2-Azaborines. *ChemMedChem* **2017**, *12*, 358–361.

⁵⁴ Nakajima, S.; Gerretsen, P.; Takeuchi, H.; Caravaggio, F.; Chow, T.; Le Foll, B.; Mulsant, B.; Pollock, B.; Graff-Guerrero, A. The Potential Role of Dopamine D₃ Receptor Neurotransmission in Cognition. *Eur. Neuropsychopharmacol.* **2013**, *23*, 799–813.

fatty acid metabolism. PPAR activity has been tied to a number of conditions including obesity, inflammation, pain, cancer, Parkinson's disease, and Alzheimer's disease.⁵⁵

Compound **1.37** was evaluated as an inhibitor of CDK2, which is a kinase that has been identified as a useful target for treatment and prevention of cancer.⁵⁶

Figure 1.10 Effects of BN/CC Isosterism on Biological Activity and Solubility⁵³

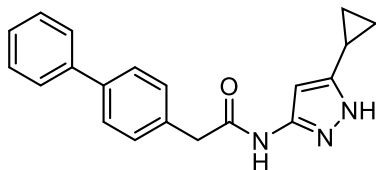
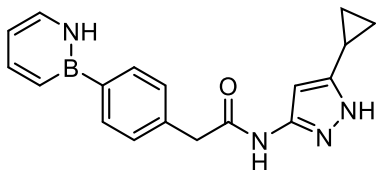


⁵⁵ Tyagi, S.; Gupta, P.; Saini, A. S.; Kaushal, C.; Sharma, S. The Peroxisome Proliferator-Activated Receptor: A Family of Nuclear Receptors Role in Various Diseases. *J. Adv. Pharm. Technol. Res.* **2011**, *2*, 236–240.

⁵⁶ Peng, C.; Zeng, W.; Su, J.; Kuang, Y.; He, Y.; Zhao, S.; Zhang, J.; Ma, W.; Bode, A. M.; Dong, Z.; Chen, X. Cyclin-Dependent Kinase 2 (CDK2) is a Key Mediator for EGF-Induced Cell Transformation Mediated through the ELK4/c-Fos Signaling Pathway. *Oncogene* **2016**, *35*, 1170–1179.

When evaluated relative to their all carbonaceous isosteres, the three BN compounds all showed comparable potency. Of particular note was compound **1.37**, which had an IC₅₀ of 87 nM. The carbonaceous molecule (**1.36**), on the other hand, had a significantly larger IC₅₀ of 320 nM. Further investigation of the properties of **1.36** and **1.37** showed that the half-life, mean residence time, maximum concentration, clearance rate, bioavailability, and area under the curve were all improved in the BN isostere (**Table 1.5**). The addition of the BN unit results in **1.36** having increased bioavailability relative to **1.37**. This enhanced biological activity can in part be attributed to the hydrogen bonding interaction at the N–H of the azaborine. Binding models of **1.37** in the cavity of CDK2 indicated a likely hydrogen bond between the backbone carbonyl of Ile10 and the azaborine N–H. ADMET behavior of the molecules indicates increased solubility of the BN compounds, which can also help explain biological activity.

Table 1.5 Pharmacokinetic Parameters of **1.36** and **1.37** after Administration to Rats⁵³

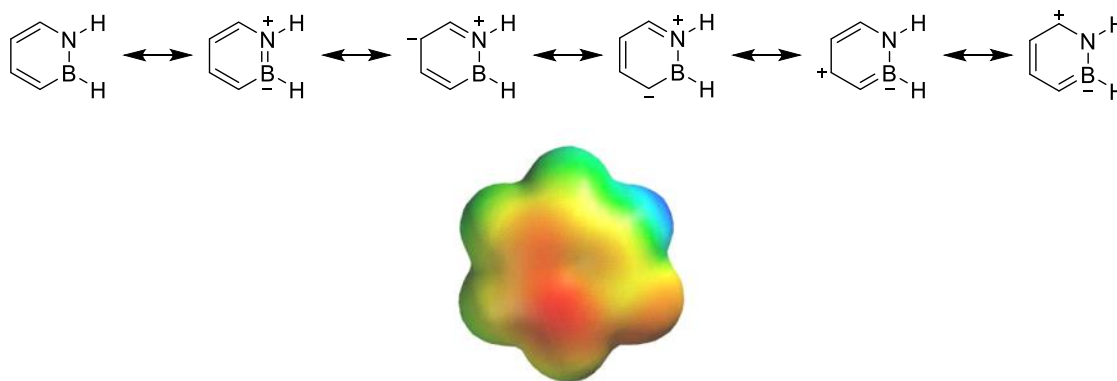
		
	1.36	1.37
i.v. dose (mg kg ⁻¹)	0.5	1.0
oral dose (mg kg ⁻¹)	5.0	5.0
AUC _{iv} (nM·h) ^a	1261	2092
AUC _{po} (nM·h) ^a	283	613
F (%) ^b	22.5	29.3
Cl _{int} (mL min ⁻¹ kg ⁻¹)	39.2	23.7
t _{max} (h)	0.5	1.5
Mean residence time (h)	0.8	2.7
C _{max} (nM)	692	746

^aArea under the curve normalized to 1 mg kg⁻¹ dose. ^bBioavailability.

1.2.2 Late Stage Functionalization of 1,2-Azaborines

The study of 1,2-azaborines as pharmacophores in medicinal chemistry requires synthetic strategies for their incorporation into the molecular framework of complex drug-like molecules. To this end, one focus of recent azaborine research has been on late stage functionalization of 1,2-azaborines. Unlike benzene, each position on the azaborine ring is electronically distinct; there is significant electron density at the C3- and C5-positions,⁵⁷ which can be illustrated by electrostatic potential maps and explained via resonance structures. (**Figure 1.11**)⁵⁸ This electronic distinction should theoretically allow for each position of the azaborine ring to be activated selectively. For the purpose of this chapter, only the carbon positions of 1,2-azaborine, i.e. positions C3-C6, will be discussed.

Figure 1.11 Resonance Structures and Electrostatic Potential Map of 1,2-Dihydro-1,2-azaborine^{37,58}



The electron-rich C3-position of 1,2-azaborine will selectively undergo electrophilic aromatic substitution. This transformation was first reported by Ashe in

⁵⁷ Marwitz, A. J. V.; Matus, M. H.; Zakharov, L. N.; Dixon, D. A. Liu, S.-Y. A Hybrid Organic/Inorganic Benzene. *Angew. Chem. Int. Ed.* **2009**, *48*, 973–977.

Electrostatic Potential map at the 0.002 electron/a.u.³ density iso-contour level. Blue is positive potential, red is negative potential, and green represents near zero potential.

⁵⁸ Electrostatic Potential map at the 0.002 electron/a.u.³ density iso-contour level. Blue is positive potential, red is negative potential, and green represents near zero potential.

2007.⁵⁹ A number of functional groups were installed via this transformation with complete regioselectivity, including bromine, iodine, nitrile, and deuterium. While Ashe was able to functionalize the 3-position in *N*-Ethyl-*B*-phenyl-1,2-azaborine, electrophilic substitution in the presence of a B–Cl bond has also been demonstrated, notably by the Liu group in 2009⁶⁰ and 2015⁶¹. Development of late stage functionalization in the presence of a B–Cl bond is significant as this bond is labile and can be readily functionalized to add further chemical diversity. In the 2015 report, the Liu group was also able to demonstrate functionalization of the C3-Br in the presence of a B–Cl bond via a Negishi cross coupling, a method tolerant of alkyl, alkenyl, and aryl zinc halides at room temperature (**Scheme 1.2**). An additional study in 2019 further expanded the Negishi reaction to 1,2-azaborines with a B–H bond.⁶² The presence of the more stable B–H bond allowed for more electron rich arenes to be used as substrates, which otherwise would generate a mixture of B–O species in the presence of a B–Cl bond.

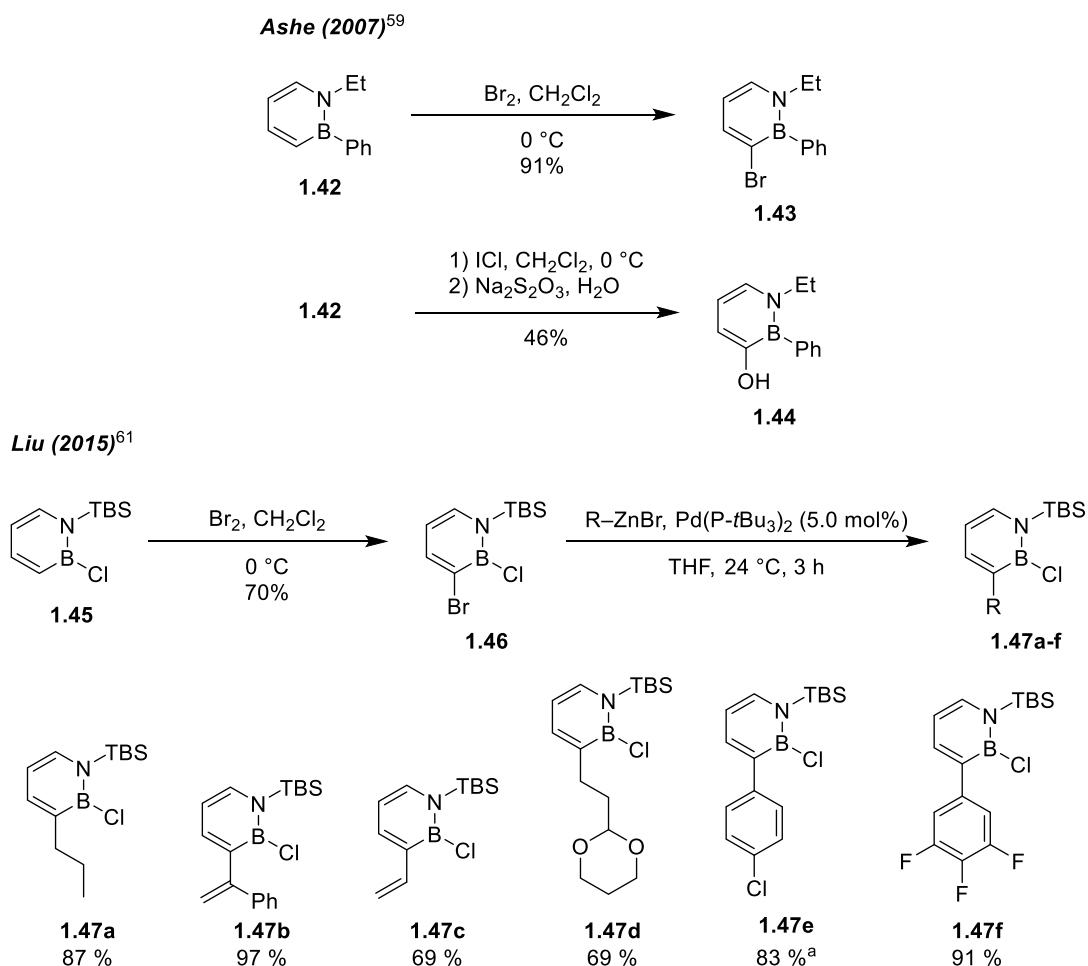
⁵⁹ Pan, J.; Kampf, J. W.; Ashe, A. J –681.

⁶⁰ Lamm, A. N.; Liu, S.-Y. How Stable are 1,2-Dihydro-1,2-azaborines toward Water and Oxygen? *Mol. BioSyst.* **2009**, *5*, 1303–1305.

⁶¹ Brown, A. N.; Li, B.; Liu, S.-Y. Negishi Cross-Coupling with a Reactive B–Cl Bond: Development of a Versatile Late-Stage Functionalization of 1,2-Azaborines and Its Application to the Synthesis of New BN Isosteres of Naphthalene and Indenyl. *J. Am. Chem. Soc.* **2015**, *137*, 8932–8935.

⁶² Brown, A. N.; Li, B.; Liu, S.-Y. Expanding the Functional Group Tolerance of Cross-Coupling in 1,2-Dihydro-1,2-azaborines: Instillation of Alkyl, Alkenyl, Aryl, and Heteroaryl Substituents While Maintaining a B–H Bond. *Tetrahedron* **2019**, *75*, 580–583.

Scheme 1.2 Late Stage Functionalization of 1,2-Azaborines at the C3-Position



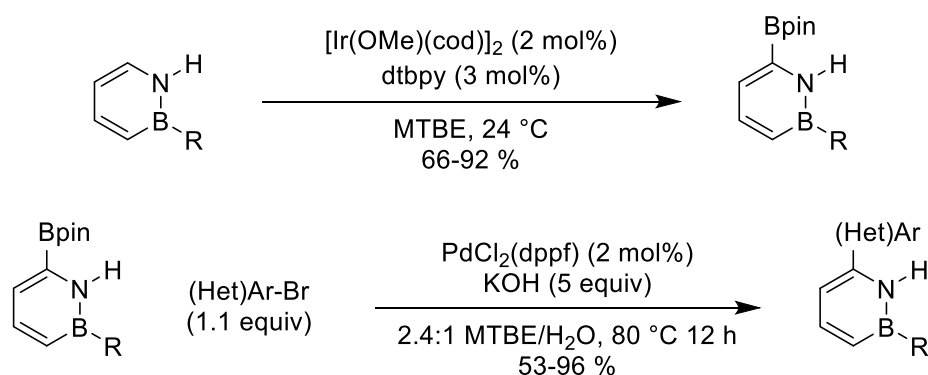
C–H borylation is currently the only published method for late-stage functionalization at the C6-position of 1,2-azaborines.⁶³ Borylation takes place selectively at the 6-position through iridium catalysis. Iridium catalyzed C–H borylation of arenes has been shown to favor activation of the most acidic C–H bonds.⁶⁴ Calculations have shown that that the C6-position of 1,2-azaborine has the lowest pK_a,⁶³

⁶³ Baggett, A. W.; Vasiliu, M.; Li, B.; Dixon, D. A.; Liu, S.-Y. Late-Stage Functionalization of 1,2-Dihydro-1,2-azaborines via Regioselective Iridium-Catalyzed C–H Borylation: The Development of a New N,N-Bidentate Ligand Scaffold. *J. Am. Chem. Soc.* **2015**, *137*, 5536–5541.

⁶⁴ Vanchura II, B. A.; Prshlock, S. M.; Roosen, P. C.; Kallepalli, V. A.; Staples, R. J.; Maleczka Jr., R. E.; Singleton, D. A.; Smith III, M. R. Electronic Effects in Iridium C–H Borylations: Insights from Unencumbered Substrates and Variation of Boryl Ligand Substituents. *Chem. Comm.* **2010**, 7724–7726.

in agreement with its electron deficient nature. The reaction was carried out on 1,2-azaborines with hydride, alkoxy, alkyl, or aryl groups at the B-position and a proton at the N-position. The borylated azaborines can then be submitted to Suzuki cross coupling conditions with an aryl- and heteroaryl-bromide cross coupling partner, further introducing diversity to the azaborine core (**Scheme 1.3**).

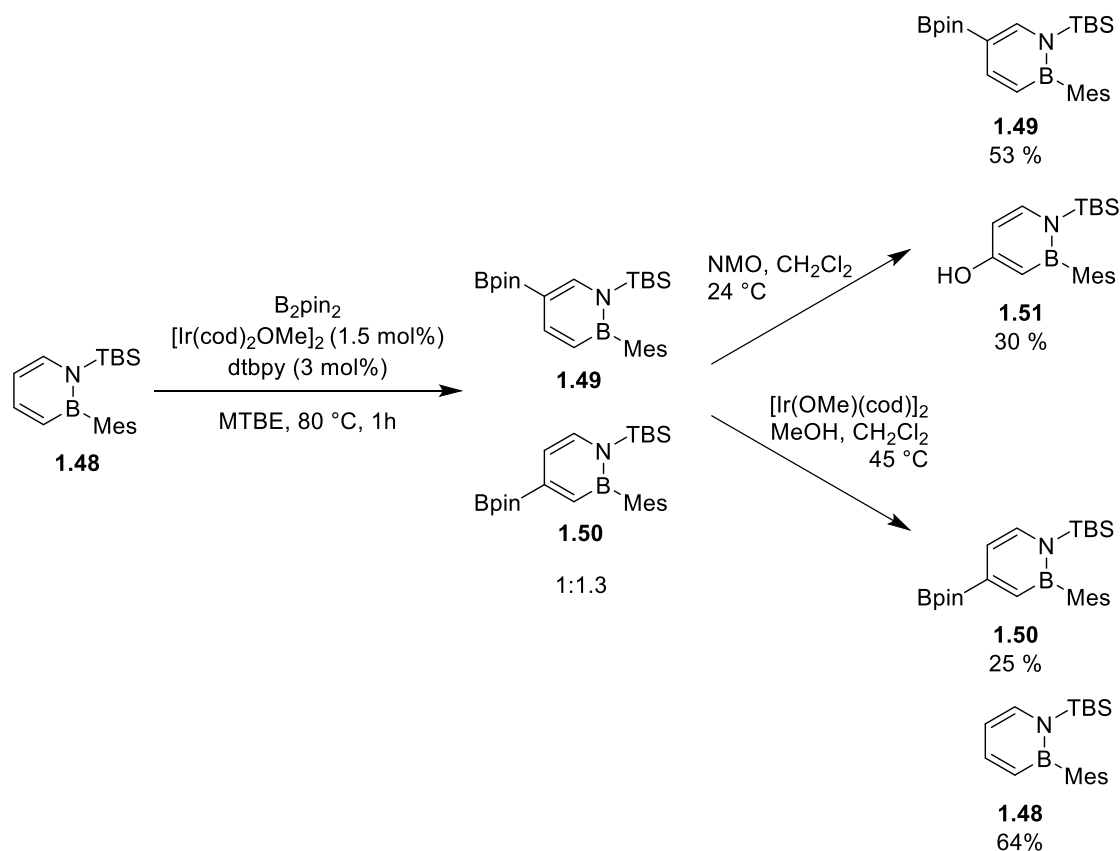
Scheme 1.3 Late Stage Functionalization of 1,2-Azaborines at the C6-Position⁶³



In the presence of a bulky TBS group at the N-position, iridium catalyzed borylation will install Bpin at both the C4- and C5-position in a ratio of 1:1.3 (**Scheme 1.4**).⁶⁵ The electronic differences at the C4- and C5- position allow for resolution and isolation of these two products, **1.49** and **1.50**. *N*-methylmorpholine-*N*-oxide selectively oxidizes **1.50**, allowing **1.49** to be isolated. An iridium catalyzed deborylation is selective for **1.49**, allowing **1.50** to be isolated. While this method is effective, it limits the maximum theoretical yield of borylation of either position on azaborine to 50%. Additionally, both resolutions were only demonstrated to be effective on B-mesityl-1,2-azaborines, which makes further modification of the azaborine core at the B-position challenging.

⁶⁵ McConnell, C. R.; Haeffner, F.; Baggett, A. W.; Liu, S.-Y. 1,2-Azaborine's Distinct Electronic Structure Unlocks Two New Regioisomeric Building Blocks via Resolution Chemistry. *J. Am. Chem. Soc.* **2019**, *141*, 9072–9078.

Scheme 1.4 Borylation and Chemical Resolution of 1,2-Azaborines at the C4- and C5-Positions⁶⁵



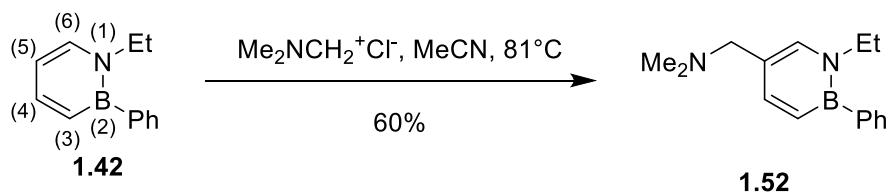
Electrophilic aromatic substitution has been demonstrated to be selective for the C5-position of 1,2-azaborines under select conditions (**Scheme 1.5**). Ashe demonstrated that a Mannich reaction will take place selectively at the C5-position of **1.42** to afford product **1.52** in 60 % yield.⁵⁹ In a study of the acylation of 1,2-azaborines, Fang found that acylation of **1.53** could proceed selectively at the C5-position to yield products **1.54a-h**. This selectivity is likely in part due to the steric bulk of the mesityl group.⁶⁶ In a separate report, Fang reported conditions for selectively nitrating the C5-position of the same substrate to yield the C5-nitrated product **1.55**.⁶⁷

⁶⁶ Zhang, Y.; Sun, F.; Dan, W.; Fang, X. Friedel–Crafts Acylation Reactions of BN-Substituted Arenes. *J. Org. Chem.* **2017**, *82*, 12877–12887.

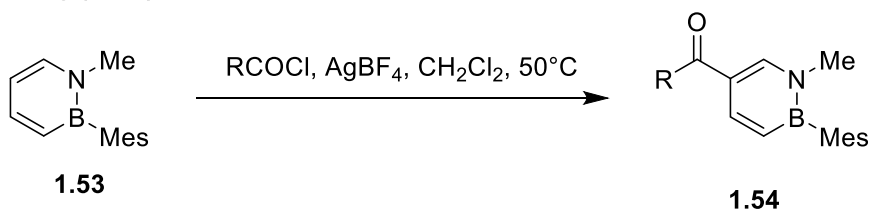
⁶⁷ Zhang, Y.; Dan, W.; Fang, X. Metal Nitrated Mediated Regioselective Nitration of BN-Substituted Arenes. *Organometallics* **2017**, *36*, 1677–1680.

Scheme 1.5 Selective Functionalization of 1,2-Azaborine at the C5-Position

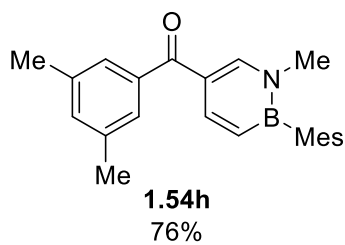
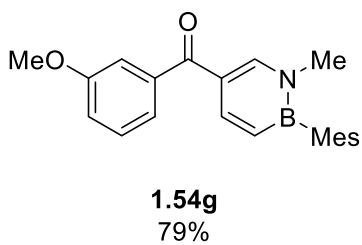
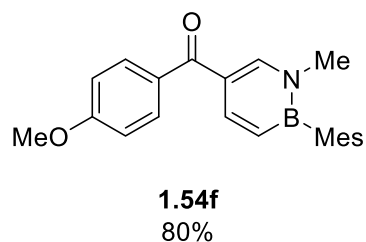
Ashe (2007)⁵⁹



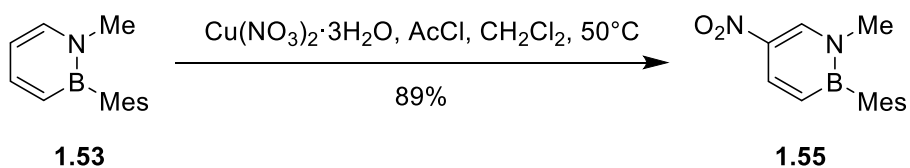
Fang (2017)⁶⁵



R = Me, **1.54a**, 94%
Ph, **1.54b**, 87%
*i*Pr, **1.54c**, 58%
 NMe_2 , **1.54d**, 61%
1-naphthyl, **1.54e**, 79%



Fang (2017)⁶⁶



While these methods exist for functionalizing the C5-position, there is no known protocol for selectively installing a functional group handle with broad synthetic utility. Additionally, all selective transformations at the C5-position have been demonstrated with a bulky mesityl or other aryl group at the B-position, making further functionalization of the molecule at that position difficult. No methods currently exist for directly installing functionality exclusively at the C4-position. In the following section, efforts to increase the scope and utility of the late stage functionalization of 1,2-azaborines will be detailed. Specifically, the installation of chemical handles on the core of 1,2-azaborines with the explicit goal of synthesizing biologically active azaborine-containing compounds will be detailed.

1.3 Towards the Synthesis of a Tetra-Orthogonally Reactive 1,2-Azaborine

1.3.1 Identifying 3,5-Dibromo-*N*-TBS-*B*-Cl-1,2-azaborine as a Synthetic Target

To date, the only 1,2-azaborine containing druglike compounds that have been synthesized and published have had substitution exclusively at the 2-position. This is due in part to synthetic limitations of functionalizing 1,2-azaborines at other positions. Many biphenyl druglike molecules, which are prime candidates for investigating BN/CC isosterism, have more complex substitution patterns that are currently inaccessible on azaborines using known functionalization methods. In order to broaden the scope of targets in which we can incorporate azaborine, it is imperative to develop site selective and orthogonally reactive methods of substituting around the core of the 1,2-azaborine.

Our vision is to develop a tetra-orthogonally reactive azaborine with electronically distinct handles at the C3- and C5-positions. Such a molecule would enable us to access a wider array of biaryl structures with substituents ortho and para to the group at the boron position. This would allow for the development of more targets to explore the medicinal chemistry profile of 1,2-azaborine. Because of the preference of the C3-position for electrophilic aromatic substitution, it was hypothesized that the C5- and C3-positions of a 3,5-dibromo-*N*-TBS-*B*-Cl-1,2-azaborine would be electronically distinct enough to selectively undergo further transformations selectively. Of utmost importance was maintaining the TBS- and Cl-functionality at the N- and B-positions, respectively, so that these positions could easily undergo further transformations. We have previously demonstrated that the TBS and Cl groups can easily be removed from the 1,2-azaborine and replaced with an array of other functionalities.^{56,61,68,69,70}

⁶⁸ Rudebusch, G. E.; Zakharov, L. N.; Liu, S.-Y. Rhodium-Catalyzed Boron Arylation of 1,2-Azaborines. *Angew. Chem. Int. Ed.* **2013**, *52*, 9316–9319.

1.3.2 Synthesis and Evaluation of 3,5-Dibromo-*N*-TBS-*B*-Cl-1,2-azaborine

N-TBS-*B*-Cl-1,2-azaborine (**1.45**), which is commercially available,⁷¹ was selectively brominated at the C3-position through conditions that have been previously described.⁵⁸ A successive bromination was accomplished by resubjecting purified **1.46** to bromination conditions, affording **1.56** in 60% yield. Because C5 was the only nucleophilic position available for bromination on the azaborine, the reaction could be run at room temperature. Additionally, a slight excess of bromine was required for full bromination to take place. Attempts to synthesize **1.56** directly from **1.46** using multiple equivalents of bromine were unsuccessful.

A Suzuki reaction was attempted to test whether the C3–Br bond and the C5–Br bond of **1.57** were sufficiently electronically distinguishable to be selectively activated. As the labile B–Cl bond was likely to lead to undesired reactions, substitution at the B-position was performed to convert **1.56** to **1.57** via a Grignard reaction. We envision our tetra-orthogonally reactive scaffold would be used as a starting point to synthesize a number of different biologically-relevant azaborine-containing molecules, and methods for addition of a wide range of groups at the B-position will be discussed in the following chapter.

For the purpose of exploring fundamental reactivity, a B–phenyl-1,2-azaborine was chosen as a model compound. The transformation was achieved by reacting **1.56** with phenyl magnesium bromide in tetrahydrofuran to afford **1.57** in good yield. Our

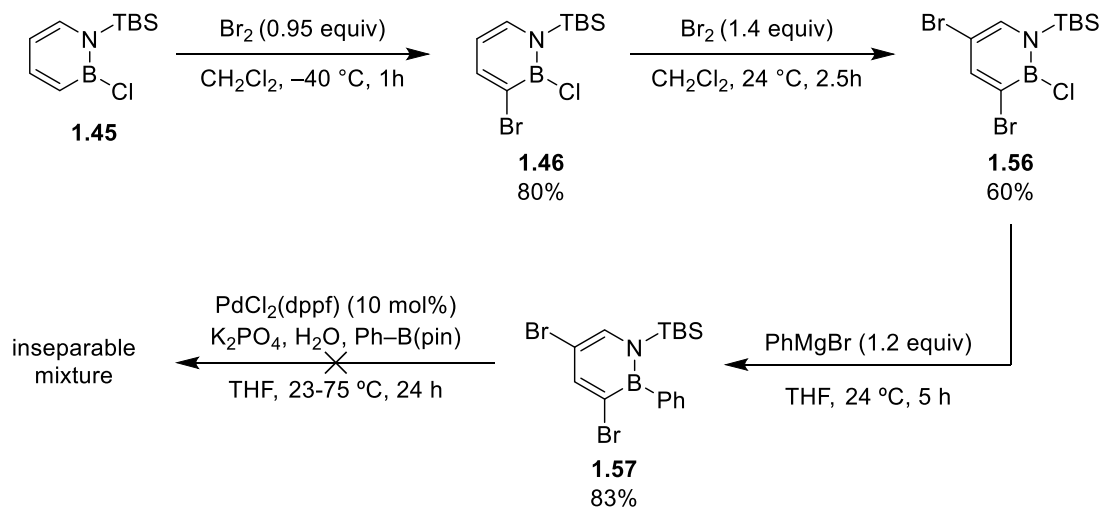
⁶⁹ Marwitz, A. J. V.; Abbey, E. R.; Jenkins, J. T.; Zakharov, L. N.; Liu, S.-Y. Diversity through Isosterism: The Case of Boron-Substituted 1,2-Dihydro-1,2-azaborines. *Org. Lett.* **2007**, *9*, 4905–1908.

⁷⁰ Lamm, A. N.; Garner, E. B.; Dixon, D. A.; Liu, S.-Y. Nucleophilic Aromatic Substitution Reactions of 1,2-Dihydro-1,2-Azaborine. *Angew. Chem. Int. Ed.* **2011**, *50*, 8157-8160.

⁷¹ Compound **1.45** is now commercially available from www.strem.com, catalog number 05-0150. Accessed on 27 Sept 2019.

model compound (**1.57**) was subjected to Suzuki conditions, but we were unable to identify any positional selectivity amongst the mixture of products. It was determined that the C3-Br and C5-Br were too electronically similar to realize our goal of a tetra-orthogonally reactive azaborine with this substitution pattern.

Scheme 1.6 Synthesis and Evaluation of 3,5-Dibromo-1,2-azaborine



1.3.3 Synthesis of 3-Bromo-5-iodo-*N*-TBS-*B*-OH-1,2-azaborine

Our limited tests indicated that **1.57** was not a suitable substrate to achieve selective activation of either the C5- or C3-position. To allow for adequate distinction between chemical handles we believed that different moieties would need to be installed at the C3- and C5-positions. Because an (Csp²)–I bond is significantly weaker than an (Csp²)–Br bond,³⁰ the installation of iodine at the C5-position while maintaining a C3–Br bond should provide sufficient electronic distinction between the two sites.

A number of conditions were screened to achieve iodination of **1.46** at the C5-position (**Table 1.6**). Unlike in the bromination reaction, molecular iodine was not reactive enough to achieve the desired addition. Several Lewis acids were screened in an effort to increase the electrophilicity of iodine, and only gold (III) trichloride was

effective. However, yields above 17% could not be achieved with gold (III) trichloride, and stoichiometric amounts of Lewis acid led to decomposition of the azaborine. As Lewis acids were unable to promote iodination with molecular iodine, we screened two reagents bearing more electrophilic iodine moieties. While iodine monochloride led to decomposition of 1,2-azaborine, ¹H NMR indicated that N-iodosuccinimide did undergo electrophilic aromatic substitution at the C5-position, warranting further investigation.

Table 1.6 Screening of Conditions for Iodination of 3-Br-*N*-TBS-*B*-Cl-1,2-azaborine

Reaction scheme: 3-Br-*N*-TBS-*B*-Cl-1,2-azaborine (**1.46**) reacts with an Iodine Source and Additive in CD₂Cl₂ at 24 °C for 18-24 h to form 5-iodo-3-bromo-1,2-azaborine (**1.58**).

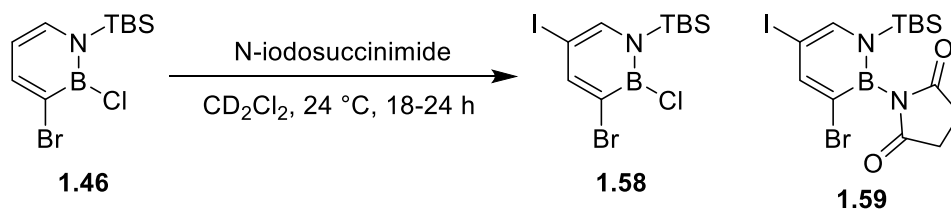
Iodine Source	Additive	Yield ^a
I ₂ (2.0 equiv)	none	0%
I ₂ (2.0 equiv)	AuCl ₃ (0.1 equiv)	17%
I ₂ (2.0 equiv)	AuCl ₃ (0.2 equiv)	16%
I ₂ (2.0 equiv)	AuCl ₃ (2.0 equiv)	0%
I ₂ (2.0 equiv)	FeCl ₃ (0.1 equiv)	0%
I ₂ (2.0 equiv)	AlCl ₃ (0.2 equiv)	0%
I ₂ (2.0 equiv)	CuCl ₂ (2.0 equiv)	0%
I ₂ (2.0 equiv)	Cu(OAc) ₂ (2.0 equiv)	0%
ICl (3.0 equiv)	none	0%
ICl (2.2 equiv)	AlCl ₃ (0.2 equiv)	0%
<i>N</i> -iodosuccinimide (1.3 equiv)	none	22%

^aYields based on ¹H NMR observation with internal standard

Use of *N*-iodosuccinimide presented a unique challenge, however. During the course of the reaction a negatively charged, nucleophilic nitrogen species is produced after abstraction of iodine by **1.46**. This nucleophilic species can then attack the azaborine, forming a side product (**1.59**) in which the succinimide group added to the

azaborine at the electrophilic B-position, breaking the labile B–Cl bond. As a result, both **1.58** and **1.59** were observed in the crude reaction mixture by ^1H NMR analysis. This challenge notwithstanding, optimization of the reaction conditions was pursued. The reaction proceeded to its highest conversion (61%, 1:1.3 **1.58** to **1.59**) with three equivalents of *N*-iodosuccinimide. The remaining mass balance was unreacted **1.46**. Four equivalents of *N*-iodosuccinimide led to decreased yield and decomposition of starting material (**Table 1.7**).

Table 1.7 Screening of Conditions for Iodination of 3-Br-*N*-TBS-B-Cl-1,2-azaborine

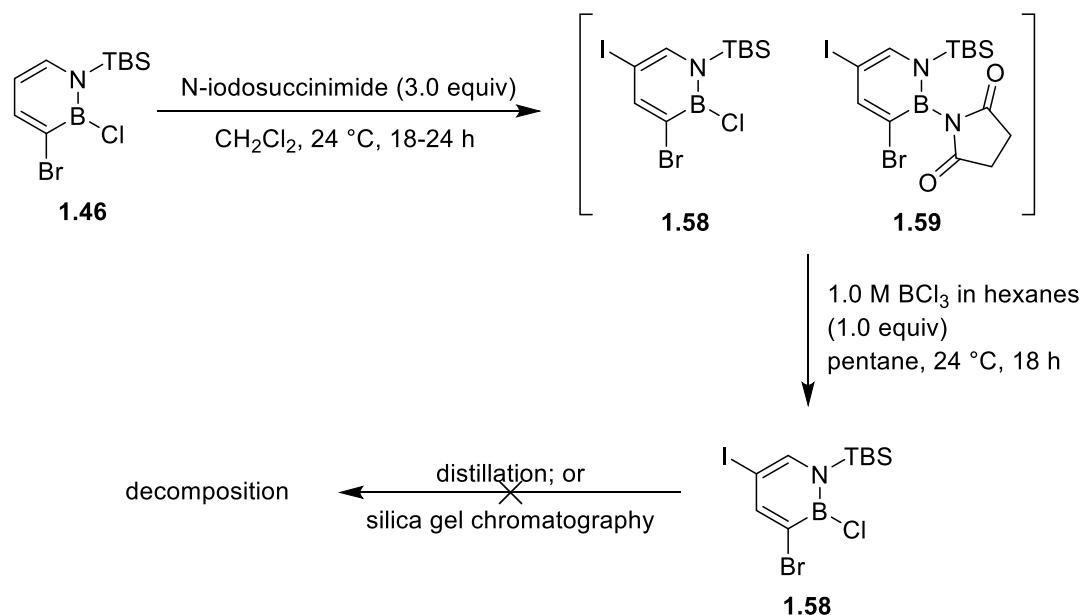


Iodine Source	Yield 1.58 ^a	Yield 1.59 ^a
<i>N</i> -iodosuccinimide (1.3 equiv)	15%	7%
<i>N</i> -iodosuccinimide (2.0 equiv)	21%	16%
<i>N</i> -iodosuccinimide (3.0 equiv)	26%	35%
<i>N</i> -iodosuccinimide (4.0 equiv)	14%	16%

^aYields based on ^1H NMR observation with internal standard

It was found that by passing the crude reaction mixture through a PTFE filter in pentane, the azaborine species could largely be separated from the other species in the reaction. By allowing this filtrate to stir in the presence of boron trichloride, a comproportionation reaction takes place, regenerating **1.58** as the only azaborine species in solution (as determined by ^1H NMR). However, **1.58** proved to be unstable both towards silica gel chromatography and at the elevated temperature that is needed for distillation, and as such could not be purified (**Scheme 1.7**).

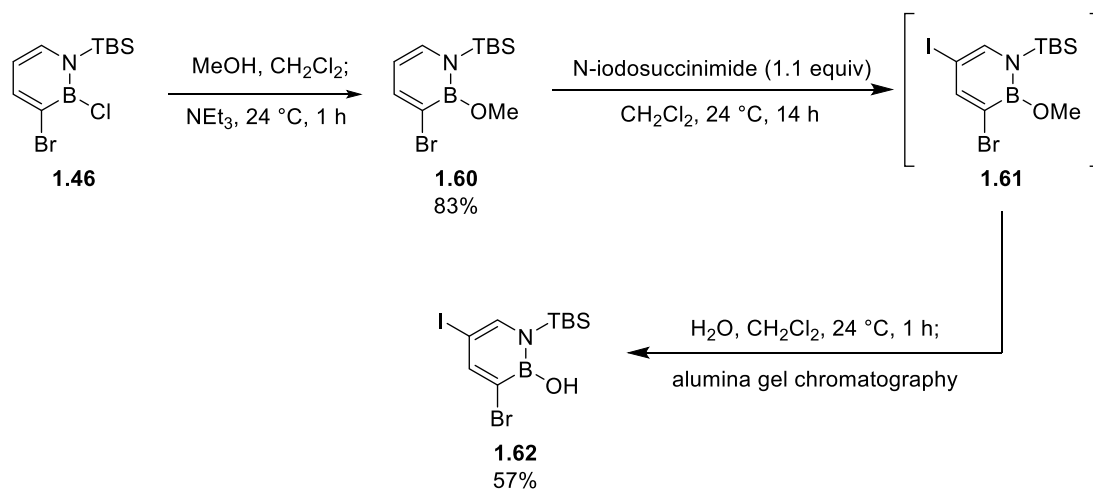
Scheme 1.7 Synthesis and Attempted Purification of 3-Br-5-I-1,2-azaborine



While decomposition at high temperatures needed for the distillation of bromine and iodine substituted 1,2-azaborine would be difficult to avoid, an appropriate group at the B-position could help protect the azaborine from decomposition during chromatography. We have previously demonstrated that unlike B–Cl azaborine, B–OR species are stable on silica.⁷² Compound **1.46** was thus treated with methanol in the presence of triethyl amine to yield **1.60**, which was purified via silica gel chromatography. Compound **1.60** was stirred in the presence of *N*-iodosuccinimide to generate intermediate **1.61**. Presence of a B–OMe bond instead of a B–Cl bond had several effects on this reaction. A smaller amount of *N*-iodosuccinimide was necessary to achieve full conversion of starting material. Additionally, the B–OMe protects against nucleophilic attack by succinimide and no B–N species were observed.

⁷² (a) Abbey, E. R.; Lam, A. N.; Baggett, A. W.; Zakharov, L. N.; Liu, S.-Y. Protecting Group-Free Synthesis of 1,2-Azaborines: A Simple Approach to the Construction of BN-Benzenoids. *J. Am. Chem. Soc.* **2013**, *135*, 12908–12913. (b) Baggett, A. W.; Liu, S.-Y. A Boron Protecting Group Strategy for 1,2-Azaborines. *J. Am. Chem. Soc.* **2017**, *137*, 15259–15264.

Scheme 1.8 Synthesis and Purification of 3-Br-5-I-B-OH-1,2-azaborine



Species **1.61** showed some decomposition to an unknown azaborine species when purified via silica gel chromatography. However, chromatography on alumina gel yielded product with both C3–Br and C5–I bonds intact. Curiously, after being passed through an alumina gel column, the B–OMe bond was replaced with a B–OH bond (**1.62**). To ensure full conversion to **1.62**, the reaction mixture was washed with pentane and passed through a PTFE filter to isolate **1.61**. Isolated **1.61** was stirred in the presence of water to generate **1.62** before purification via alumina gel chromatography. **1.62** was found to be stable to silica and under air at ambient temperatures. Several attempts were made to convert the B–OH species to a B–OR species without success.⁷³

⁷³ See section 1.5.4.3: Attempts to Regenerate *N*-TBS-*B*-OMe-3-bromo-5-iodo-1,2-azaborine

1.4 Conclusions

It has been demonstrated that 1,2-azaborines can act as bioisosteres of benzene.^{46,47} The unique electronic properties of 1,2-azaborines can be leveraged to change not only the ADMET properties of target molecules but also influence their mechanisms of binding within enzymatic pockets. Despite the proven value of 1,2-azaborines in drug development, improved synthetic accessibility is necessary for further studies, particularly with regard to addition of functionality at the carbon positions of the azaborine ring.

Towards this end, we have described the synthesis of *N*-TBS-*B*-OH-3-bromo-5-iodo-1,2-azaborine, which may act as a tetra-orthogonally reactive azaborine core. By installing different halogens at the C3- and C5-positions, it could be possible to selectively and sequentially functionalize these positions through any number of transformations that proceed from halogenated starting materials. *N*-TBS deprotection and further functionalization at the N-position has been well documented in 1,2-azaborines. While B–OH species have yet to be studied, other B–OR species have been shown to be competent precursors to a number of different B–R substituted azaborine species. Reactivity of B–O species will be discussed in depth in the following chapter.

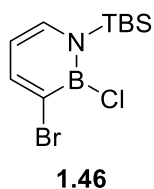
1.5 Experimental

1.5.1 General Considerations

Unless otherwise noted, all oxygen- and moisture-sensitive manipulations were carried out in flame- or oven-dried glassware under an atmosphere of nitrogen using either standard Schlenk technique or a nitrogen-filled glove box. Oxygen-sensitive manipulations carried out in the presence of degassed water were done so in a nitrogen filled, wet glove box. THF, CH₂Cl₂, and pentane were dried using a Brady[®] solvent purification system, which consisted of columnar molecular sieves under argon atmosphere. All column chromatography was performed by hand in a nitrogen-filled glove box. Silica gel (230-400 mesh) and alumina gel were dried for 18 hours at 240 °C under high vacuum. All reagents were purchased from commercial vendors (Acros Organics[®], Millipore Sigma[®], TCI[®]) and used as received unless otherwise noted.

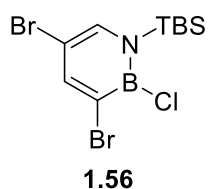
All NMR spectra were recorded on a Varian VNMRs 500 MHz or INOVA 500 MHz spectrometer at ambient temperature in the Michael Gerson Magnetic Resonance and Instrumentation Laboratory at Boston College. ¹¹B NMR spectra were externally referenced to BF₃·Et₂O (δ 0.0 ppm). ¹H NMR spectra were internally referenced to chloroform-d₃ (δ 7.26 ppm). Infrared spectroscopy was performed on a Bruker ALPHA-Platinum FT-IR Spectrometer with an ATR-sampling module. High-resolution mass spectrometry analysis was performed by Marek Domin on a JEOL AccuTOF instrument equipped with a DART ion source in positive ion mode at the Boston College Center for Mass Spectrometry.

1.5.2 Synthesis of 1,2-Azaborines



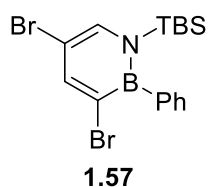
1.45 (1.50 g, 6.59 mmol) was dissolved in 10.0 mL of dichloromethane in a 100 mL roundbottom flask and allowed to stir under nitrogen. The reaction mixture was cooled to $-40\text{ }^{\circ}\text{C}$ in a dry ice/acetone bath. Molecular bromine (1.11 g, 6.92 mmol) was dissolved in 1.5 mL of dichloromethane and added dropwise to the flask. The reaction mixture changed from clear and colorless to a shallow orange color after addition of bromine. The reaction was allowed to warm to $0\text{ }^{\circ}\text{C}$ over the course of 1 hour. At the conclusion of the reaction, the reaction mixture was concentrated *in vacuo*. The crude reaction mixture was purified *via* vacuum distillation ($140\text{ }^{\circ}\text{C}$, 200 mtorr). **1.46** was collected at $90\text{ }^{\circ}\text{C}$ as a light yellow oil (1.62 g, 80.3% yield).

Spectra of isolated compound matched previously published records.⁶¹



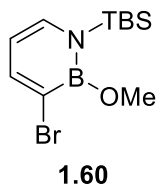
1.46 (2.90 g, 9.46 mmol) was dissolved in 3.0 mL of dichloromethane in a 50 mL roundbottom flask and allowed to stir under nitrogen at 24 °C. Molecular bromine (2.42 g, 15.14 mmol) was dissolved in 3.0 mL of dichloromethane and added dropwise to the flask, after which the reaction mixture changed from clear and colorless to a rich red color. The reaction mixture was allowed to stir for 2 hours. At the conclusion of the reaction, the reaction mixture was concentrated *in vacuo*. The crude reaction mixture was purified *via* vacuum distillation (210 °C, 300 mtorr). **1.56** was collected at 95 °C as a golden oil (1.12 g, 30.8% yield)

¹H NMR (500 MHz, CDCl₃) δ 7.96 (s, 1H), δ 7.36 (s, 1H), δ 0.96 (s, 9H), δ 0.57 (s, 6H);
¹³C NMR (125 MHz, CDCl₃) δ 148.83, 137.67, 104.12, 28.59, 19.30, -1.61 (one C bonded to B was not observed); ¹¹B NMR (160 MHz, CDCl₃) δ 33.784; FTIR (thin film) $\tilde{\nu}$ = 2953, 2929, 2884, 2858, 1603, 1440, 1348, 1317, 1260, 1103, 999, 843, 810, 759, 712, 681; HRMS (DART+) calculated for C₁₀H₁₇BNCIBr₂Si (M⁺): 384.92582, observed: 384.96750.



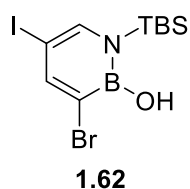
1.56 (250 mg, 0.649 mmol) was dissolved in 5 mL of tetrahydrofuran in a 25 mL roundbottom flask and allowed to stir at 24 °C. A 3M solution of phenyl magnesium bromide in diethyl ether (0.259 mL, 0.778 mmol) was added dropwise to the reaction mixture. The reaction was allowed to stir for 5 hours, after which the reaction mixture turned from a light yellow color to a clear, vibrant orange. At the conclusion of the reaction, 0.1 mL of methanol was added to the reaction mixture, which immediately produced a bright red color. The reaction mixture was concentrated *in vacuo*, and purified *via* silica gel chromatography (15-50% dichloromethane in pentane). **1.57** was collected as an off-white solid (230 mg, 83.0% yield).

^1H NMR (500 MHz, CDCl_3) δ 8.04 (s, 1H), δ 7.53 (s, 1H), δ 7.35-7.33 (m, 3H), δ 7.31-7.29 (m, 2H) δ 0.90 (s, 9H), δ 0.02 (s, 6H); ^{13}C NMR (125 MHz, CDCl_3) δ 147.28, 137.50, 132.11, 127.57, 126.97, 104.89, 28.68, 18.85, -2.30 (two Cs bonded to B were not observed); ^{11}B NMR (160 MHz, CDCl_3) δ 37.373; FTIR (thin film) $\tilde{\nu}$ = 2954, 2930, 2885, 2858, 1607, 1440, 1363, 1348, 1260, 1128, 998, 842, 811, 732, 681; HRMS (DART+) calculated for $\text{C}_{16}\text{H}_{22}\text{BNBr}_2\text{Si}$ (M^+): 424.99758, observed: 424.99827.



1.46 (4.71 g, 15.37 mmol) was dissolved in 20 mL of dichloromethane in a 100 mL roundbottom flask and allowed to stir at 24 °C. A solution of methanol (0.654 mL, 16.13 mmol), distilled off of calcium hydride, and triethylamine (3.21 mL, 23.05 mmol), distilled off of calcium hydride, in 10 mL of dichloromethane was added dropwise to the vial and allowed to stir for 1.5 hours. The reaction mixture turned from a clear yellow color to an opaque off-white color with a significant presence of a precipitate. At the conclusion of the reaction, the reaction mixture was diluted with pentane (50 mL), causing additional precipitate to crash out of solution. The crude reaction mixture was reduced *in vacuo* and purified *via* silica gel chromatography (20% dichloromethane in pentane). **1.60** was collected as a clear, lightly yellow oil (3.88 g, 83.6% yield).

^1H NMR (500 MHz, CDCl_3) δ 7.75 (d, $J = 6.5$, 1H), δ 7.00 (d, $J = 6.5$, 1H), δ 5.77 (t, $J = 7$, 3H), δ 4.03 (s, 3H) δ 0.91 (s, 9H), δ 0.37 (s, 6H); ^{13}C NMR (125 MHz, CDCl_3) δ 149.00, 138.00, 106.80, 53.88, 26.80, 18.88, -2.91 (one C bonded to B was not observed); ^{11}B NMR (160 MHz, CDCl_3) δ 27.908; FTIR (thin film) $\tilde{\nu} = 2954, 2929, 2884, 2858, 1603, 1470, 1356, 1286, 1252, 1128, 998, 906, 841, 823, 732, 681$; HRMS (DART+) calculated for $\text{C}_{11}\text{H}_{21}\text{BNOBrSi}$ (M^+): 302.07416, observed: 302.07412.

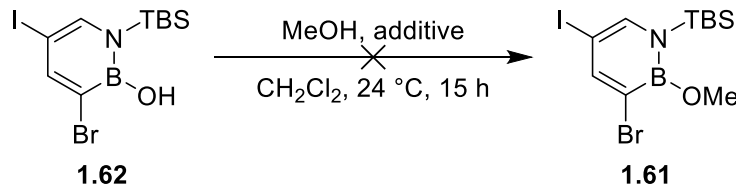


1.60 (1.50 g, 4.97 mmol) was dissolved in 20 mL of dichloromethane in a 100 mL vial and was allowed to stir at 24 °C. *N*-iodosuccinimide (1.51 g, 6.70 mmol), recrystallized from a dioxane/pentane mixture, was added to the vial as a solid. The reaction was allowed to stir for 24 hours, after which the reaction mixture changed in color from translucent red to a deep, opaque black. At the conclusion of the reaction, solvent was removed from the crude *in vacuo*. Concentrated crude was dissolved in 15% dichloromethane in pentane (20 mL) and purified *via* alumina gel chromatography (15% dichloromethane in pentane) to yield a mixture of **1.61** and **1.62** as a clear, orange liquid. This mixture was dissolved in 20 mL of dichloromethane and allowed to stir at 24 °C. Degassed water (0.270 mL, 14.91 mmol) was added to flask, which was allowed to stir under nitrogen atmosphere for 1 hour. The reaction mixture was allowed to stir over activated molecular sieves for 2 hours, after which it was transferred *via* cannula to a dry 50 mL roundbottom flask and concentrated *in vacuo*. Crude reaction mixture was purified *via* alumina gel chromatography (15% dichloromethane in pentane). **1.62** was collected as an orange solid (1.17 g, 57.0% yield). ^1H NMR (500 MHz, CDCl_3) δ 7.80 (s, 1H), δ 7.17 (s, 1H), δ 4.62 (s, 1H), δ 0.93 (s, 9H), δ 0.43 (s, 6H); ^{13}C NMR (125 MHz, CDCl_3) δ 151.48, 142.17, 26.33, 18.75, -3.67 (one C bonded to B and one C bonded to I were not observed); ^{11}B NMR (160 MHz, CDCl_3) δ 28.689; FTIR (thin film) $\tilde{\nu}$ = 3612, 2952, 2928, 2884, 2857, 1581, 1470, 1387, 1343, 1258, 1007, 842, 811, 680; HRMS (DART+) calculated for $\text{C}_{10}\text{H}_{18}\text{BNOBrSi}$ (M^+): 413.95581, observed: 413.95581.

1.5.3 Attempts to Regenerate *N*-TBS-*B*-OMe-3-bromo-5-iodo-1,2-azaborine

Several attempts were made to regenerate **1.61** from **1.62** by nucleophilic attack of methanol at the B-position (**Table 1.8**). Drying agents seemed unable to push the reaction to the product. Large excesses of methanol was equally ineffective and only served to cause decomposition of the azaborine core.

Table 1.8 Attempts to Regenerate **1.61** by Nucleophilic Displacement of -OH by Methanol

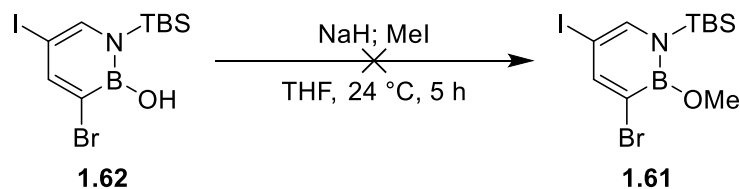


Equiv. MeOH	additive	result
1.12	4 Å mol. sieves	incomplete conversion
3.4	5 equiv. NEt ₃	decomposition
2.0	Na ₂ SO ₄	incomplete conversion
2.0	MgSO ₄	incomplete conversion
102	MgSO ₄	incomplete conversion ^a
102	4 Å mol. sieves	incomplete conversion ^a

^asome decomposition observed

An attempt was also made to deprotonate the protic hydrogen bound to oxygen and attack a methyl electrophile (**Scheme 1.9**). While deprotonation was observed via ¹¹B NMR, no reaction in the presence of methyl-iodide was observed.

Scheme 1.9 Attempt to Regenerate **1.61** by Reaction with a Methyl Electrophile



1.5.4 Spectral Data

3,5-Br-N-TBS-B-Cl-1,2-azaborine

Sample Name:

JRA-2-101_1HNMR

Data Collected on:

nmr18-vmmrs500

Archive directory:

Sample directory:

Filefile: PROTON

Pulse Sequence: PROTON (s3pul)

Solvent: cdcl3

Data collected on: Sep 3 2019

Temp: 25.0 C / 298.1 K

Operator: Liu

Relax. delay 20.000 sec

Pulse 45.0 degrees

Acq. time 2.045 sec

Width 8012.8 Hz

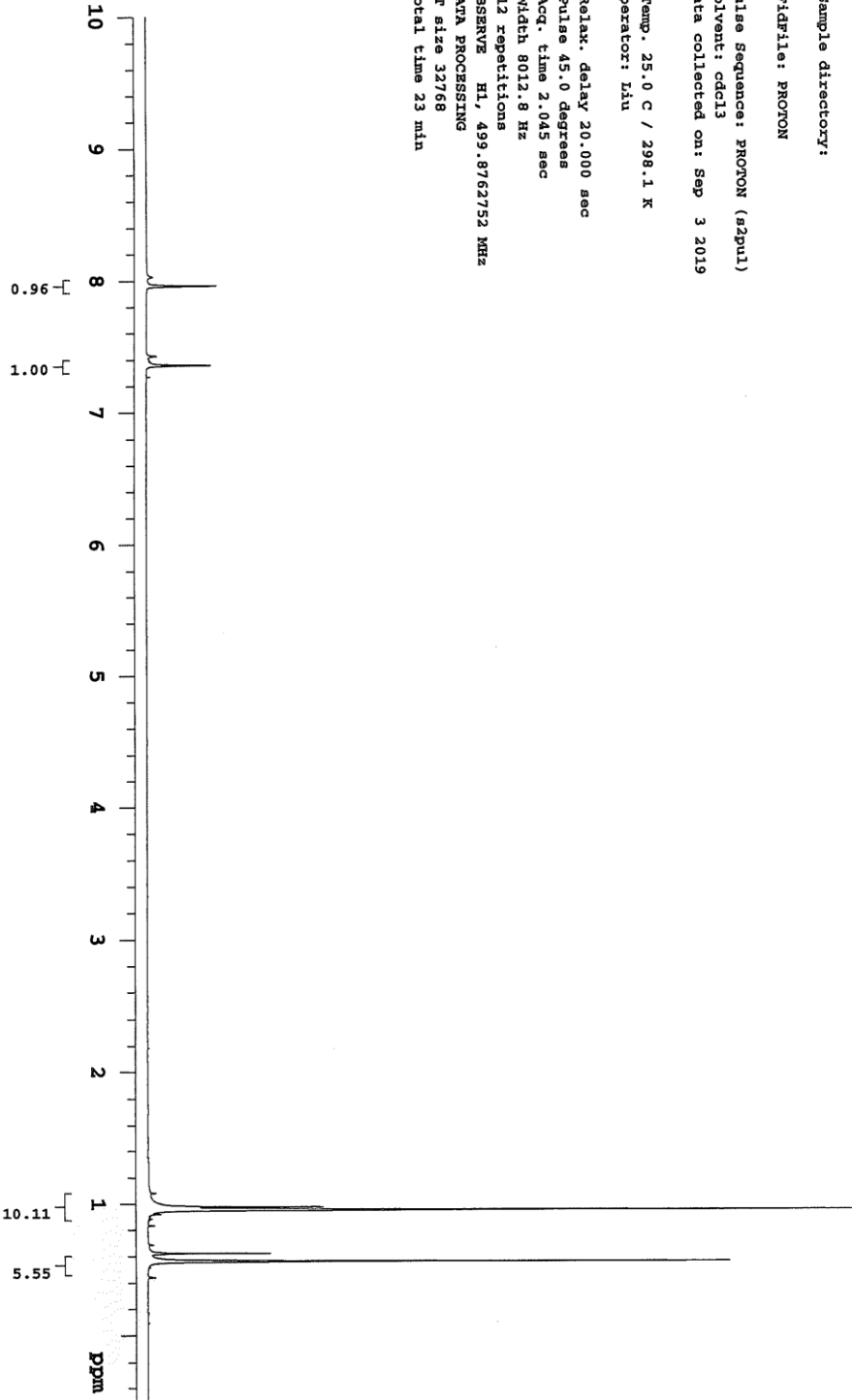
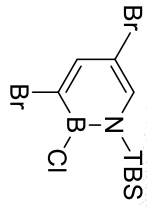
12 repetitions

OBSERVE H1, 499.8762752 MHz

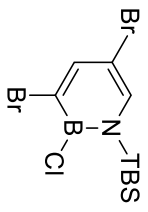
DATA PROCESSING

FW size 32768

Total time 23 min



3,5-Br-N-TBS-B-Cl-1,2-azaborine



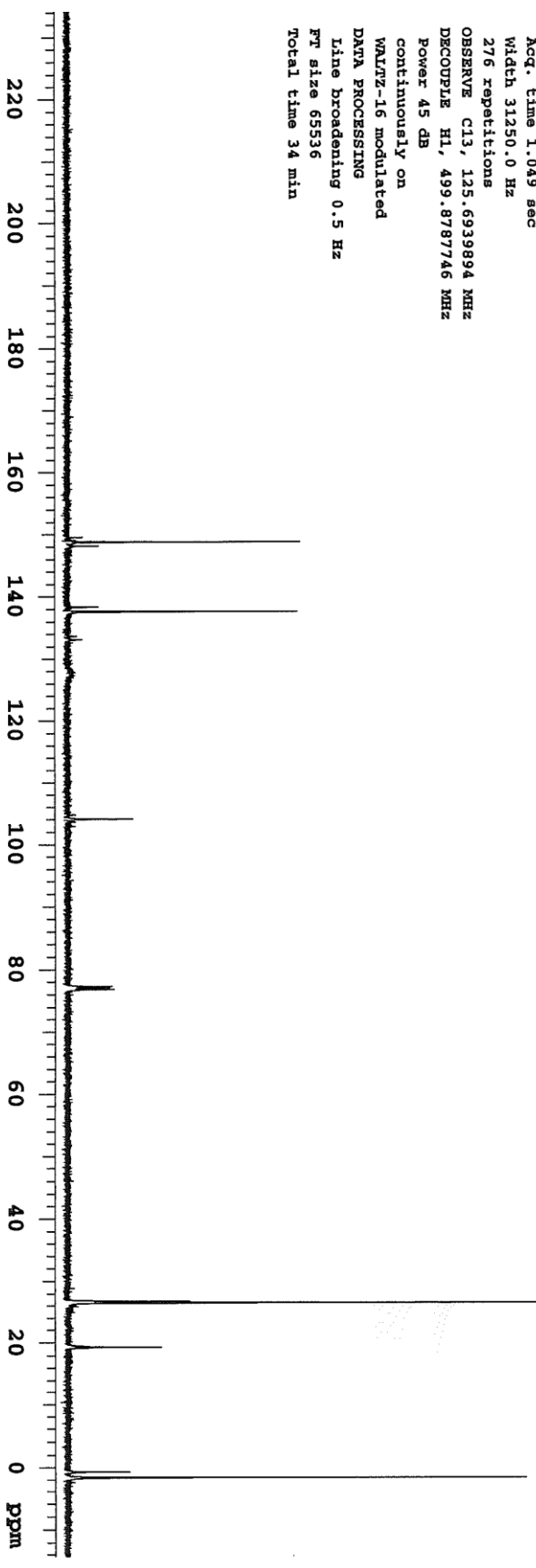
Sample Name:
JRA-2-101_13CNMR
Data Collected on:
nmr18-vnmr5500
Archive directory:

Sample directory:
FidFile: CARBON

Pulse Sequence: CARBON (s2pu1)
Solvent: cdcl3
Data collected on: Sep 3 2019

Temp. 25.0 C / 298.1 K
Operator: Liu

Relax. delay 1.000 sec
Pulse 45.0 degrees
Acq. time 1.049 sec
Width 31250.0 Hz
276 repetitions
OBSERVE C13, 125.6939894 MHz
DECOUPLE H1, 499.8787746 MHz
Power 45 dB
continuously on
WALTZ-16 modulated
DATA PROCESSING
Line broadening 0.5 Hz
FT size 65536
Total time 34 min



3,5-Br-N-TBS-B-Cl-1,2-azaborine

Sample Name:

JRA-2-101_11BMMR

Data Collected on:

mmx11-1nov2019

Archive directory:

Sample directory:

File: JRA-2-101_fr2_11BMMR

Pulse Sequence: s2pul1

Solvent: cdcl3

Data collected on: Sep 3 2019

Temp. 25.0 C / 298.1 K

Operator: lhu

Relax. delay 0.100 sec

Pulse 22.2 degrees

Acq. time 0.064 sec

Width 32064.1 Hz

106 repetitions

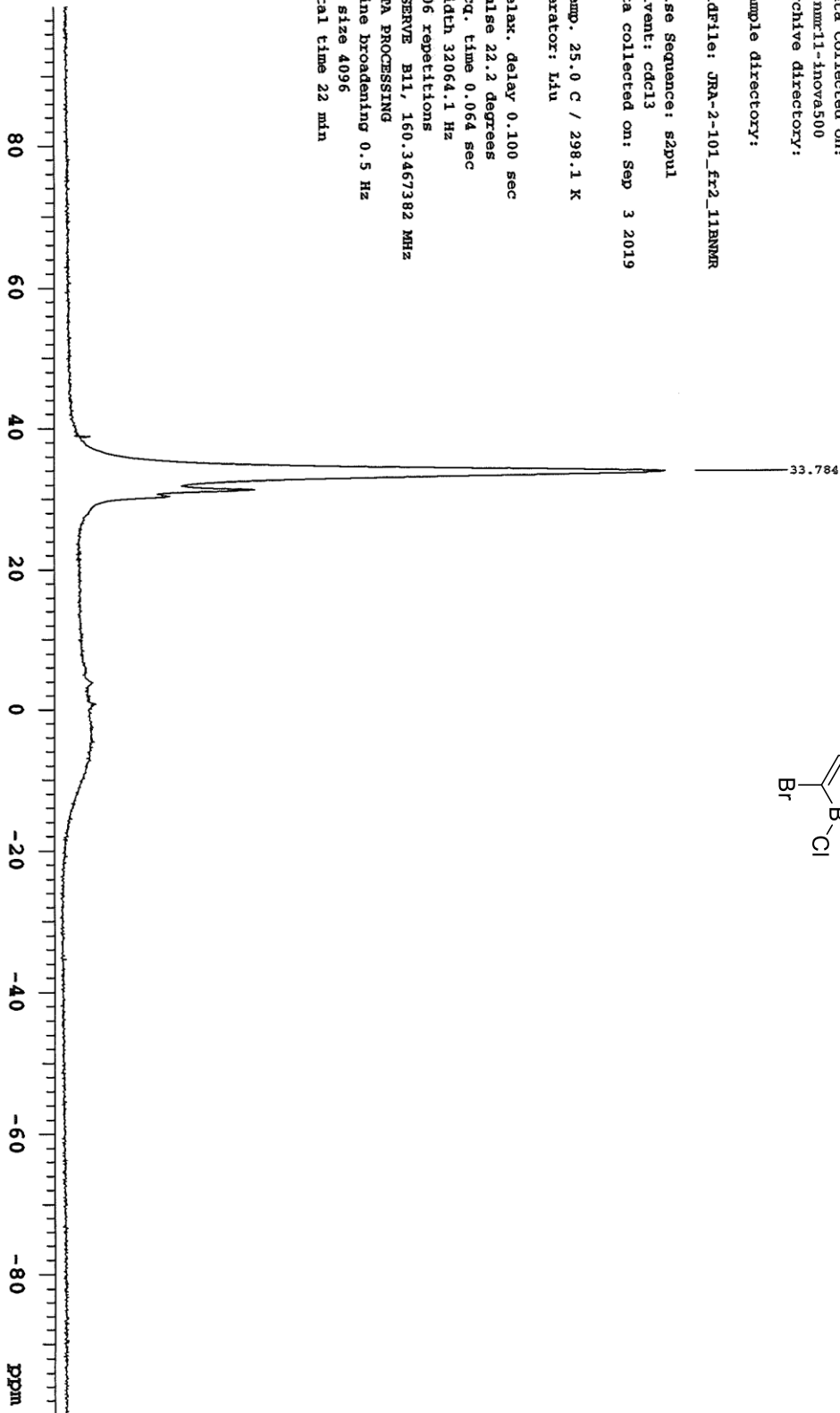
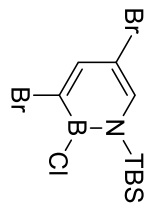
OBSERVE B11, 160.3467382 MHz

DATA PROCESSING

Line broadening 0.5 Hz

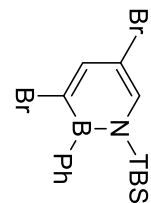
FW size 4096

Total time 22 min



5-Br-3-Br-N-TBS-B-Ph-1,2-azaborine

Sample Name:
URA-1-073_2_1HNMNR
Data Collected on:
MMX18-VNMRS500
Archive directory:



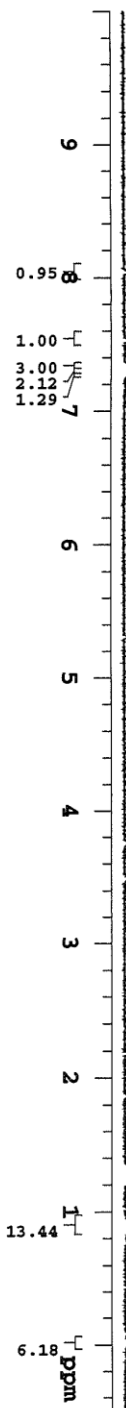
Agilent Technologies

Sample directory:
Fidfile: PROTON

Pulse Sequence: PROTON (s2pul)
Solvent: cdcl3
Data collected on: Aug 30 2019

Temp: 25.0 C / 298.1 K
Operator: kin

Relax. delay 10.000 sec
Pulse 45.0 degrees
Acq. time 2.045 sec
Width 8012.8 Hz
24 repetitions
OBSERVE H1, 499.8762752 MHz
DATA PROCESSING
Ft size 32768
Total time 6 min 25 sec



3,5-Br-N-TBS-B-Ph-1,2-azaborine

Sample Name:

Data Collected on:

nmr18-vnmr5500

Archive directory:

Sample directory:

Fidfile: CARBON

Pulse Sequence: CARBON (szpu1)

Solvent: cdcl3

Data collected on: Sep 4 2019

Temp. 25.0 C / 298.1 K

Operator: Liu

Relax. delay 1.000 sec

Pulse 45.0 degrees

Acq. time 1.049 sec

Width 31250.0 Hz

420 repetitions

OBSERVE C13, 125.6939894 MHz

DECOUPLE H1, 499.8787746 MHz

Power 45 dB

continuously on

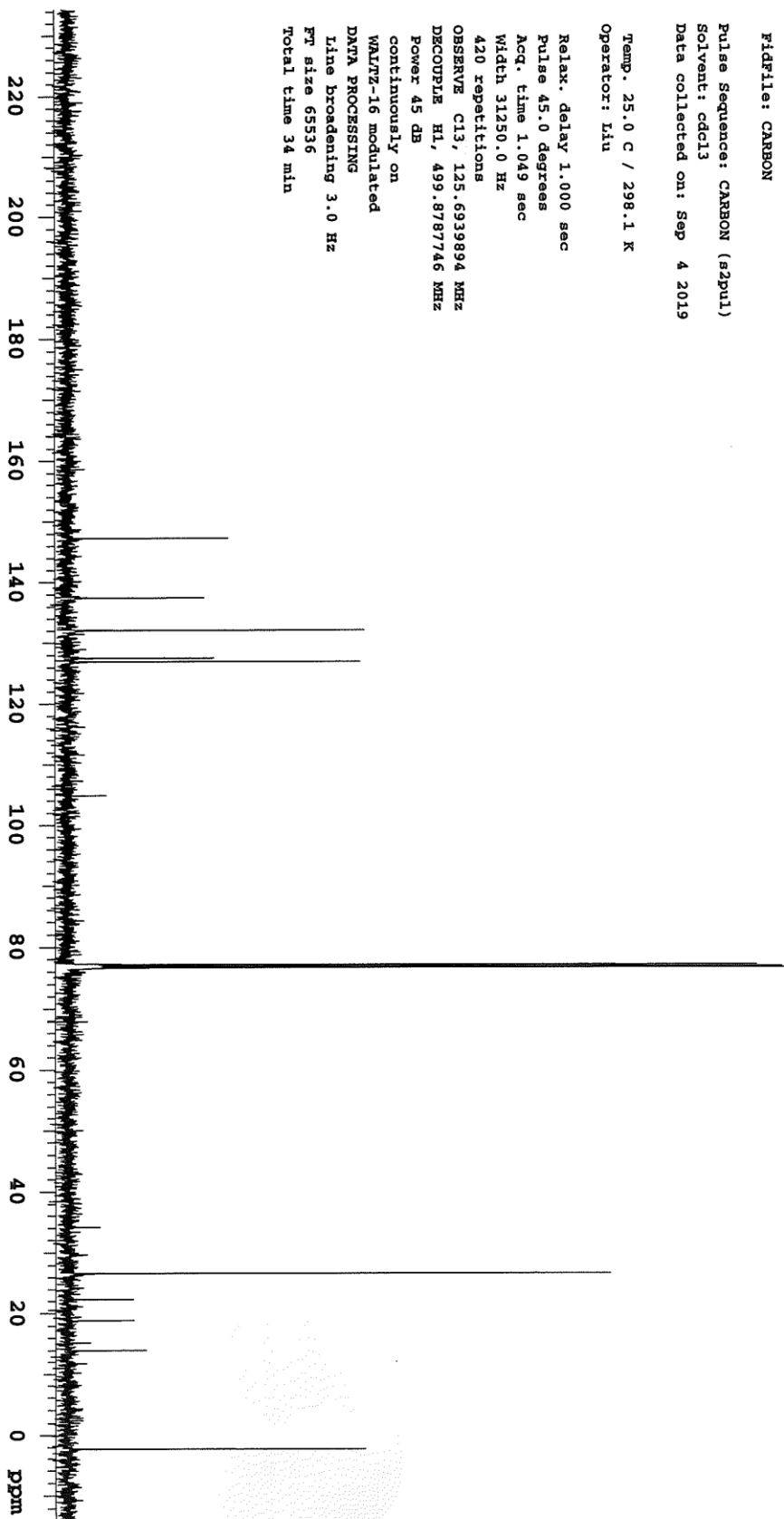
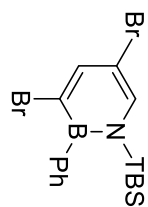
WALTZ-16 modulated

DATA PROCESSING

Line broadening 3.0 Hz

FT size 65536

Total time 34 min



5-Br-3-Br-N-TBS-B-Ph-1,2-azaborine

Sample Name:

JRA-1-073_2_11BRNR

Data Collected on:

nmr18-vmrms500

Archive directory:

Sample directory:

FidFile: B11

Pulse Sequence: s2pul1

Solvent: cdcl3

Data collected on: Aug 30 2019

Temp. 25.0 C / 298.1 K

Operator: lhu

Relax. delay 0.100 sec

Pulse 60.5 degrees

Acq. time 0.064 sec

Width 32051.3 Hz

891 repetitions

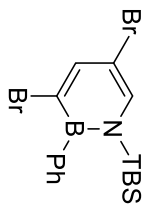
OBSERVE B11, 160.380205 MHz

DATA PROCESSING

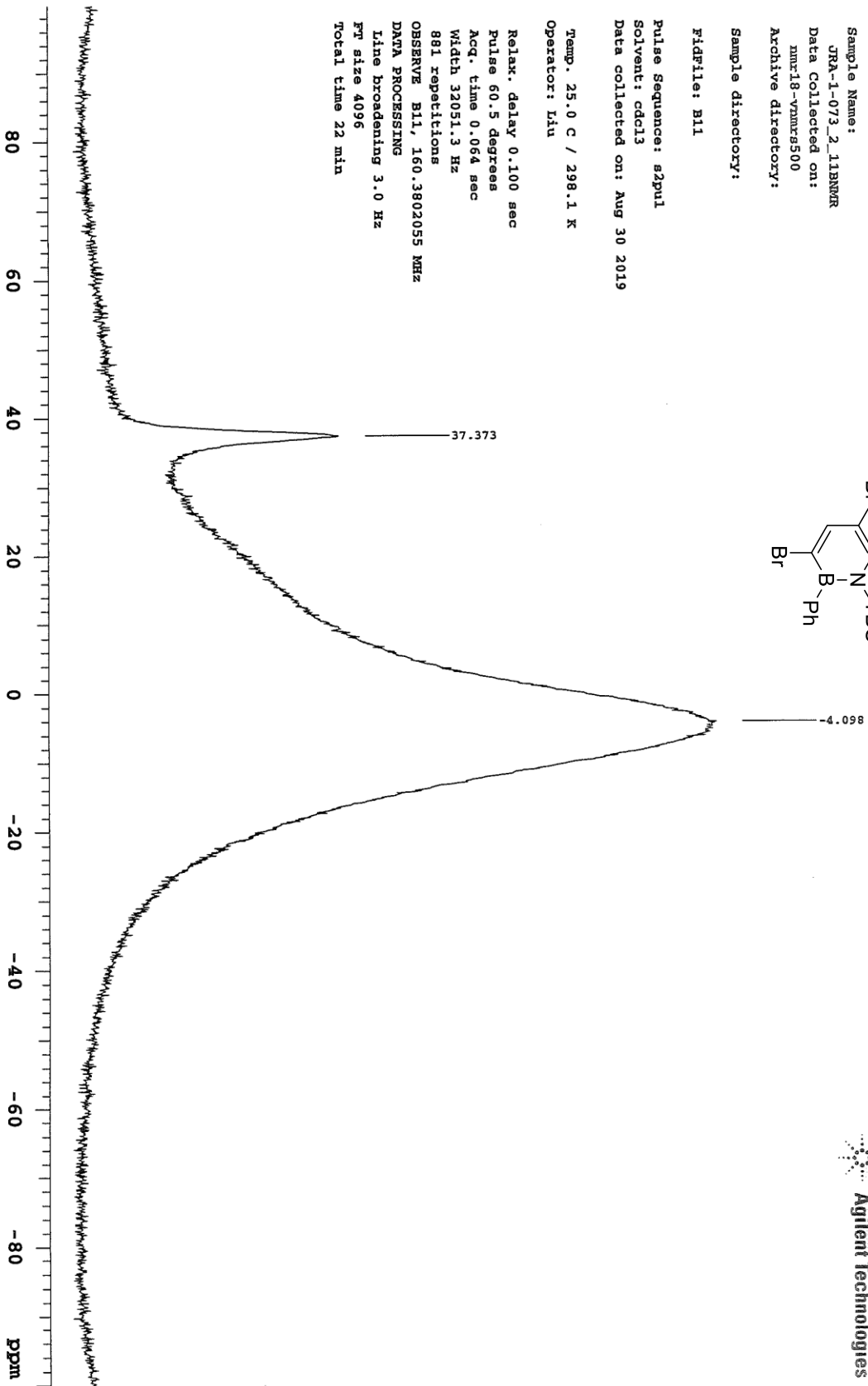
Line broadening 3.0 Hz

PR size 4096

Total time 22 min

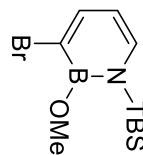


Agilent Technologies



3-Br-N-TBS-B-OMe-1,2-azaborine

Sample Name:
JRA-2-066_1HNMR
Data Collected on:
mm18-vnmr5500
Archive directory:



Sample directory:

Fidfile: JRA-2-066_1HNMR

Pulse Sequence: PROTON (s2pul)

Solvent: cdcl3

Data collected on: Jul 19 2019

Temp. 25.0 C / 298.1 K

Operator: lhu

Relax. delay 15.000 sec

Pulse 45.0 degrees

Acq. time 2.045 sec

Width 8012.8 Hz

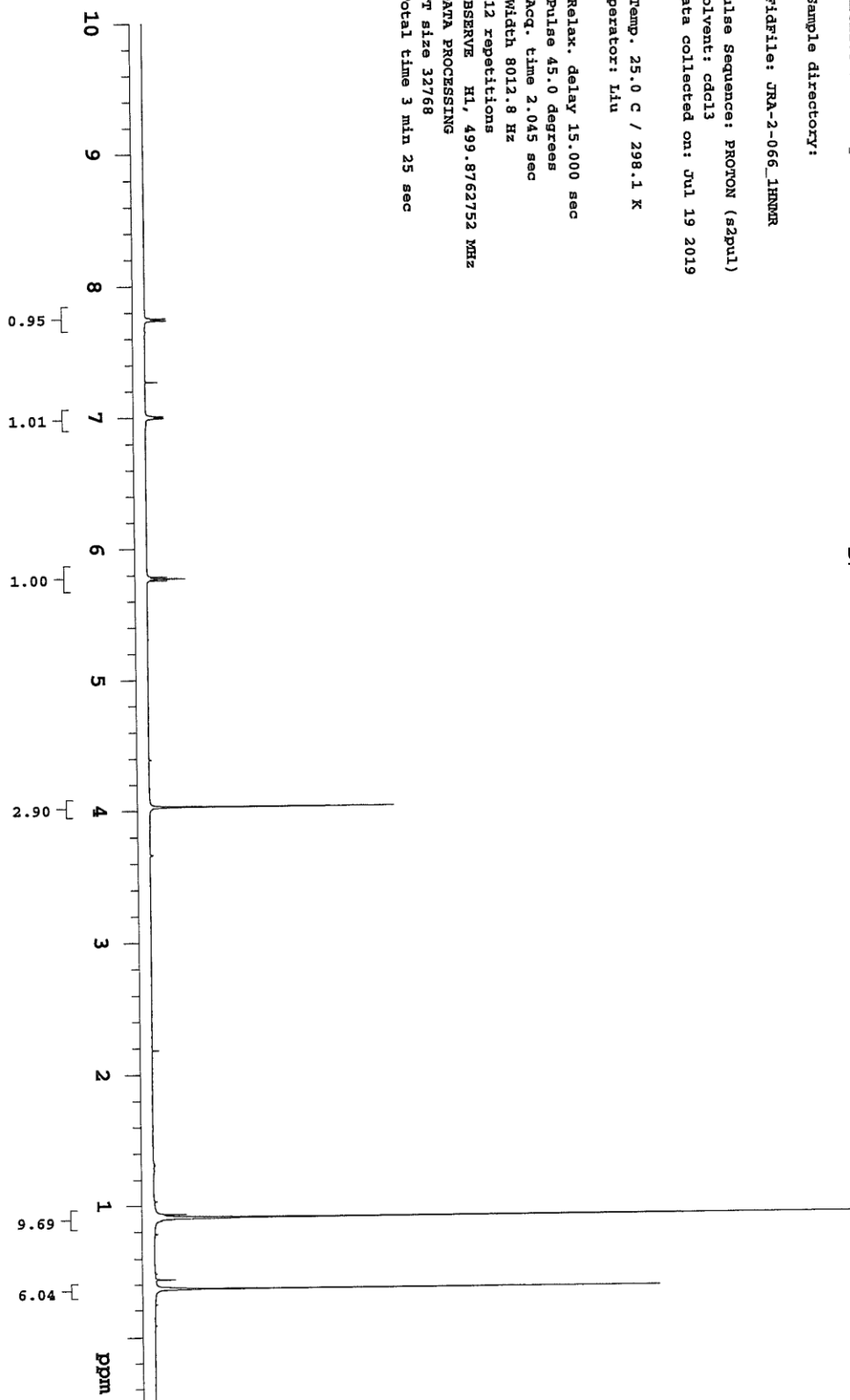
12 repetitions

OBSERVE H1, 499.8762752 MHz

DATA PROCESSING

FT size 32768

Total time 3 min 25 sec



3-Br-N-TBS-B-OMe-1,2-azaborine

Sample Name:

JRA-2-066_13CNMR

Data Collected on:

mmr18-vmmrs500

Archive directory:

Sample directory:

FidFile: JRA-2-066_13CNMR

Pulse Sequence: CARBON (s2pul)

Solvent: cdcl3

Data collected on: Jul 19 2019

Temp. 25.0 C / 298.1 K

Operator: Liu

Relax. delay 1.000 sec

Pulse 45.0 degrees

Acq. time 1.049 sec

Width 31250.0 Hz

450 repetitions

OBSERVE C13, 125.6939687 MHz

DECOUPLE H1, 499.8787746 MHz

Power 43 dB

continuously on

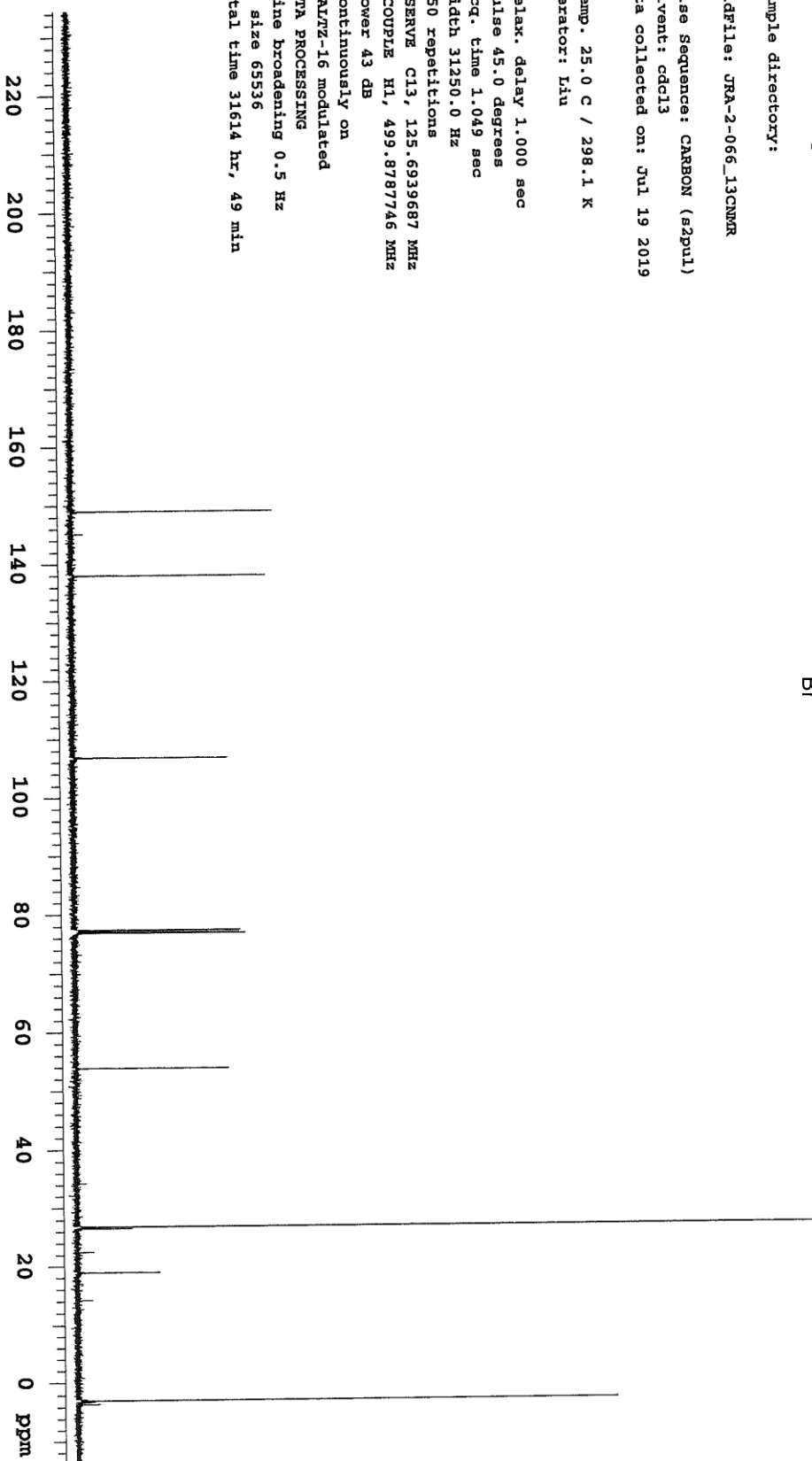
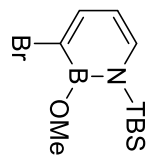
WALTZ-16 modulated

DATA PROCESSING

Line broadening 0.5 Hz

FT size 65536

Total time 31614 hr, 49 min



3-Br-N-TBS-B-OMe-1,2-azaborine

Sample Name:

URA-2-066_11BNMR

Data Collected on:

nmr18-vnmr5500

Archive directory:

Sample directory:

File: URA-2-066_11BNMR

Pulse Sequence: szpul

Solvent: cdcl3

Data collected on: Jul 19 2019

Temp. 25.0 C / 298.1 K

Operator: ldu

Relax. delay 0.100 sec

Pulse 60.5 degrees

Acq. time 0.064 sec

Width 32051.3 Hz

55 repetitions

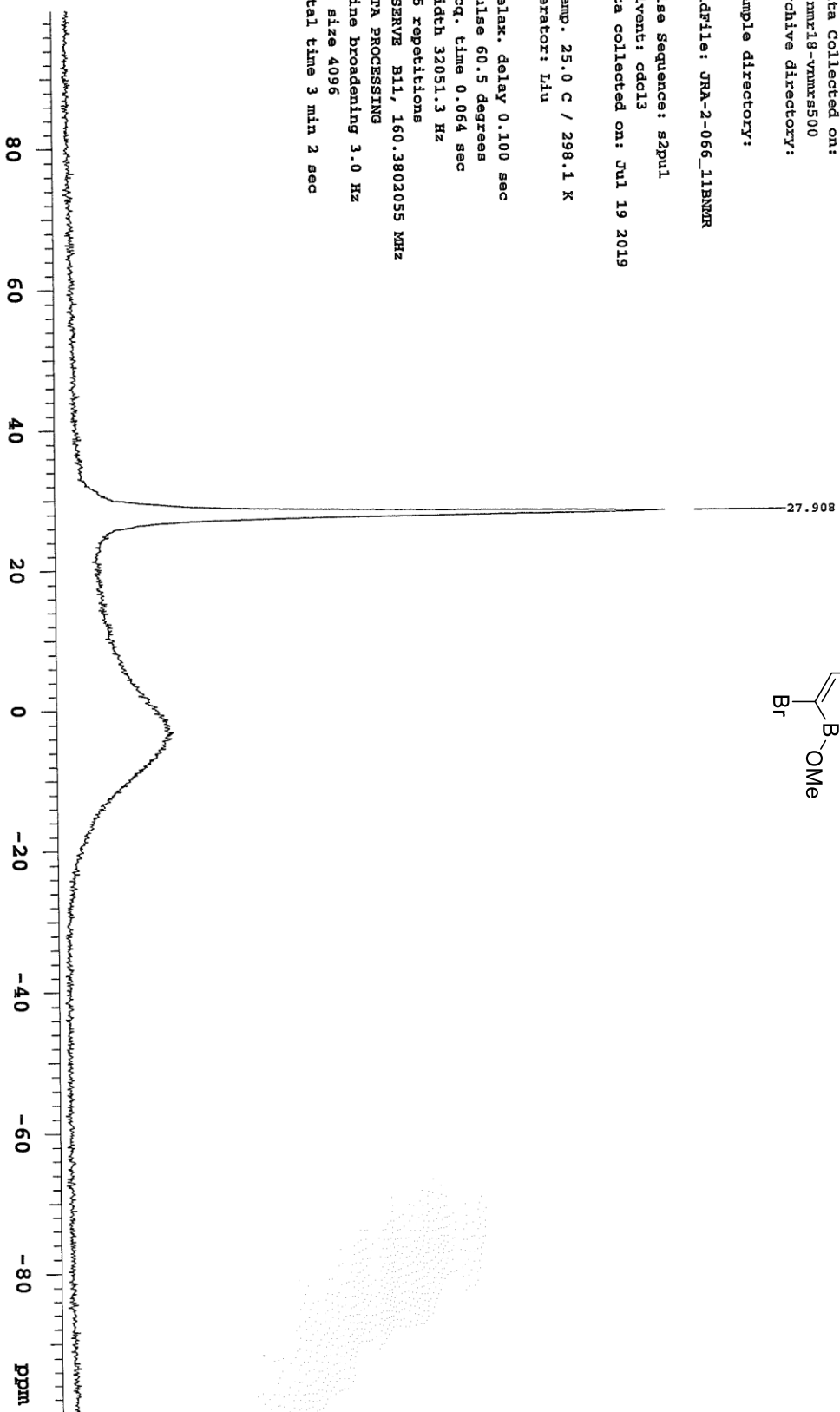
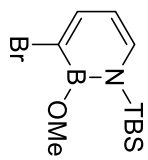
OBSERVE B11, 160.3802055 MHz

DATA PROCESSING

Line broadening 3.0 Hz

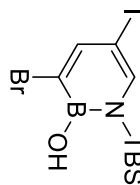
FT size 4096

Total time 3 min 2 sec



5-I-3-Br-N-TBS-B-OH-1,2-azaborine

Sample Name:
JRA-2-073_1HNMR
Data Collected on:
nmr18-vmr3500
Archive directory:



Sample directory:

Fidfile: JRA-2-073_1HNMR

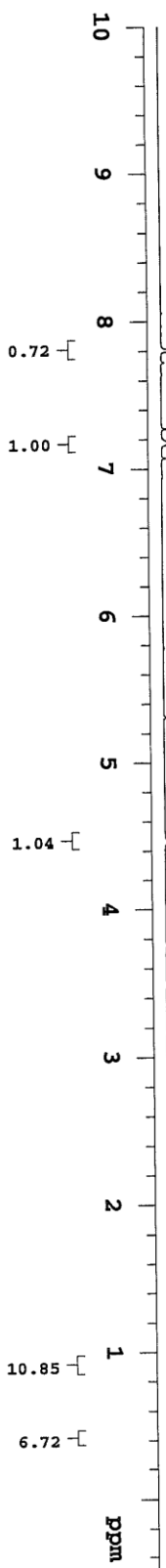
Pulse Sequence: PROTON (s2pul)

Solvent: cdcl3

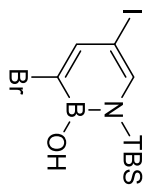
Data collected on: Aug 1 2019

Temp. 25.0 C / 298.1 K
Operator: Jlu

Relax. delay 15.000 sec
Pulse 45.0 degrees
Acq. time 2.045 sec
Width 8012.8 Hz
16 repetitions
OBSERVE H1, 499.8762752 MHz
DATA PROCESSING
F1 size 32768
Total time 4 min 33 sec



5-I-3-Br-N-TBS-B-OH-1,2-azaborine



Sample Name:
JRA-2-073_13CNMR
Data Collected on:
nmr18-vmmr5500
Archive directory:

Sample directory:

Fidfile: JRA-2-073_13CNMR

Pulse Sequence: CARBON (s2pul)
Solvent: cdcl3
Data collected on: Aug 1 2019

Temp. 25.0 C / 298.1 K
Operator: Iku

Relax. delay 1.000 sec
Pulse 45.0 degrees
Acq. time 1.049 sec
Width 31250.0 Hz
160 repetitions
OBSERVE C13, 125.6939894 MHz
DECOUPLE H1, 499.8787746 MHz
Power 43 dB
continuously on
WALTZ-16 modulated
DATA PROCESSING
Line broadening 0.5 Hz
Ft size 65536
Total time 34 min



5-I-3-Br-N-TBS-B-OH-1,2-azaborine

Sample Name:

JRA-2-073_11BNMR

Data Collected on:

mmr18-vnmrs500

Archive directory:

Sample directory:

FIDFile: JRA-2-073_11BNMR

Pulse Sequence: s2pul

Solvent: cdcl3

Data collected on: Aug 1 2019

Temp. 25.0 C / 298.1 K

Operator: Liu

Relax. delay 0.100 sec

Pulse 60.5 degrees

Acq. time 0.064 sec

Width 32051.3 Hz

793 repetitions

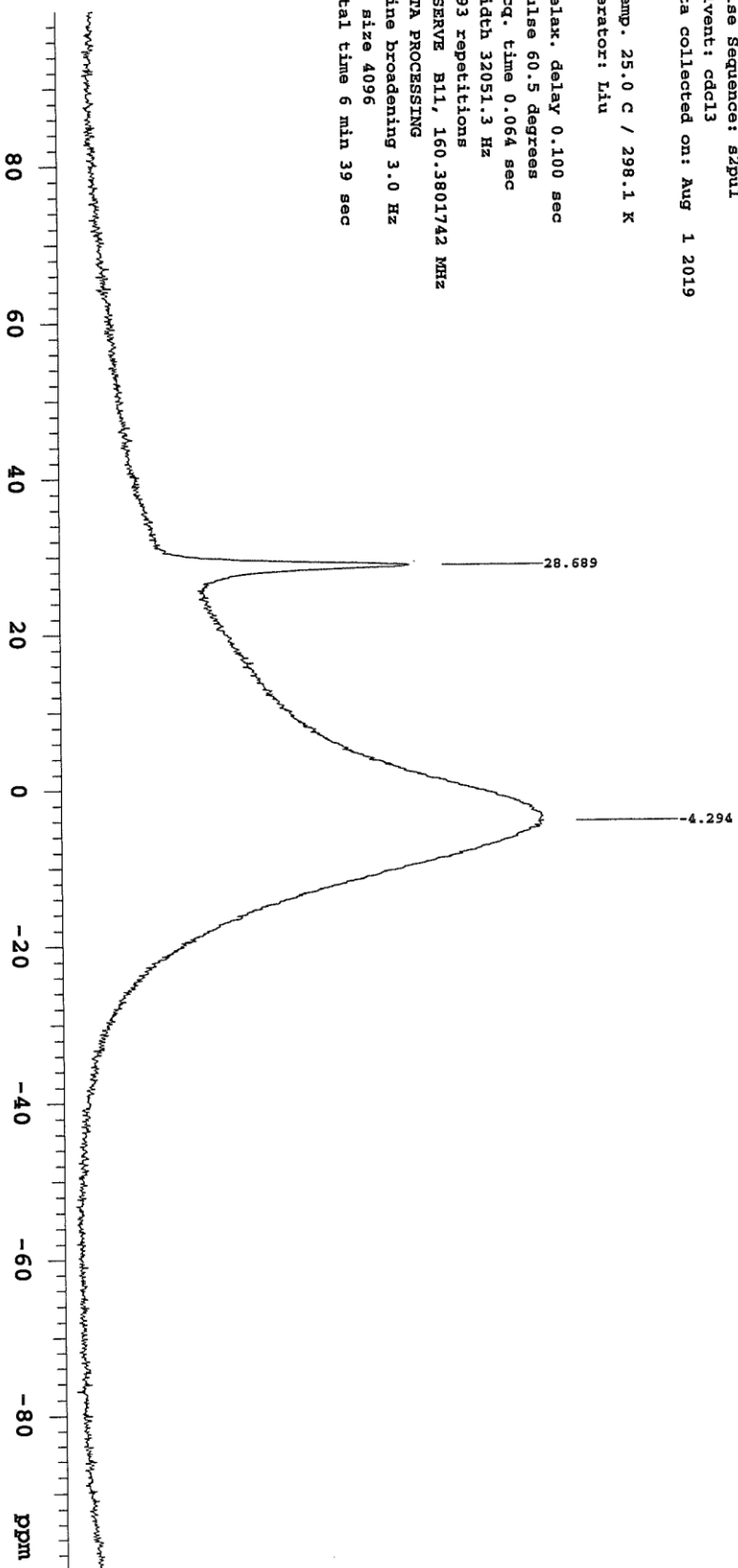
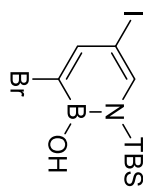
OBSERVE B11, 160.3801742 MHz

DATA PROCESSING

Line broadening 3.0 Hz

FT size 4096

Total time 6 min 39 sec



CHAPTER 2

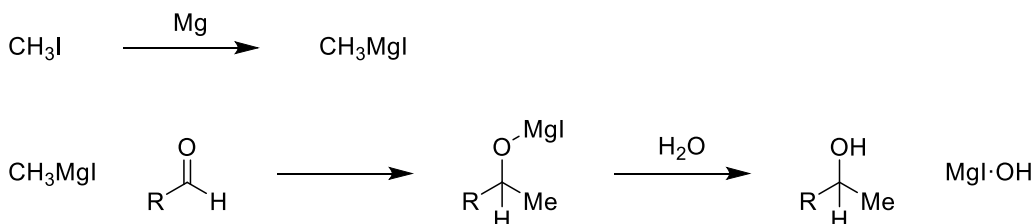
Development of a Functional Group Tolerant Grignard-Type Reaction for Addition to the B-Position of 1,2-Azaborines

2.1 Introduction: The Turbo Grignard Reagent

2.1.1 Limitations of the Traditional Grignard Reaction

What is now known as the Grignard reaction was first reported over 100 years ago by Victor Grignard. In the last year of the nineteenth century, Grignard reported the formation of secondary and tertiary alcohols by reacting alkyl magnesium halides with aldehydes and ketones (**Scheme 2.1**).¹ The importance of Grignard's reaction was quickly recognized, as he was awarded the Nobel Prize in Chemistry in 1912.² Grignard's reagent has since found a wide array of applications in organic and organometallic chemistry,³ and remains one of the most widely utilized organometallic reagents.²

Scheme 2.1 The Grignard Reaction as Originally Proposed by Victor Grignard¹



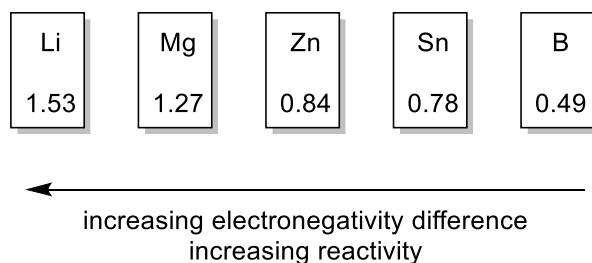
¹ (a) Grignard, V. Sur quelques nouvelles combinaisons organométalliques du magnésium et leur application à des synthèses d'alcools et d'hydrocarbures. *Compt. Rend.* **1900**, *130*, 1322–1325. (b) Rheinboldt, H. Fifty Years of the Grignard Reaction. *J. Chem. Ed.* **1950**, *27*, 476–488.

² Seyferth, D. The Grignard Reagents. *Organometallics* **2009**, *28*, 1598–1605.

³ For selected reviews on uses of Grignard reagents, see: (a) Mako, T. L.; Byers, J. A. Recent Advances in Iron-Catalyzed Cross-Coupling Reactions and Their Mechanistic Underpinning. *Inorg. Chem. Front.* **2016**, *3*, 766–790. (b) Knappke, C. E. I.; von Wangelin, A. J. 35 Years of Palladium-Catalyzed Cross-Coupling with Grignard Reagents: How Far Have We Come? *Chem. Soc. Rev.* **2011**, *40*, 4948–4962. (c) Harutyunyan, S. R.; den Hartog, T.; Geurts, K. Minnaard, A. J.; Feringa, B. L. Catalytic Asymmetric Conjugate Addition and Allylic Alkylation with Grignard Reagents. *Chem. Rev.* **2008**, *108*, 2824–2852. (d) Cherney, A. H.; Kadunce, N. T.; Reisman, S. E. Enantioselective and Enantiospecific Transition-Metal-Catalyzed Cross-Coupling Reactions of Organometallic Reagents to Construct C–C Bonds. *Chem. Rev.* **2015**, *115*, 9587–9652. (e) Sun, C.-L.; Shi, Z.-J. Transition-Metal-Free Coupling Reactions. *Chem. Rev.* **2014**, *114*, 9219–9280. (f) Jana, R.; Pathak, T. P.; Sigman, M. S. Advances in Transition Metal (Pd, Ni, Fe)-Catalyzed Cross-Coupling Reactions Using Alkyl-Organometallics as Reaction Partners. *Chem. Rev.* **2011**, *111*, 1417–1492.

The Grignard reaction allows for the formation of carbon–carbon bonds between the nucleophilic Grignard reagent and an electrophilic species. The Grignard reagent is formed when magnesium undergoes an oxidative insertion at a carbon–halogen bond. This resulting carbon–magnesium bond has partial positive charge on the magnesium and partial negative charge on the carbon, creating a nucleophilic carbon species. The strength of this nucleophilic species is dependent on the electronegativity difference between the carbon and the metal; increasingly polarized bonds result in more nucleophilic species (**Figure 2.1**).⁴

Figure 2.1 Difference in Electronegativity between Carbon and Various Metals Using the Allred-Rochow Electronegativity Scale.



For less electropositive metals, it is currently impossible to prepare organometallic compounds by direct reaction of the organic halide with the zero valent metal species.⁵ On the other hand, highly electropositive metals such as lithium form strong nucleophiles that are reactive towards most functional groups. A narrow selection of functional group tolerant organolithium compounds can be generated, but only at temperatures between -100 and -78 °C, limiting synthetic utility.⁶ Formation of classical

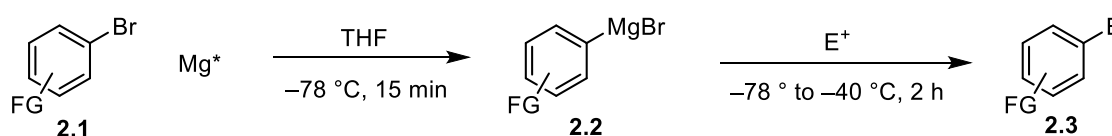
⁴ Boudieer, A.; Bromm, L. O.; Lotz, M.; Knochel, P. New Applications of Polyfunctional Organometallic Compounds in Organic Synthesis. *Angew. Chem. Int. Ed.* **2000**, *39*, 4414–4435.

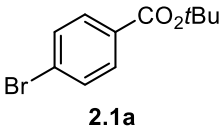
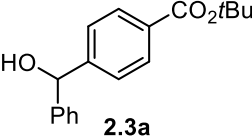
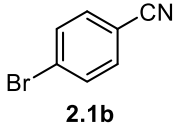
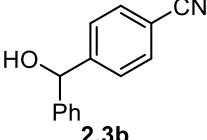
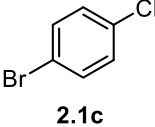
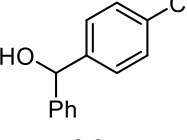
⁵ Rieke, R. D. Preparation of Organometallic Compounds from Highly Reactive Metal Powders. *Science* **1986**, *246*, 1260–1264.

⁶ (a) Parham, W. E.; Jones, L. D. Elaboration of Bromoarylnitriles. *J. Org. Chem.* **1976**, *41*, 1187–1191. (b) Parham, W. E.; Jones, L. D. Halogen–Metal Exchange in Haloaryl Acids. *J. Org. Chem.* **1976**, *41*, 2704–2706.

Grignard reagents will only tolerate a limited number of functional groups, and react readily with ketones, aldehydes, esters, nitriles, and epoxides.⁵ An effective strategy for developing more functional group tolerant Grignard reactions is to increase the reactivity of the metal towards organic substrates. This increased reactivity allows for more facile insertion into the C–X bond, which allows the reaction to occur at lower temperatures, safeguarding sensitive functional groups.

Table 2.1 Scope of Functional Group Tolerance for Grignard Reaction Using Activated Magnesium⁸



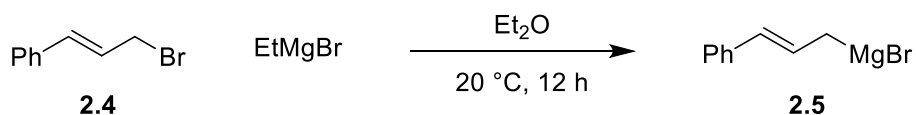
Substrate	Electrophile	Product	Yield (%)
 <p>2.1a</p>	 <p>PhCHO</p>	 <p>2.3a</p>	86
 <p>2.1b</p>	 <p>PhCHO</p>	 <p>2.3b</p>	65
 <p>2.1c</p>	 <p>PhCHO</p>	 <p>2.3c</p>	72

Rieke was able to generate highly reactive magnesium by reducing MgCl₂ or MgBr₂ in the presence of Li with naphthalene as an electron carrier. This activated magnesium could undergo oxidative insertion with bromobenzene at temperatures as low as -78 °C, and even could undergo oxidative insertion with fluorobenzene, which is the

most stable of the carbon–halogen bonds.^{5,7} While this more reactive magnesium was an improvement, it still required temperatures of $-78\text{ }^{\circ}\text{C}$ and could only tolerate a narrow selection of functional groups.⁸ For example, only bulky esters, nitriles, and chlorine groups were tolerated, and the reactions occurred at such low temperatures that only aldehydes could act as competent electrophiles (**Table 2.1**).

Another method for increasing functional group tolerance of Grignard reactions is using alkyl–magnesium bromide species to form Grignard reagents (**Scheme 2.2**) via magnesium-bromine exchange. Use of alkyl–magnesium reagents is particularly useful for forming $\text{C}(\text{sp}^2)\text{--Mg}$ bonds, as the thermodynamic stability of the product *vis-à-vis* the alkyl–magnesium reagent is the driving force behind generation of the Grignard reagent.

Scheme 2.2 Use of Alkyl–Magnesium Reagents as Originally Described by Prevost¹⁰



This strategy was first employed by Prévost in 1931 by generating an allylic Grignard reagent using ethyl magnesium bromide as a magnesium source.^{9,10} Additional work was performed in the 1970s on heavily fluorinated bromobenzenes,¹¹ and further studies determined that the rate of magnesium-bromine exchange was increased with

⁷ (a) Rieke, R. D.; Hudnall, P. M. Activated Metals. I. Preparation of Highly Reactive Magnesium Metal. *J. Am. Chem. Soc.* **1972**, *94*, 7178–7179. (b) Rieke, R. D.; Li, P. T.-J.; Burns, T. P.; Uhm, S. T. Preparation of Highly Reactive Metal Powders. New Procedure for the Preparation of Highly Reactive Zinc and Magnesium Metal Powders. *J. Org. Chem.* **1981**, *46*, 4323–4324. (c) Burns, T. P.; Rieke, R. D. Highly Reactive Magnesium and Its Application to Organic Syntheses. *J. Org. Chem.* **1987**, *52*, 3674–3680.

⁸ Lee, J.-S.; Velarde-Ortiz, R.; Guijarro, A.; Wurst, J. R.; Rieke, R. D. Low-Temperature Formation of Functionalized Grignard Reagents from Direct Oxidative Addition of Active Magnesium to Aryl Bromides. *J. Org. Chem.* **2000**, *65*, 5428–5430.

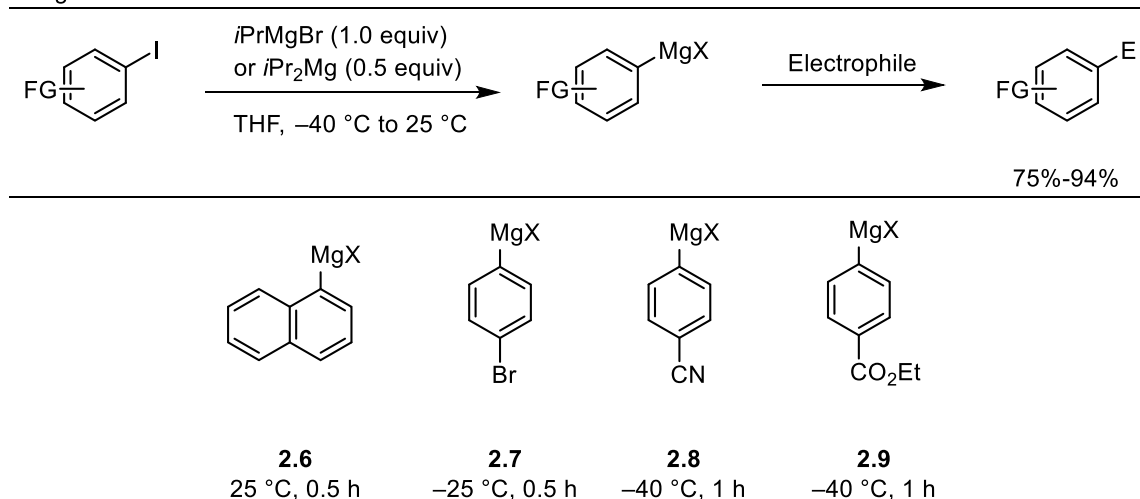
⁹ Prévost, C. The Action of Action of α -Ethyleneic Bromides on Organomagnesium Bromides-Collected Results. *Bull. Soc. Chim. Fr.* **1931**, *49*, 1372.

¹⁰ Knochel, P.; Dohle, W.; Gommermann, N.; Kneisel, F. F.; Kopp, F.; Korn, T.; Sapountzis, I.; Vu, V. A. Highly Functionalized Organomagnesium Reagents Prepared through Halogen–Metal Exchange.

¹¹ Tamborski, C.; Moore, G. J. Synthesis of Polyfluoroaromatic Magnesium Compounds through the Exchange Reaction. *J. Organometal. Chem.* **1971**, *26*, 153–156.

additional electron withdrawing groups present.¹² Even bromobenzenes with electron donating methoxy groups were found to undergo magnesium-halogen exchange with *i*PrMgCl, though this was likely due to the directing effect of oxygen adjacent to the labile C–Br bond.¹³ While magnesium-bromine exchange using *i*PrMgBr or related alkyl–magnesium species faced difficulties in activating C–Br bonds without additional electron withdrawing groups present, it was found to be effective in activating C–I bonds in the presence of sensitive functional groups or non-directing electron donating groups (Table 2.2).¹⁴ The weaker C–I bond allowed for a more facile magnesium-iodine exchange that could be carried out at reduced temperatures, leading to higher functional group tolerance.

Table 2.2 New Functional Group Tolerance Displayed by Mg-I Exchange Using Alkyl–Magnesium Reagents¹⁴



¹² Abarbri, M.; Dehmel, F.; Knochel, P. Bromine-Magnesium-exchange as a General Tool for the Preparation of Polyfunctional Aryl and Heteroaryl Magnesium-Reagents. *Tetrahedron Lett.* **1999**, *40*, 7449–7453.

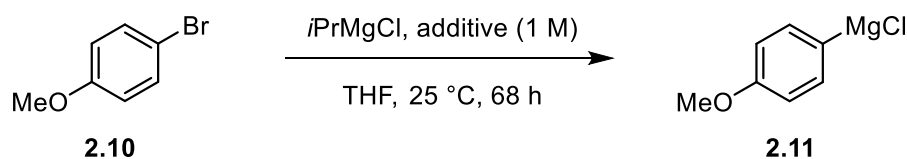
¹³ Nishiyama, H.; Isaka, K.; Itoh, K.; Ohno, K.; Nagase, H.; Matsumoto, K.; Yoshiwara, H. Metal–Halogen Exchange between Polybromoanisoles and Aliphatic Grignard Reagents: A Synthesis of Cyclopenta[*b*]benzofurans. *J. Org. Chem.* **1992**, *57*, 407–410.

¹⁴ (a) Rottländer, M.; et al. New Polyfunctional Magnesium Reagents for Organic Synthesis. *Chem. Eur. J.* **2000**, *6*, 767–770. (b) Boymond, L.; Rottländer, M.; Cahiez, G.; Knochel, P. Preparation of Highly Functionalized Reagents by an Iodine–Magnesium Exchange Reaction and its Application in Solid-Phase Synthesis. *Angew. Chem. Int. Ed.* **1998**, *37*, 1701–1703.

2.1.2 Use of *i*PrMgCl·LiCl to Achieve Broad Functional Group Tolerance

Despite advances of alkyl–magnesium reagents, methods for forming functional group tolerant Grignard reagents still excluded many sensitive moieties and there is still difficulty in activating C–Br bonds, especially in the presence of sensitive chemical groups.¹⁵ In 2004, Knochel discovered that by adding LiCl salt to a solution of *i*PrMgCl, more challenging magnesium-bromine exchanges could be achieved (**Table 2.3**). Thus, the turbo Grignard reagent, *i*PrMgCl·LiCl, was discovered as a powerful tool for creating polyfunctionalized Grignard reagents.¹⁶

Table 2.3 Addition of LiCl Allows for Magnesium-Bromine Exchange of Unactivated C–Br Bonds¹⁶



Additive	Conversion (%)
none	18
LiBF ₄	5
LiBr	40
LiI	38
LiClO ₄	38
LiCl	70

Knochel's method allowed him to access a wealth of new Grignard reagents that were previously inaccessible through simpler alkyl–magnesium reagents (**Table 2.4**). Use of *i*PrMgCl·LiCl resulted in higher yields than traditional *i*PrMgCl or *i*Pr₂Mg reagents at room temperature, suggesting more facile insertion between the C–Br bond.¹⁶ The power of the turbo Grignard reaction is due to the presence of the Lewis acidic lithium. The

¹⁵ Ziegler, D. S.; Wei, B.; Knochel, P. Improving the Halogen–Magnesium Exchange by Using New TurboGrignard Reagents. *Chem. Eur. J.* **2018**, *25*, 2695–2703.

¹⁶ Krasovskiy, A.; Knochel, P. A LiCl-Mediated Br/Mg Exchange Reaction for the Preparation of Functionalized Aryl- and Heteroarylmagnesium Compounds from Organic Bromides. *Angew. Chem. Int. Ed.* **2004**, *43*, 3333–3336.

lithium gives more magnesiate character to the Grignard reagent, resulting in species with the distinct charge distribution of $[\text{Li}]^+[\text{RMgCl}_2]^-$. In this way, lithium “activates” $i\text{PrMgCl}$ and increases the nucleophilic character of the isopropyl group, leading to quicker exchange with carbon–halogen bonds. Additionally, the LiCl salt likely breaks up polymeric aggregates of $i\text{PrMgCl}$ in solution, improving solubility.^{17,18}

Table 2.4 Substrate Scope of Knochel's Initial Study of $i\text{PrMgCl}\cdot\text{LiCl}$ Mediated Grignard Reactions¹⁶

Grignard reagent ^[a]	Electrophile	Yield	Grignard reagent ^[a]	Electrophile	Yield
	PhCHO	70		CIPPh ₂	85
	PhCHO	87 ^[b]		PhCHO	83
	PhCOCl	81		PhCHO	90
	allyl bromide	93 ^[b]		allyl bromide	88 ^[b]

[a] Y = Cl·LiCl. [b] The Grignard reagent as transmetalated with $\text{CuCN}\cdot 2\text{LiCl}$ before reaction with an electrophile.

In addition to the nitrile and bulky esters tolerated in Knochel's original work, a number of other sensitive functional groups have been shown to survive magnesium–

¹⁷Blasberg, F.; Bolte, M.; Wagner, M.; Lerner, H.-W. An Approach to Pin Down the Solid-State Structure of the “Turbo Grignard”. *Organometallics* **2012**, *31*, 1001–1005.

¹⁸Bao, R. L.-Y.; Zhao, R.; Shi, L. Progress and Developments in the Turbo Grignard Reagent $i\text{-PrMgCl}\cdot\text{LiCl}$: A Ten-Year Journey. *Chem. Comm.* **2015**, *51*, 6884–6900.

halogen exchange with the turbo Grignard reagent (**Scheme 2.3**). The year following Knochel's initial paper, he published two reports expanding the functional group tolerance of his reagent. In the first report, Knochel showed that he could form Grignard reagents in the presence of both a triazine moiety and a simple ester, in this case an ethyl ester.¹⁹ While bulky esters such as *tert*-butyl ester were tolerated by reagents such as *i*PrMgCl, simpler esters had presented more of a challenge. In the second report, Knochel showed that a Grignard reagent could be formed in the presence of an electrophilic boronic pinacol ester.²⁰

Additional work five years later demonstrated the utility of the method in the presence of phosphate esters. While most other examples of its application to that point had been in aryl systems, this magnesium-halogen exchange was shown to occur with a vinyl C–I bond.²¹ In 2009, Zhang showed that the formation of a Grignard using the turbo Grignard reagent could occur both in pyridine *N*-oxides as well as in the presence of substituted amides.²² While these are just a few representations of functional group tolerance, many more examples exist demonstrating the broad utility of the turbo Grignard reagent in forming new carbon–carbon bonds in the presence of sensitive electrophilic moieties.²³

¹⁹ Liu, C.-Y.; Knochel, P. Preparation of Polyfunctional Arylmagnesium Reagents Bearing a Triazine Moiety. A New Carbazole Synthesis. *Org. Lett.* **2005**, *7*, 2543–2546.

²⁰ Baron, O.; Knochel, P. Preparation and Selective Reaction of Mixed Bimetallic Aromatic and Heteroaromatic Boron–Magnesium Reagents. *Angew. Chem. Int. Ed.* **2005**, *44*, 3133–3135.

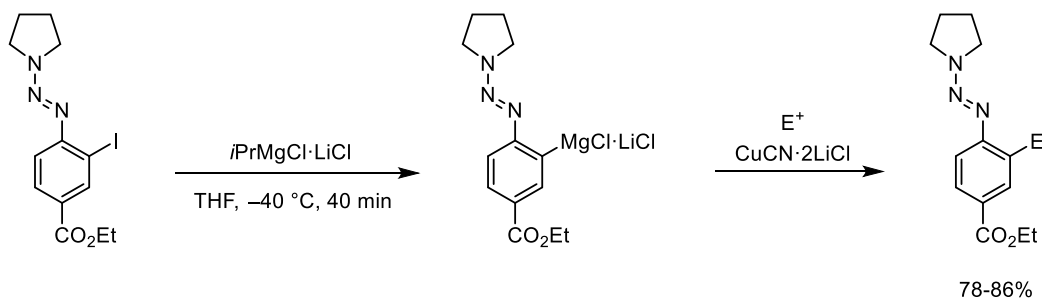
²¹ Piller, F. M.; Bresser, T.; Fischer, M. K. R.; Knochel, P. Preparation of Functionalized Cyclic Enol Phosphates by Halogen-Magnesium Exchange and Directed Deprotonation Reactions. *J. Org. Chem.* **2010**, *75*, 4365–4375.

²² Duan, X.-F.; Ma, Z.-Q.; Zhang, F.; Zhang, Z.-B. Magnesiumation of Pyridine *N*-Oxides via Iodine or Bromine-Magnesium Exchange: A Useful Tool for Functionalizing Pyridine *N*-Oxides. *J. Org. Chem.* **2009**, *74*, 939–942.

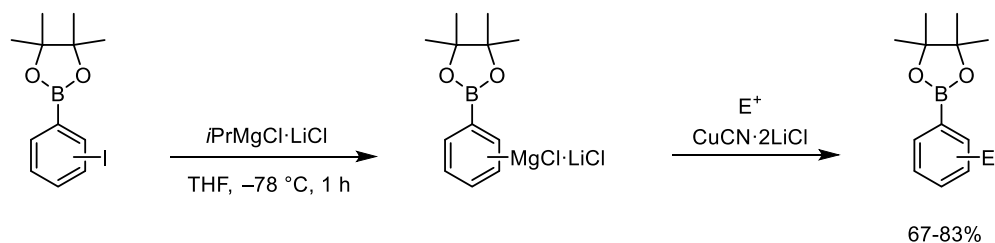
²³ For further examples, see: (a) Ren, H.; Knochel, P. Regioselective Functionalization of Trisubstituted Pyridines Using a Bromine–Magnesium Exchange. *Chem. Commun.* **2006**, 726–728. (b) Frischmuth, A.; Unsinn, A.; Groll, K.; Stadtmüller, H.; Knochel, P. Preparations and Reactions of SF₅-Substituted Aryl and Heteroaryl Derivatives via Mg and Zn Organometallics. *Chem. Eur. J.* **2012**, *18*, 10234–10238. (c) Kopp,

Scheme 2.3 Selected Examples of the Functional Group Tolerance of the Turbo Grignard Reagent

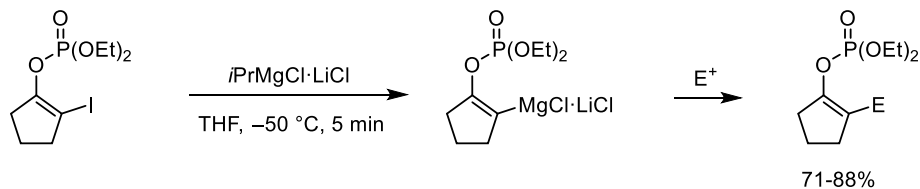
Knochel (2005)¹⁹



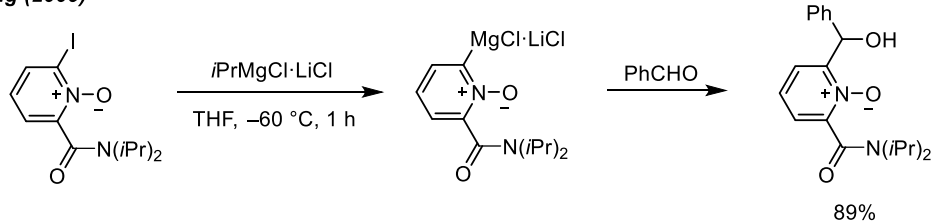
Knochel (2005)²⁰



Knochel (2010)²¹



Zhang (2009)²²



Because the turbo Grignard reagent is so reactive, it can undergo magnesium-halogen exchange at temperatures as low as $-78\text{ }^\circ\text{C}$. This flexibility in temperature allows for the tuning of reactivity of the eventual Grignard reagent. Many functional groups that

F.; Krasovskiy, A.; Knochel, P. Convenient Magnesiumation of Aromatic and Heterocyclic Rings Bearing a Hydroxy Group in Presence of LiCl. *Chem. Commun.* **2004**, 2288–2289. (d) Kopp, F.; Wunderlich, S.; Knochel, P. Halogen–Magnesium Exchange on Unprotected Aromatic and Heteroaromatic Carboxylic Acids. *Chem. Commun.* **2007**, 2075–2077. (e) Kopp, F.; Knochel, P. Functionalization of Unprotected Uracil Derivatives Using the Halogen-Magnesium Exchange. *Org. Lett.* **2007**, *9*, 1639–1641. (f) Kopp, F.; Knochel, P. Iodine-Magnesium Exchange on Unprotected Imidazoles in the Presence of LiCl. *Synlett* **2007**, 980–982.

are not reactive with the turbo Grignard reagent at lower temperatures can act as effective electrophiles at higher temperatures. For example, substituted amides are non-reactive during Grignard formation at $-60\text{ }^{\circ}\text{C}$, they can serve as electrophiles at higher temperatures.²⁴ Though nitrile groups are well tolerated, a number of methods have been developed to install them using the turbo Grignard as well.^{24,25}

Like traditional Grignard reagents, use of the turbo Grignard is a reliable way of forming carbon–carbon bonds. Of particular interest, however, is the use of the turbo Grignard to attack non-carbon electrophiles to form carbon–heteroatom bonds. While boronic esters are tolerated as functional groups, they can also be formed by using borate esters as electrophiles in the presence of the turbo Grignard reagent (**Scheme 2.4**). Both boronic esters²⁶ and boronic acids²⁷ can be generated following nucleophilic attack by the generated Grignard and the cleavage of a B–OR bond. In addition, a wide variety of electrophiles can be used to form carbon–nitrogen bonds,²⁸ carbon–sulfur bonds,²⁹ carbon–phosphorus bonds,²¹ carbon–tin bonds,²² and carbon–halogen bonds.³⁰

²⁴ Liu, C.-Y.; Ren, H.; Knochel, P. Magnesiated Unsaturated Silylated Cyanohydrins as Synthetic Equivalents of Aromatic and Heterocyclic Grignard Reagents Bearing a Ketone or and Aldehyde. *Org. Lett.* **2006**, *8*, 617–619.

²⁵ Anbarasan, P.; Neumann, H.; Beller, M. A Novel and Convenient Synthesis of Benzonitriles: Electrophilic Cyanation of Aryl and Heteroaryl Bromides. *Chem. Eur. J.* **2011**, *17*, 4217–4222.

²⁶ Leermann, T.; Leroux, F. R.; Colobert, F. Highly Efficient One-Pot Access to Functionalized Arylboronic Acid via Noncryogenic Bromine/Magnesium Exchange. *Org. Lett.* **2011**, *13*, 4479–4481.

²⁷ Demory, E.; Blandin, V.; Einhorn, J.; Chavant, P. Y. Noncryogenic Preparation of Functionalized Arylboronic Esters through a Magnesium–Iodine Exchange with in Situ Quench. *Org. Process Res. Dev.* **2011**, *15*, 710–716.

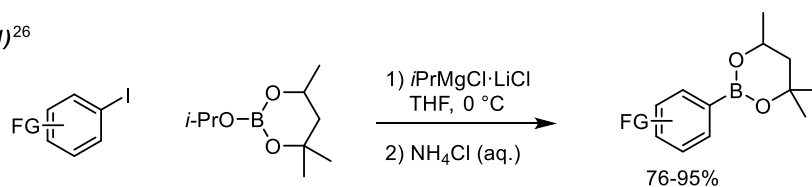
²⁸ (a) Sinha, P.; Knochel, P. Preparation of Polyfunctional Tertiary Amines via the Electrophilic Amination of Arylmagnesium Compounds Using *N*-Chloroamines. *Synlett* **2006**, 3304–3308. (b) Frischmuth, A.; Unsinn, A.; Groll, K.; Stadtmüller, H.; Knochel, P. Preparations and Reactions of SF₅-Substituted Aryl and Heteroaryl Derivatives via Mg and Zn Organometallics. *Chem. Eur. J.* **2012**, *18*, 10234–10238.

²⁹ (a) Krasovskiy, A.; Gavryushin, A.; Knochel, P. A General Thiolation of Magnesium Organometallics Using Tetramethylthiuram Disulfide. *Synlett* **2005**, 2691–2693. (b) Reeves, J. T.; Camara, K.; Han, Z. S.; Xu, Y.; Lee, H.; Busacca, C. A.; Senanayake, C. H. The Reaction of Grignards Reagents with Bunte Salts: A Thiol-Free Synthesis of Sulfides. *Org. Lett.* **2014**, *16*, 1196–1199.

³⁰ (a) Despotopoulou, C.; Bauer, R. C.; Krasovskiy, A.; Mayer, P.; Stryker, J. M.; Knochel, P. Selective Mono- and 1,2-Difunctionalization of Cyclopentene Derivatives via Mg and Cu Intermediates. *Chem. Eur.*

Scheme 2.4 Boron Electrophiles as Substrates in the Turbo Grignard Reaction.

Colobert (2011)²⁶



Chavant (2011)²⁷



In summary, the Grignard reagent has emerged as a versatile strategy for not only forming new carbon–carbon bonds, but also forming carbon–heteroatom bonds. The molecular structure of *i*PrMgCl·LiCl allows for more facile magnesium-halogen exchange. This increase in reactivity allows the reaction to take place at lower temperatures, which allows for more reliable tuning of the reactivity of the resultant Grignard species. By modulating reaction temperatures, magnesium-halogen exchange can be achieved in the presence of a wide array of sensitive functional groups. By increasing the temperature, those same functional groups can act as electrophiles in the resulting Grignard reaction.

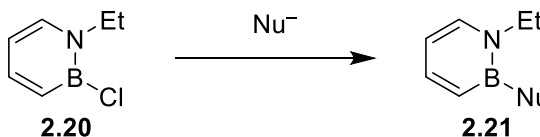
J. **2008**, *14*, 2499–2506. (b) Anbarasan, P.; Neumann, H.; Beller, M. Efficient Synthesis of Aryl Fluorides. *Angew. Chem. Int. Ed.* **2010**, *49*, 2219–2222.

2.2 Late Stage Functionalization of 1,2-Azaborines at the B-Position

2.2.1 Nucleophilic Addition to the B-Position

The B-position is unique amongst positions on the ring of 1,2-azaborine because of boron's formally vacant *p*-orbital. This empty orbital causes the boron at this position to be susceptible to nucleophilic attack, allowing for a method of substitution that is completely orthogonal to functionalization at every other position of the 1,2-azaborine ring.³¹ Nucleophilic addition to the B-position has been demonstrated with several B–X groups present. In 2007, Liu demonstrated that a number of different carbon, oxygen, nitrogen, sulfur, and hydride nucleophiles could add to 1,2-azaborine **2.20** in good to great yields (**Table 2.5**). In addition to these nucleophiles, it was also shown that oxygen nucleophiles could be generated *in situ* in the presence of a base (**Scheme 2.5**).³²

Table 2.5 Nucleophilic Attack on B–Cl Bond of 1,2-Azaborines³²

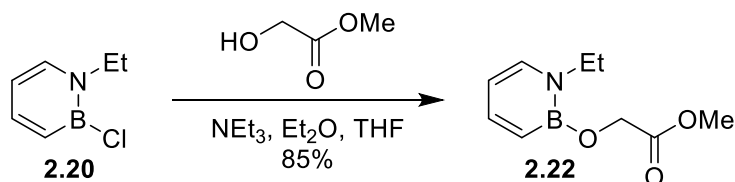


Nucleophile (Nu)	Product	Yield (%)
Li–Bu	2.21a	79
Li–vinyl	2.21b	50
BrMg–Ph	2.21c	76
BrMg–≡–Ph	2.21d	83
Li–NMe ₂	2.21e	66
Li–SBn	2.21f	80
Li–OtBu	2.21g	71
LiBEt ₃ –H	2.21h	92

³¹ McConnell C. R.; Liu, S.-Y. Late-Stage Functionalization of BN-Heterocycles. *Chem. Soc. Rev.* **2019**, *48*, 3436–3453.

³² Marwitz, A. J. V.; Abbey, E. R.; Jenkins, J. T.; Zakharov, L. N.; Liu, S.-Y. Diversity through Isosterism: The Case of Boron-Substituted 1,2-Dihydro-1,2-azaborines. *Org. Lett.* **2007**, *9*, 4095–4908.

Scheme 2.5 Nucleophilic Attack by *in situ* Generated Nucleophile³²



In addition to the *B*-Cl-1,2-azaborine, 1,2-dihydro-1,2-azaborine also served as a competent substrate for nucleophilic addition.³³ It was found that the protic N–H bond was attacked by the nucleophilic/basic partner in the reaction. A second equivalent of nucleophile was necessary to first deprotonate the N–H, which could then be regenerated with subsequent addition of a proton source (**Table 2.6**).

Table 2.6 Nucleophilic Attack on B–H Bond of 1,2-Azaborines³³

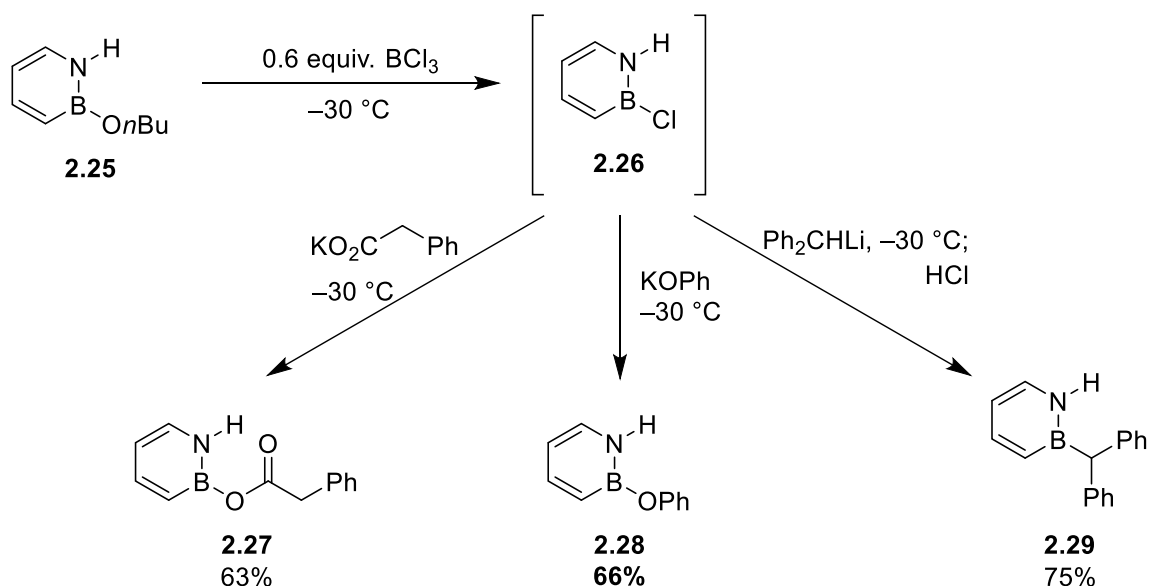
M–Nu	E–X	Product	Yield (%)
Na– <i>o</i> tBu	H–Cl	2.24a	63
K–Oallyl	H–Cl	2.24b	79
Li– <i>t</i> Bu	H–Cl	2.24c	81
Li– <i>n</i> Bu	H–Cl	2.24d	80
Li–Ph	H–Cl	2.24e	98
BrMg–vinyl	H–Cl	2.24f	59
BrMg–≡–Ph	H–Cl	2.24g	71
Li– <i>n</i> Bu	TMS–Cl	2.24h	89
Li– <i>n</i> Bu	Me–I	2.24i	67
Li– <i>n</i> Bu	Bn–Br	2.24j	60

Similar attempts to perform a nucleophilic attack on **2.25** were relatively more challenging. While it was possible to replace the B–OR bond with strong nucleophiles

³³ Lamm, A. N.; Garner III, E. B.; Dixon, D. A.; Liu, S.-Y. Nucleophilic Aromatic Substitution of 1,2-Dihydro-1,2-Azaborines. *Angew. Chem. Int. Ed.* **2011**, *50*, 8157–8160.

such as simple organolithiates or Grignard reagents, weaker nucleophiles were unable to add to the B-position. However, B–Cl could be regenerated *in situ* from B–OR bonds in the presence of BCl₃. Intermediate **2.26** could then undergo a subsequent nucleophilic addition to form products **2.27-2.29**.³⁴ In summary, B–Cl, B–H, and B–OR bonds have all proven suitable substrates for nucleophilic addition.

Scheme 2.6 Nucleophilic Addition to B–OR Substituted 1,2-Azaborines *via* a B–Cl Intermediate



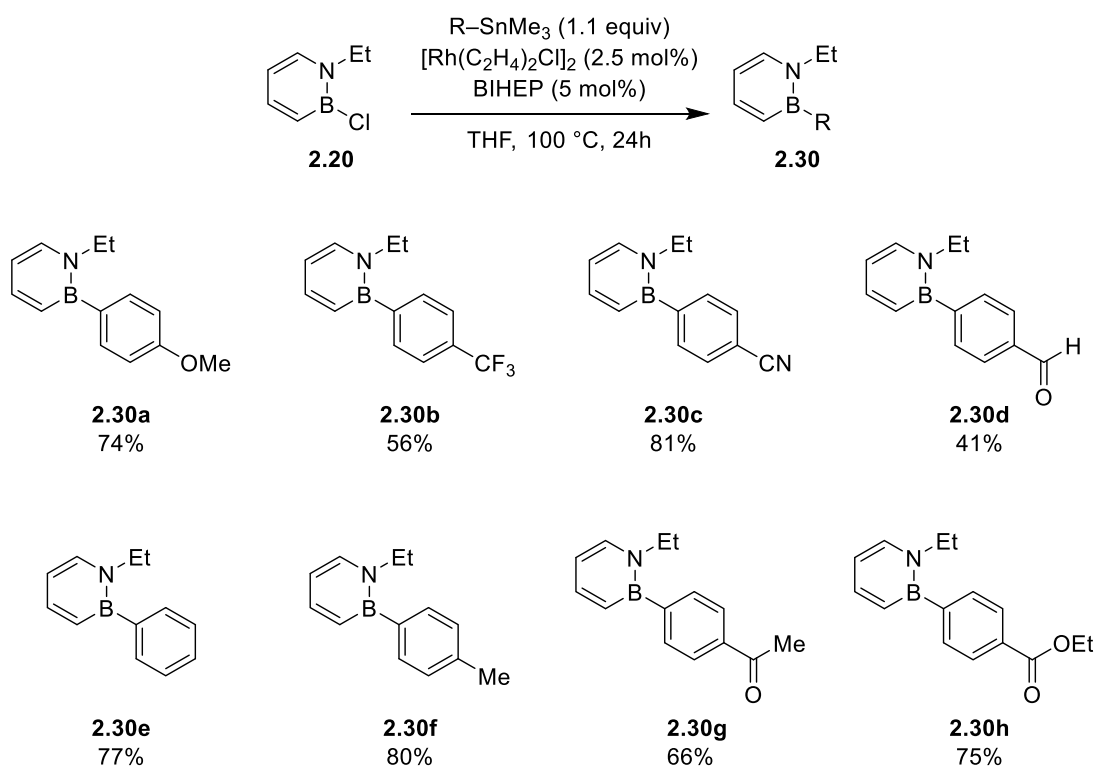
2.2.2 Non-Nucleophilic Activation of the B–R and B–X Bond

While nucleophilic addition to the B-position is a reliable method for adding chemical diversity to the core of 1,2-azaborines, other metal mediated methods can be used to either add sensitive functionality or break more stable B–C bonds. In 2013, a rhodium-catalyzed arylation of B–Cl substituted 1,2-azaborines was reported by the Liu

³⁴ Abbey, E. R.; Lamm, A. N.; Baggett, A. W.; Zakharov, L. N.; Liu, S.-Y. Protecting Group-Free Synthesis of 1,2-Azaborines: A Simple Approach to the Construction of BN-Benzenoids. *J. Am. Chem. Soc.* **2013**, *135*, 12908–12913.

group.³⁵ This cross-coupling takes place *via* sequential transmetalations with the azaborine and an arylstannane. Mechanistic studies suggest that the arylstannane first transfers its arene from the tin to the rhodium, followed by transfer of the aryl group to the 1,2-azaborine. A number of functional groups, such as esters, nitriles, and aldehydes, which are generally too sensitive to be tolerated by nucleophilic Grignard reagents or organolithiates can be coupled to 1,2-azaborines using this method (**Scheme 2.7**).

Scheme 2.7 Selected Products of Rh-Catalyzed Arylation of B–Cl Substituted 1,2-Azaborine³⁵



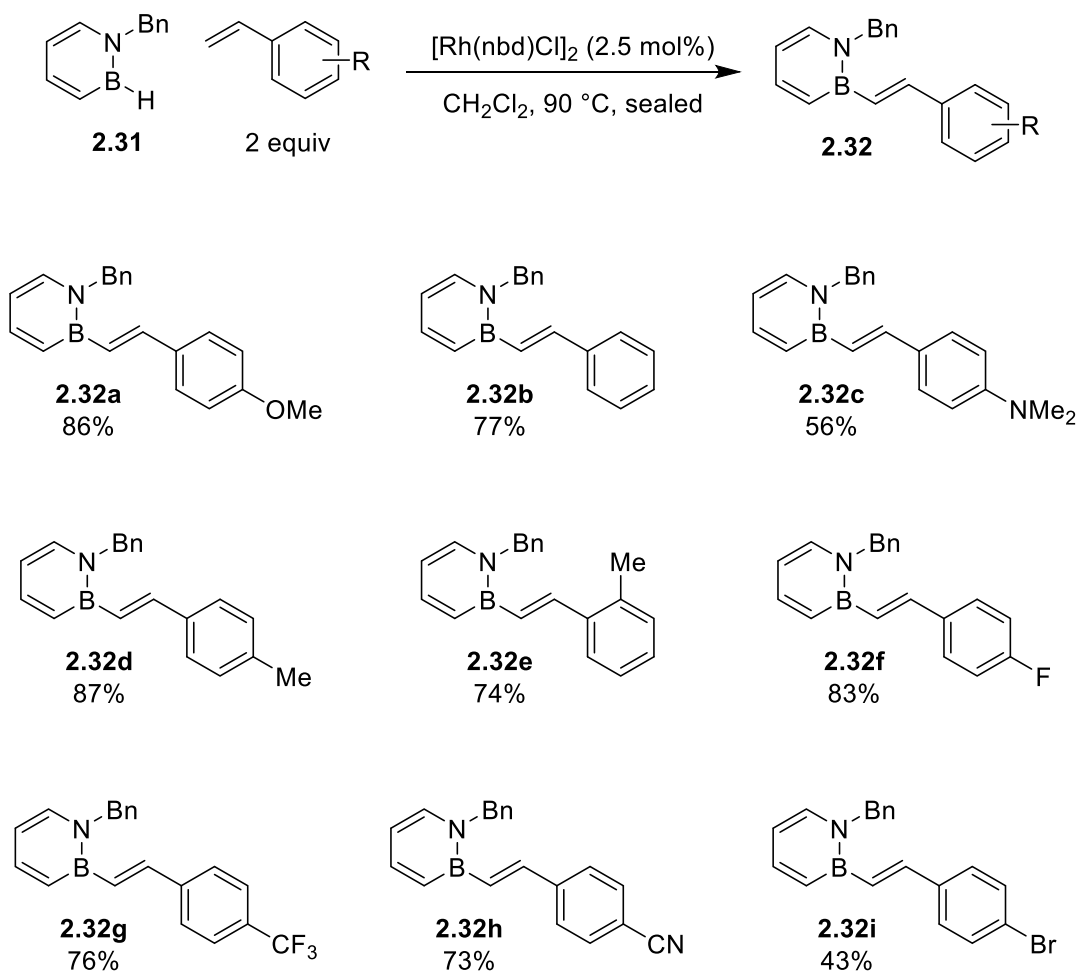
In addition to B–Cl activation, B–H activation was also demonstrated in a separate rhodium-catalyzed synthesis of BN isosteres of stilbene.³⁶ A potential

³⁵ Rudebusch, G. E.; Zakharov, L. N.; Liu, S.-Y. Rhodium-Catalyzed Boron Arylation of 1,2-Azaborines. *Angew. Chem. Int. Ed.* **2013**, *52*, 9316–9319.

³⁶ Brown, A. N.; Zakharov, L. N.; Mikulas, T.; Dixon, D. A.; Liu, S.-Y. Rhodium-Catalyzed B–H Activation of 1,2-Azaborines: Synthesis and Characterization of BN Isosteres of Stilbenes. *Org. Lett.* **2014**, *16*, 3340–3343.

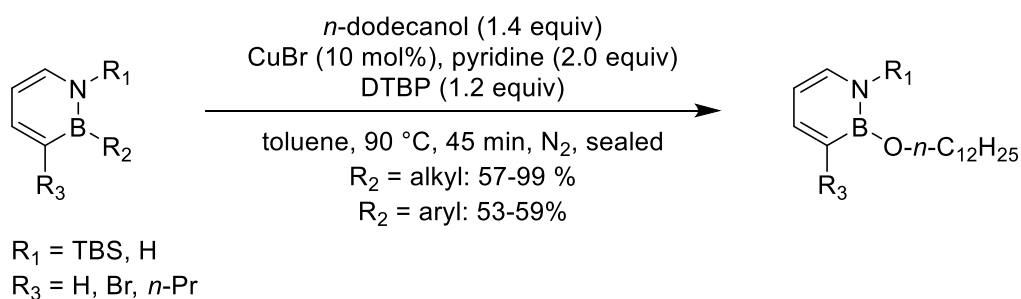
mechanism included oxidative addition of the B–H bond to the rhodium catalyst followed by a β -migratory insertion of the styrene coupling partner. Subsequent β -hydride elimination would yield the BN stilbene product and a rhodium dihydride complex. This rhodium dihydride complex can hydrogenate a second styrene coupling partner to regenerate the active catalyst, consistent with the need for two equivalents of styrene. This method was used to synthesize a number of different BN-stilbene analogues (Scheme 2.8).

Scheme 2.8 Rh-Catalyzed B–H Activation of 1,2-Azaborines³⁶



While it has been shown that B–H, B–Cl, and B–OR bonds are readily modifiable, B–C bonds, in particular aryl groups, are far more robust,³¹ and their removal is not trivial. A recent report from the Liu group details a copper-mediated oxidation of alkyl and aryl B–C bonds.³⁷ An alkoxy group first adds to the B-position in the presence of a stoichiometric oxidant, forming a tetracoordinate boron species. Either a Cu(I) or Cu(II) compound then promotes homolytic cleavage of the B–C bond, regenerating a tricoordinate boron species. This yields a B–OR substituted 1,2-azaborine, which is easily modifiable by methods previously described. Alkyl substituted 1,2-azaborines proceeded with good to great yields, while aryl substituted 1,2-azaborines proceeded with modest yields (**Scheme 2.9**).

Scheme 2.9 Copper Catalyzed Oxidation of B–C Bonds of 1,2-Azaborines³⁷



³⁷ Bagget, A. W.; Liu, S.-Y. A Boron Protecting Group Strategy for 1,2-Azaborines. *J. Am. Chem. Soc.* **2017**, *139*, 15259–15264.

2.3 Development of a Functional Group Tolerant B–Aryl Nucleophilic Substitution Method

2.3.1 Biaryl Molecules as a Privileged Class in Medicinal Chemistry

A privileged structure in medicinal chemistry is defined as “a single molecular framework able to provide ligands for diverse receptors.”³⁸ Biaryl compounds are one example of a privileged motif, as they have been shown to bind to a wide range of protein receptors across a number of different therapeutic areas.³⁹ Because of the privileged status of biaryl compounds, and as 1,2-azaborine is an isostere of benzene, we believe biaryl compounds are an attractive synthetic target for exploring the biological effects of BN-CC isosterism. Additionally, aryl substitution at the B-position affords enhanced oxidative stability to 1,2-azaborines.

As previously discussed, we have developed two general methods of adding arenes at the 2-position: nucleophilic addition or a rhodium-catalyzed boron arylation. These methods both have shortcomings that limit their usefulness in preparing drug like molecules. In the case of Grignard and lithiate reactions, we are unable to add sensitive electrophilic moieties such as carbonyl or nitrile containing arenes to 1,2-azaborine. While the rhodium-catalyzed method can tolerate these groups, it requires stoichiometric amounts of toxic organotin reagents. To increase the scope of sensitive aryl functional groups that can be added to the B-position of 1,2-azaborine while obviating the need for toxic heavy metal reagents, a LiCl mediated Grignard-type reaction developed by Knochel¹⁶ has been adapted to use with *N*-TBS-*B*-Cl-1,2-azaborines.

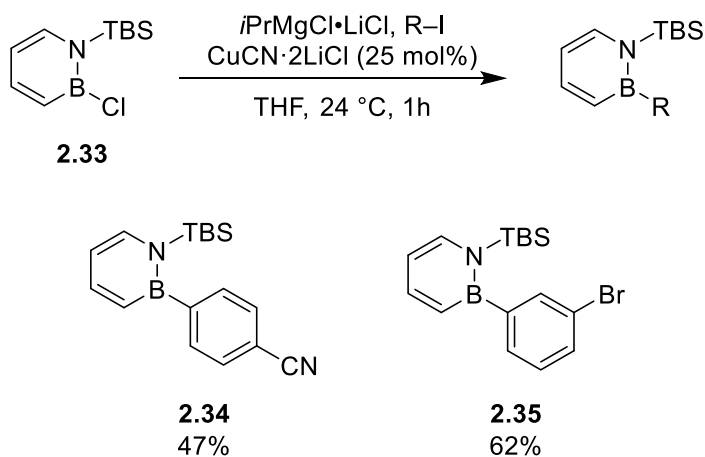
³⁸ Horton, D. A.; Bourne, G. T.; Smythe, M. L. The Combinatorial Synthesis of Bicyclic Privileged Structures or Privileged Substructures. *Chem. Rev.* **2003**, *103*, 893–930

³⁹ Hajduk, P. J.; Bures, M.; Praestgaard, J.; Fesik, S. W. Privileged Molecules for Protein Binding Identified from NMR-Based Screening. *J. Med. Chem.* **2000**, *43*, 3443–3447.

2.3.2 Adapting the Turbo Grignard Reaction to 1,2-Azaborines

The procedure for the turbo Grignard reaction was adapted directly from Knochel's 2004 report¹⁶ and was used with the commercially available *N*-TBS-*B*-Cl-1,2-azaborine (**2.33**). The two initial addition partners chosen were *para*-iodo-benzonitrile and *meta*-iodo-bromobenzene, both of which were effective in moderate yields (**Scheme 2.10**). The reaction was also attempted without the presence of the copper catalyst, though no desired product was observed.

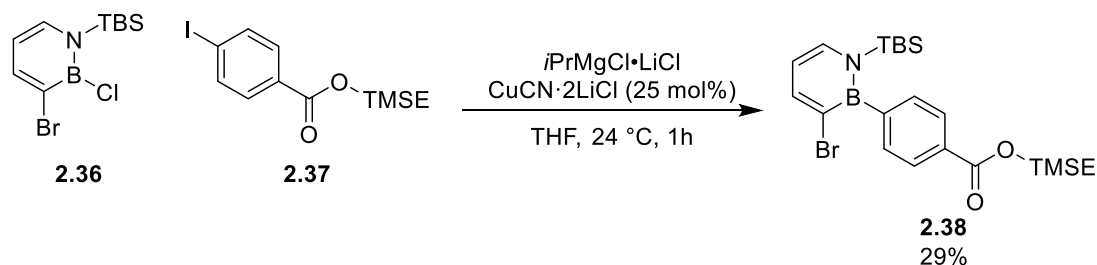
Scheme 2.10 Turbo Grignard Reaction with *N*-TBS-*B*-Cl-1,2-azaborine



These reaction conditions were then attempted with a halogenated 1,2-azaborine (**2.36**) and an ester bearing aryl addition partner (**2.37**). This protected phenyl ester has been used as a synthetic precursor to a number of BN isosteres of biologically active molecules.⁴⁰ Previously, however, this group had to be installed using the rhodium-catalyzed cross coupling method that required stoichiometric amounts of organotin reagents. We have demonstrated that this same functionality can be installed onto the azaborine core using the turbo Grignard reaction in comparable yields (**Scheme 2.11**).

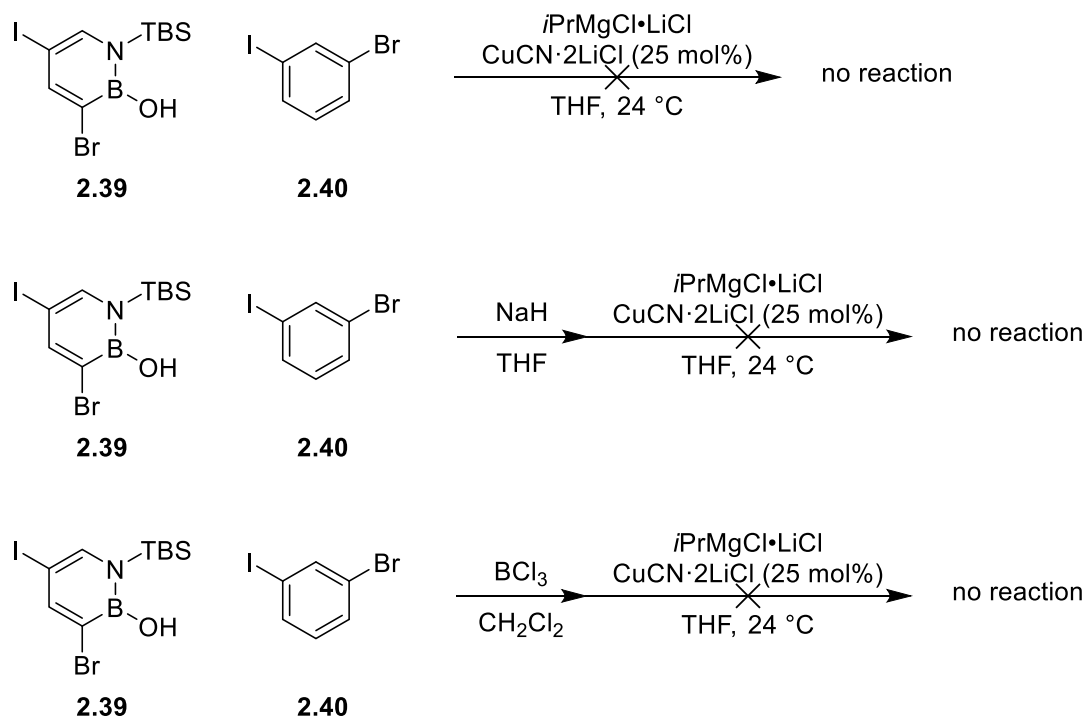
⁴⁰ Zhao, P.; Nettleton, D. O.; Karki, R. G.; Zécari, F. J.; Liu, S.-Y. Medicinal Chemistry Profiling of Monocyclic 1,2-Azaborines. *ChemMedChem* **2017**, *12*, 358–361.

Scheme 2.11 Turbo Grignard Reaction with 3-Br-*N*-TBS-*B*-Cl-1,2-azaborine



Having demonstrated the utility of the turbo Grignard reaction with B–Cl bearing 1,2-azaborines, we attempted to apply the reaction to 1,2-azaborines that contained B–O bonds. Attempts were made to apply this reaction to our tetra-substituted 1,2-azaborine **2.39**⁴¹. Unfortunately, direct application of the turbo Grignard reaction conditions was unsuccessful. Additionally, deprotonation of the group and an attempted ligand exchange with BCl_3 also did not yield product (**Scheme 2.12**).

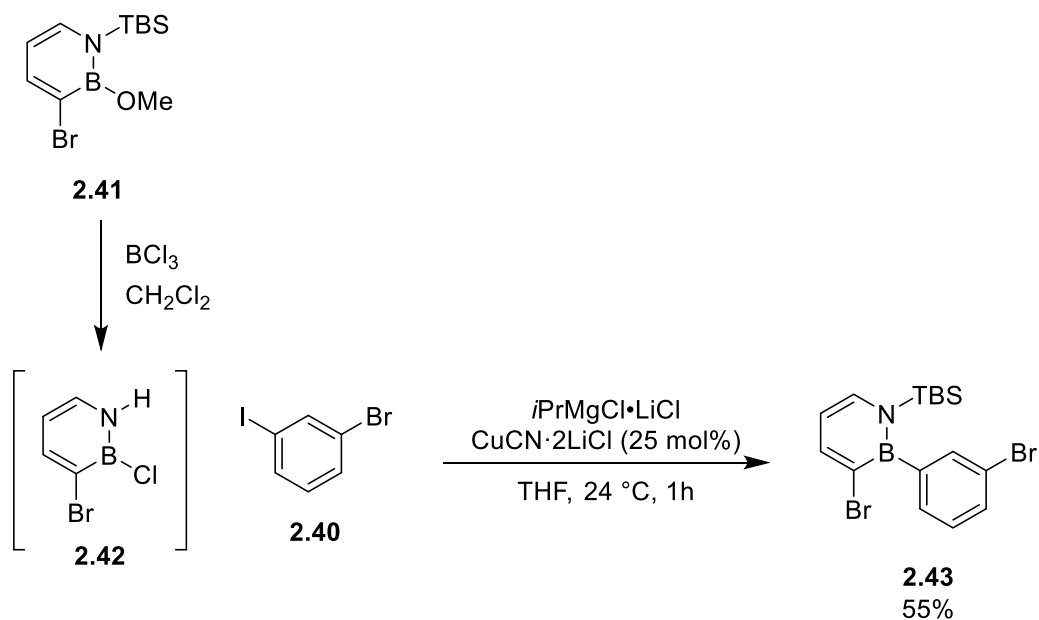
Scheme 2.12 Attempts to Adapt Turbo Grignard Reaction to 3-Br-5-I-*N*-TBS-*B*-Cl-1,2-azaborine



⁴¹ See section 1.3.3 Synthesis of *N*-TBS-*B*-OH-3-Br-5-I-1,2-azaborine

To demonstrate that this method could be applied to B–OR systems, the reaction was attempted with **2.41**, which is the synthetic precursor of **2.39**,⁴¹ as a substrate and **2.40** as the addition partner. As has been previously reported,³⁴ a comproportionation reaction generated **2.42** in situ. **2.42** was then isolated and subjected to turbo Grignard conditions, which yielded the product **2.43**.

Scheme 2.13 Turbo Grignard Reaction with 3-Br-N-TBS-B-OMe-1,2-azaborine



2.4 Conclusions

While the current scope of the turbo Grignard reaction with 1,2-azaborines is limited, it demonstrates a clear ability to tolerate sensitive electrophilic groups, including esters and nitriles, that previously could only be installed with rhodium-catalyzed cross-coupling. We have shown that it can be effective with both B–Cl and B–OR substituted 1,2-azaborines. Additionally, we have shown that halogenation on the 1,2-azaborine core does not inhibit this reaction.

Our ultimate goal for this chemistry is to develop a tetra-orthogonally reactive azaborine in order to study the effects of BN-CC isosterism of 1,2-azaborines in biological settings. In order to achieve this, we must be able to synthesize complex isosteres of biologically active molecules. Application of the turbo Grignard reaction demonstrates that sensitive aryl groups can be installed on the core of 1,2-azaborines in a way that is simple and does not require organotin or other harmful reagents.

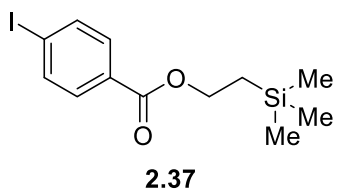
2.5 Experimental

2.5.1 General Considerations

Unless otherwise noted, all oxygen- and moisture-sensitive manipulations were carried out in flame- or oven-dried glassware under an atmosphere of nitrogen using either standard Schlenk technique or a nitrogen-filled glove box. THF, CH₂Cl₂, and pentane were dried using a Brady[®] solvent purification system, which consisted of columnar molecular sieves under argon atmosphere. All column chromatography was performed by hand in a nitrogen-filled glove box. Silica gel (230-400 mesh) was dried for 18 hours at 240 °C under high vacuum. All reagents were purchased from commercial vendors (Acros Organics[®], Millipore Sigma[®], TCI[®]) and used as received unless otherwise noted.

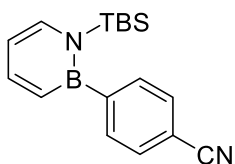
All NMR spectra were recorded on a Varian VNMRS 500 MHz, Varian VNMRS 600 MHz, or INOVA 500 MHz spectrometer at ambient temperature in the Michael Gerson Magnetic Resonance and Instrumentation Laboratory at Boston College. ¹¹B NMR spectra were externally referenced to BF₃·Et₂O (δ 0.0 ppm). ¹H NMR spectra were internally referenced to chloroform-d₃ (δ 7.26 ppm) or benzene-d₆ (δ 7.16). Infrared spectroscopy was performed on a Bruker ALPHA-Platinum FT-IR Spectrometer with an ATR-sampling module. High-resolution mass spectrometry analysis was performed by Marek Domin on a JEOL AccuTOF instrument equipped with a DART ion source in positive ion mode at the Boston College Center for Mass Spectrometry.

2.5.2 Addition of Turbo Grignard Reagents to 1,2-Azaborines



4-iodobenzoic acid (1.80 g, 7.26 mmol), 2-trimethylsilylethanol (3.12 mL, 21.77 mmol), and *N,N*-dimethylaminopyridine (88.66 mg, 0.725 mmol) were dissolved in 45 mL of CH₂Cl₂ in a 250 mL roundbottom flask and allowed to stir at 0 °C under ambient atmosphere. While stirring, liquid *N,N*-dicyclohexylcarbodiimide (1.65 g, 7.98 mmol) was slowly added to the solution, which was allowed to warm to 24 °C while stirring over 4 hours. As the reaction progressed, a solid, white precipitate was observed in the reaction mixture. At the conclusion of the reaction, the crude reaction mixture was passed through a glass fritted funnel and the filtrate was concentrated *in vacuo*. **2.37** was purified *via* silica gel chromatography (1:3 dichloromethane in pentane) and collected as a salmon colored liquid (2.13 g, 84.3% yield). Spectra of isolated compound matched previously published records.⁴²

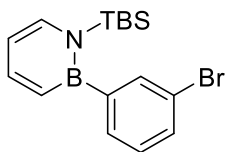
⁴² Mallagaray, A.; Canales, A.; Domínguez, G.; Pérez-Castells, J.; Jiménez-Barbero, J. Rigid Lanthanide Binding Tag for NMR 3D Structure Determination of Carbohydrates. *Chem. Comm.* **2011**, 47, 7179–7181.



2.34

A dry 20 mL glass vial flushed with nitrogen was filled with a solution of *i*PrMgCl·LiCl in tetrahydrofuran (0.535 mL, 0.862 M, 0.461 mmol) and cooled to $-15\text{ }^{\circ}\text{C}$. para-Iodo-benzonitrile (101 mg, 0.439 mmol) was dissolved in 2 mL of THF and slowly added to the flask. After allowing to stir for 30 minutes, **2.33** (100 mg, 0.439 mmol) was dissolved in 2 mL of THF and added dropwise to the flask, followed by Cu(I)CN·(LiCl)₂ in THF (0.110 mL, 0.110 mmol, 1.00 M). The reaction was allowed to stir for 12 hours as it warmed to $24\text{ }^{\circ}\text{C}$. At the conclusion of the reaction, the crude reaction mixture was concentrated *in vacuo* and dissolved in 2 mL of a 2:1 pentane/dichloromethane mixture and purified via silica gel chromatography (5-20% dichloromethane in pentane). **2.34** was collected as a white solid (60.5 mg, 46.8% yield).

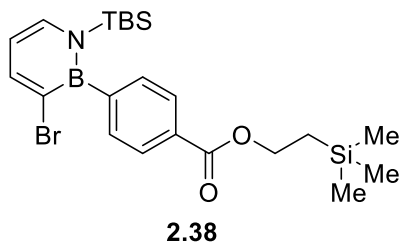
¹H NMR (500 MHz, C₆D₆) δ 7.50 (dd, $J = 6.5, 11.5$ Hz, 1H), δ 7.15 (d, $J = 7.5$, 1H), δ 7.04 (m, 4H), δ 6.71 (d, $J = 11$ Hz) δ 6.26 (t, $J = 6.5$, 1H), δ 0.96 (s, 9H), δ 0.57 (s, 6H); ¹³C NMR (150 MHz, C₆D₆) δ 143.44, 137.78, 132.20, 129.95, 119.01, 112.50, 110.87, 26.33, 18.45, -2.54 (two Cs bonded to B was not observed); ¹¹B NMR (160 MHz, C₆D₆) δ 38.252; FTIR (thin film) $\tilde{\nu} = 2956, 2930, 2886, 2858, 2226, 1603, 1504, 1453, 1389, 1265, 1096, 998, 957, 810, 562$; HRMS (DART+) calculated for C₁₇H₂₄BN₂Si (M⁺): 295.17963, observed: 295.18024.



2.35

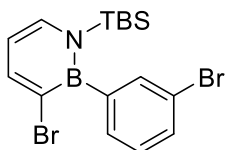
A dry 20 mL glass vial flushed with nitrogen was filled with a solution of *i*PrMgCl·LiCl in tetrahydrofuran (0.535 mL, 0.862 M 0.461 mmol) and cooled to $-15\text{ }^{\circ}\text{C}$. **2.40** (124 mg, 0.439 mmol) was dissolved in 2 mL of THF and slowly added to the flask. After allowing to stir for 30 minutes, **2.33** (100 mg, 0.439 mmol) was dissolved in 2 mL of THF and added dropwise to the flask, followed by Cu(I)CN·(LiCl)₂ in THF (0.110 mL, 0.110 mmol, 1.00 M). The reaction was allowed to stir for 12 hours as it warmed to $24\text{ }^{\circ}\text{C}$. At the conclusion of the reaction, the crude reaction mixture was concentrated *in vacuo* and dissolved in 2 mL of a 2:1 pentane/dichloromethane mixture and purified via silica gel chromatography (15-30% dichloromethane in pentane). **2.35** was collected as an orange solid (95.5 mg, 62.4% yield).

¹H NMR (500 MHz, C₆D₆) δ 7.62 (s, 1H) δ 7.50 (dd, $J = 6.0, 10.5\text{ Hz}, 11.5\text{ Hz}$, 1H), δ 7.29 (d, $J = 8.5\text{ Hz}$, 1H) δ 7.19 (d, $J = 7.5$, 1H), δ 7.17 (d, $J = 7.0\text{ Hz}$, 1H), δ 6.83 (m, 2H), δ 6.26 (t, $J = 7.0$, 1H), δ 0.70 (s, 9H), δ -0.16 (s, 6H); ¹³C NMR (150 MHz, C₆D₆) δ 143.26, 137.80, 134.97, 130.33, 129.65, 128.58, 121.83, 112.30, 26.43, 18.54, -2.46 (two Cs bonded to B was not observed); ¹¹B NMR (160 MHz, C₆D₆) δ 38.349; FTIR (thin film) $\tilde{\nu} = 3612, 2953, 2928, 2884, 2857, 1606, 1585, 1389, 1346, 1256, 1209, 1015, 810, 680$; HRMS (DART+) calculated for C₁₆H₂₄BNSiBr (M⁺): 348.09490, observed: 348.09486.



A dry 50 mL roundbottom flask flushed with nitrogen was filled with *i*PrMgCl·LiCl in THF (0.230 mL, 0.743 M, 0.171 mmol) and cooled to $-15\text{ }^{\circ}\text{C}$. **2.37** (56.81 mg, 163 μmol) was dissolved in 0.5 mL of THF and slowly added to the flask.. After allowing to stir for 20 minutes, **2.36** (50 mg, 163 μmol) was dissolved in 0.5 mL of THF and added dropwise to the flask, followed by Cu(I)CN·(LiCl)₂ in THF (0.55 mL, 0.55 mmol, 1.00 M). The reaction was allowed to stir for 1 hour at $0\text{ }^{\circ}\text{C}$. At the conclusion of the reaction, the crude reaction mixture was concentrated *in vacuo* and dissolved in 2 mL of a 2:1 pentane/dichloromethane mixture and purified via silica gel chromatography (25-50% dichloromethane in pentane). **2.38** was collected as an off-white solid (23.0 mg, 28.6% yield).

¹H NMR (500 MHz, CDCl₃) δ 8.01 (d, *J* = 6.5 Hz, 2H) δ 7.95 (d, *J* = 7.5 Hz, 1H) δ 7.43 (m, 3H), δ 6.36 (t, *J* = 7.0, 1H), δ 0.89 (s, 9H), δ 0.09 (s, 12H) δ 0.16 (s, 6H); ¹³C NMR (125 MHz, CDCl₃) δ 167.19, 145.03, 137.81, 132.21, 129.48, 127.86, 112.15, 63.03, 26.72, 18.88, 17.50, -1.45, -2.12 (two Cs bonded to B was not observed); ¹¹B NMR (160 MHz, CDCl₃) δ 37.607; FTIR (thin film) $\tilde{\nu}$ = 2955, 2930, 2886, 2858, 2226, 1712, 1602, 1504, 1453, 1389, 1271, 1096, 997, 823, 747; HRMS (DART+) calculated for C₂₂H₃₅BNO₂Si₂Br (M⁺): 491.14773, observed: 491.14938.



2.43

2.41 (200.0 mg, 0.662 mmol) was dissolved in 2 mL of CH_2Cl_2 in a dry 20 mL vial and allowed to stir under nitrogen at room temperature. BCl_3 in hexanes (728 μL , 1.0 M, 0.728 mmol) was added dropwise to the vial and allowed to stir for 3 hours. The crude reaction mixture was concentrated in vacuo and redissolved in pentane, which was then passed through a PTFE filter. The pentane filtrate was again concentrated in vacuo and redissolved in 3 mL of THF. A dry 25 mL roundbottom flask flushed with nitrogen was filled with *i*PrMgCl·LiCl in THF (0.806 mL, 0.862 M, 695 μmol) and cooled to -15°C . **2.40** (187 mg, 662 μmol) in was dissolved in 3 mL of THF and was slowly added to the flask. After allowing to stir for 30 minutes, the solution containing isolated **2.42** was added dropwise to the flask, followed by $\text{Cu(I)CN}\cdot(\text{LiCl})_2$ (165 μL , 165 μmol , 1M in THF). The reaction was allowed to warm to room temperature while stirring for 12.5 hours. At the conclusion of the reaction, the reaction mixture was concentrated *in vacuo* and purified *via* silica gel chromatography (5-15% dichloromethane in pentane). **2.43** was collected as an off-white solid (155.8 mg, 55.1% yield).

^1H NMR (500 MHz, CDCl_3) δ 7.95 (d, $J = 7.5$ Hz, 1H) δ 7.47 (m, 2H), δ 7.42 (d, $J = 7.0$ Hz, 1H) δ 7.28 (d, $J = 7.5$, 1H) δ 7.22 (t, $J = 7.5$, 1H), δ 6.35 (t, $J = 7.0$, 1H), δ 0.90 (s, 9H), δ 0.04 (s, 6H); ^{13}C NMR (125 MHz, CDCl_3) δ 145.11, 137.85, 134.99, 130.75, 130.26, 128.72, 121.73, 112.19, 26.17, 18.92, -2.13 (two Cs bonded to B was not observed); ^{11}B NMR (160 MHz, CDCl_3) δ 37.412; FTIR (thin film) $\tilde{\nu} = 2956, 2930, 2885, 2858, 1601, 1550, 1471, 1337, 1265, 1110, 996, 841, 811, 758, 699, 623, 412$; HRMS (DART+) calculated for $\text{C}_{16}\text{H}_{22}\text{BNSiBr}_2$ (M⁺): 428.06470, observed: 428.00260.

2.5.3 Spectral Data

N-TBS-3-(p-CN-Ph)-1,2-azaborine

Sample Name:
JRA-2-096_2_1HRMR
Data Collected on:
mmx18-vmmr5500
Archive directory:

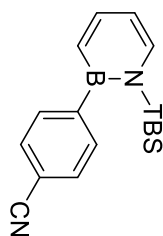
Sample directory:

File: PROTON

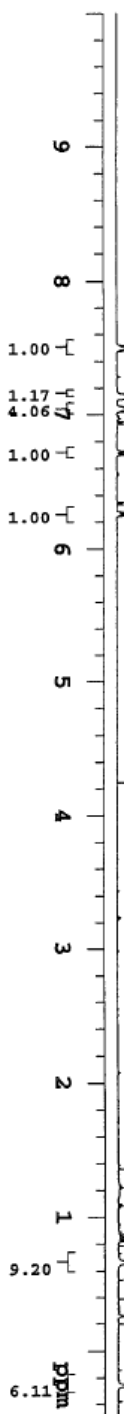
Pulse Sequence: PROTON (s2pu1)
Solvent: c6d6
Data collected on: Aug 30 2019

Temp. 25.0 C / 298.1 K
Operator: Liu

Relax. delay 10.000 sec
Pulse 45.0 degrees
Acq. time 2.045 sec
Width 8012.8 Hz
12 repetitions
OBSERVE H1, 499.8763203 MHz
DATA PROCESSING
F2 size 32768
Total time 6 min 25 sec



2.34



N-TBS-B-(p-CN-Ph)-1,2-azaborine

Sample Name:

JRA-2-096_2_13CNMR

Data Collected on:

mmx18-vnmr6500

Archive directory:

Sample directory:

FIDFile: JRA-2-096_2_13CNMR

Pulse Sequence: CARBON (s2pm1)

Solvent: c6d6

Data collected on: Aug 30 2019

Temp. 25.0 C / 298.1 K

Operator: Jlu

Relax. delay 1.000 sec

Pulse 45.0 degrees

Acq. time 1.049 sec

Width 31250.0 Hz

248 repetitions

OBSERVE C13, 125.6940007 MHz

DECODEDIE H1, 499.8788196 MHz

Power 45 dB

continuously on

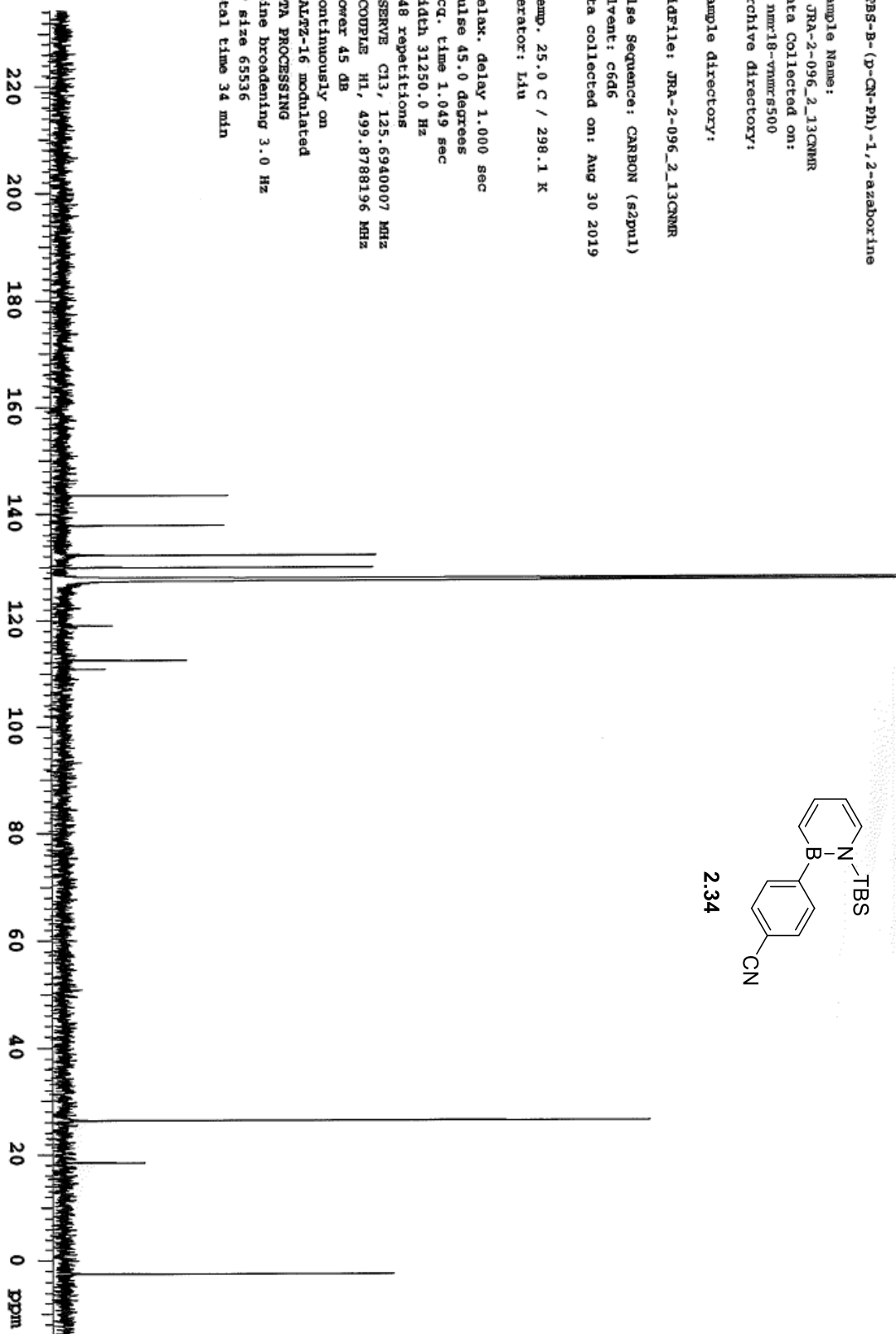
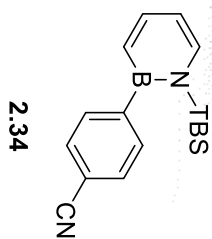
WALTZ-16 modulated

DATA PROCESSING

Line broadening 3.0 Hz

FT size 65536

Total time 34 min



N-TBS-B-(m-Br-Ph)-1,2-azaborine

Sample Name:

JRA-2-095_2_13CNMR

Data Collected on:

nmr18-vnmr5500

Archive directory:

Sample directory:

Fidfile: JRA-2-095_2_13CNMR

Pulse Sequence: CARBON (s2pu1)

Solvent: c6d6

Data collected on: Aug 30 2019

Temp. 25.0 C / 298.1 K

Operator: lhu

Relax. delay 1.000 sec

Pulse 45.0 degrees

Acq. time 1.049 sec

Width 31250.0 Hz

248 repetitions

OBSERVE C13, 125.694007 MHz

DECUPLE H1, 499.8788196 MHz

Power 45 db

continuously on

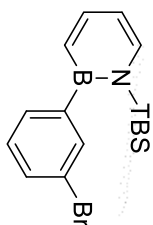
WALTZ-16 modulated

DATA PROCESSING

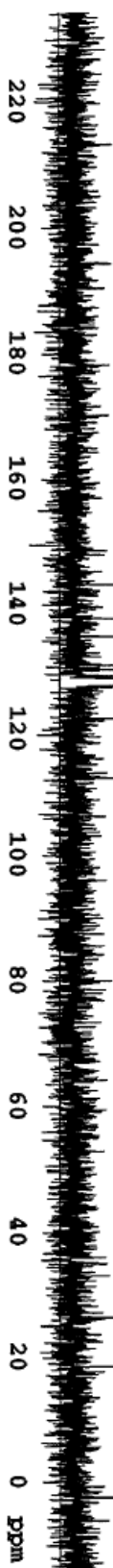
Line broadening 3.0 Hz

FT size 65536

Total time 34 min



2.35



N-TBS-B-(m-Br-Ph)-1,2-azaborine

Sample Name:

JRA-2-095_2_11BMR

Data Collected on:

nmr18-vnmr5500

Archive directory:

Sample directory:

FidFile: JRA-2-095_2_11BMR

Pulse Sequence: s2pul

Solvent: c6d6

Data collected on: Aug 30 2019

Temp. 25.0 C / 298.1 K

Operator: Liu

Relax. delay 0.100 sec

Pulse 60.5 degrees

Acq. time 0.064 sec

Width 32051.3 Hz

508 repetitions

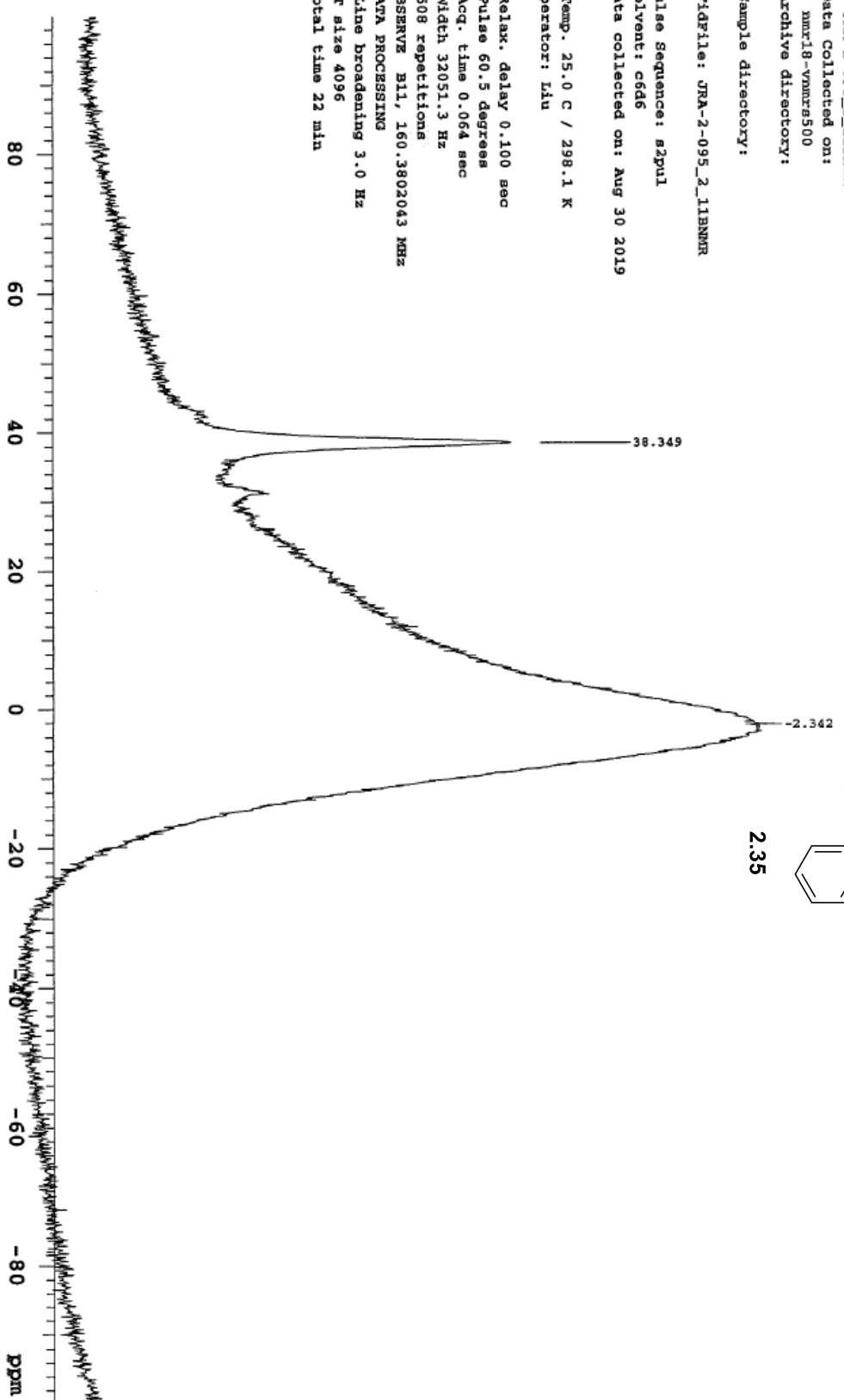
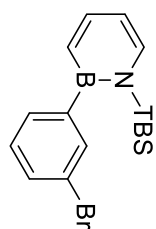
OBSERVE B1, 160.3802043 MHz

DATA PROCESSING

Line broadening 3.0 Hz

FT size 4096

Total time 22 min



3-Br-N-TBS-B-(p-TMSPester-Ph)-1,2-azaborine

Sample Name:

Data Collected on:

nmr18-vmrms500

Archive directory:

Sample directory:

F1dfile: CARBON

Pulse Sequence: CARBON (s2pu1)

Solvent: cdcl3

Data collected on: Sep 4 2019

Temp. 25.0 C / 298.1 K

Operator: Liu

Relax. delay 1.000 sec

Pulse 45.0 degrees

Acq. time 1.049 sec

Width 31250.0 Hz

400 repetitions

OBSERVE C13, 125.6939894 MHz

DECOUPLE H1, 499.8787746 MHz

Power 45 dB

continuously on

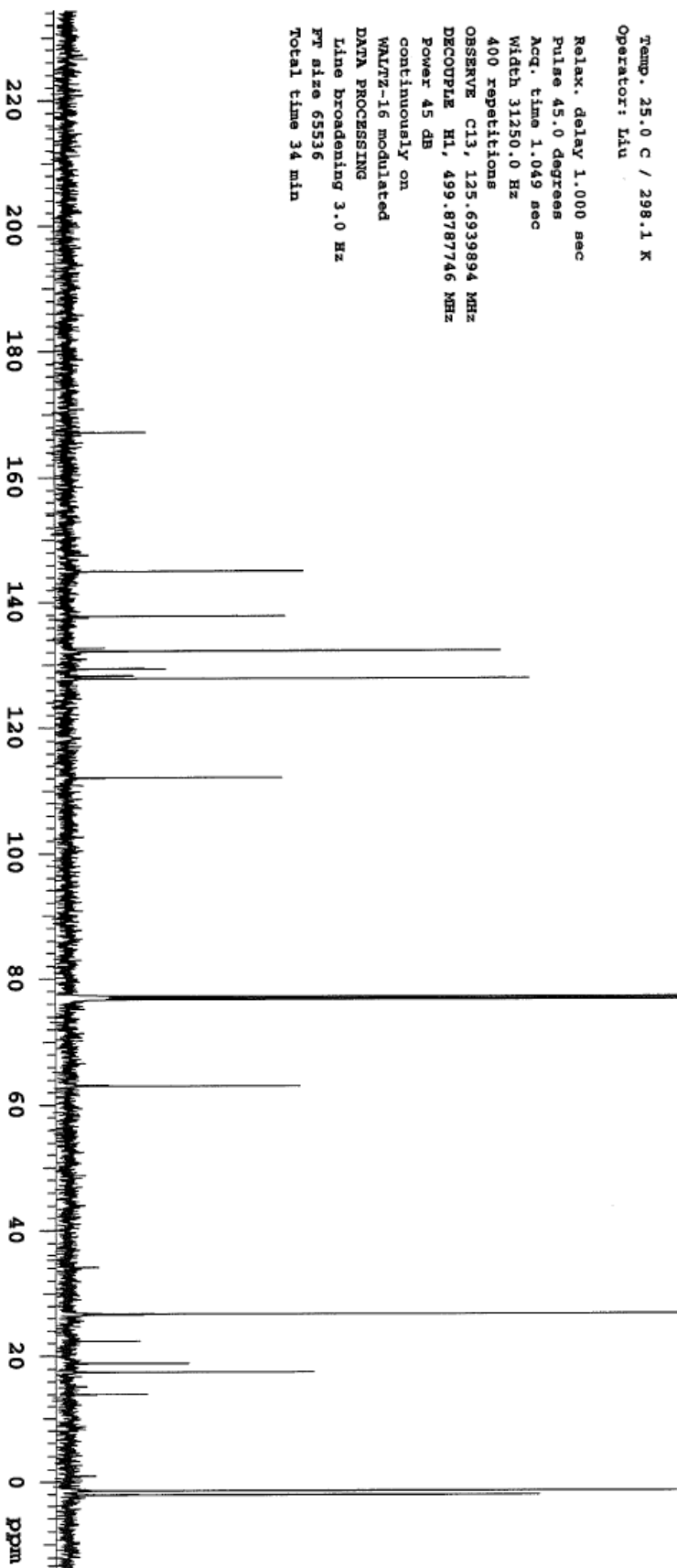
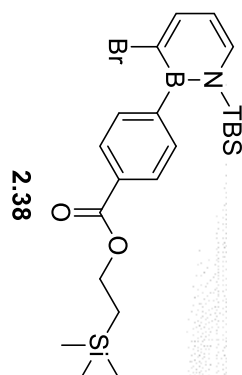
WALTZ-16 modulated

DATA PROCESSING

Line broadening 3.0 Hz

FT size 65536

Total time 34 min



3-Br-N-TBS-B-(p-TMSRestor-Ph)-1,2-azaborine

Sample Name:

Data Collected on:

mmx11-Inova500

Archive directory:

Sample directory:

F1dFile: B11

Pulse Sequence: szpul

Solvent: cdcl3

Data collected on: Sep 4 2019

Temp: 25.0 C / 298.1 K

Operator: Lhu

Relax. delay 0.100 sec

Pulse 22.2 degrees

Acq. time 0.054 sec

Width 32064.1 Hz

1680 repetitions

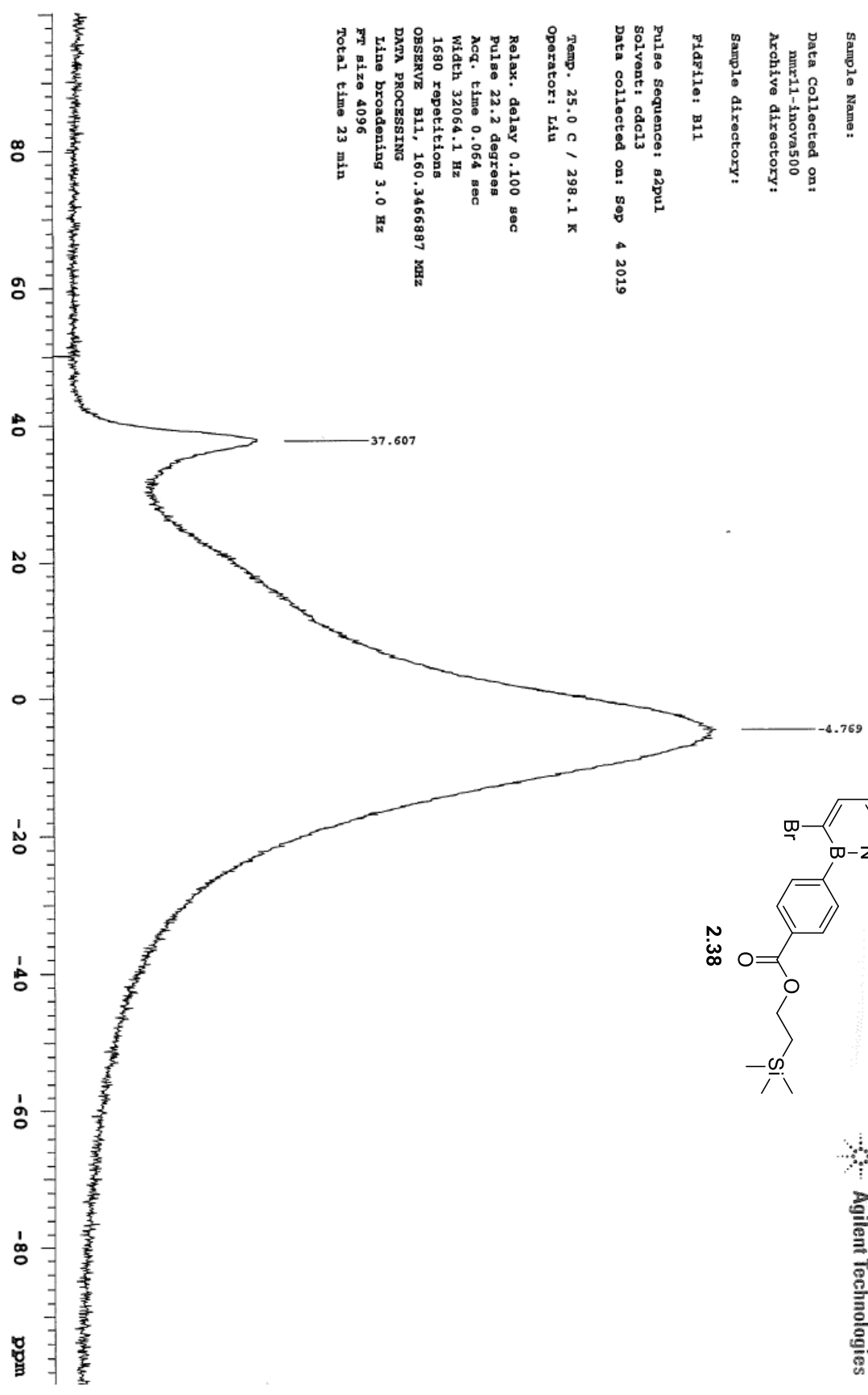
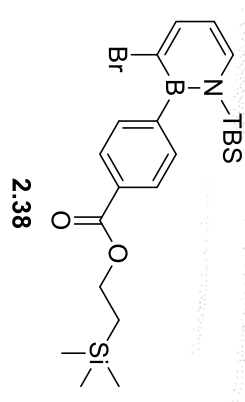
OBSERVE B11, 160.3466887 MHz

DATA PROCESSING

Line broadening 3.0 Hz

FW size 4096

Total time 23 min



3-Br-N-TBS-3-(m-Br-Ph)-1,2-azaborine

Sample Name:
JRA-2-100_1HMNR
Data Collected on:
mmr18-vmmr5500
Archive directory:

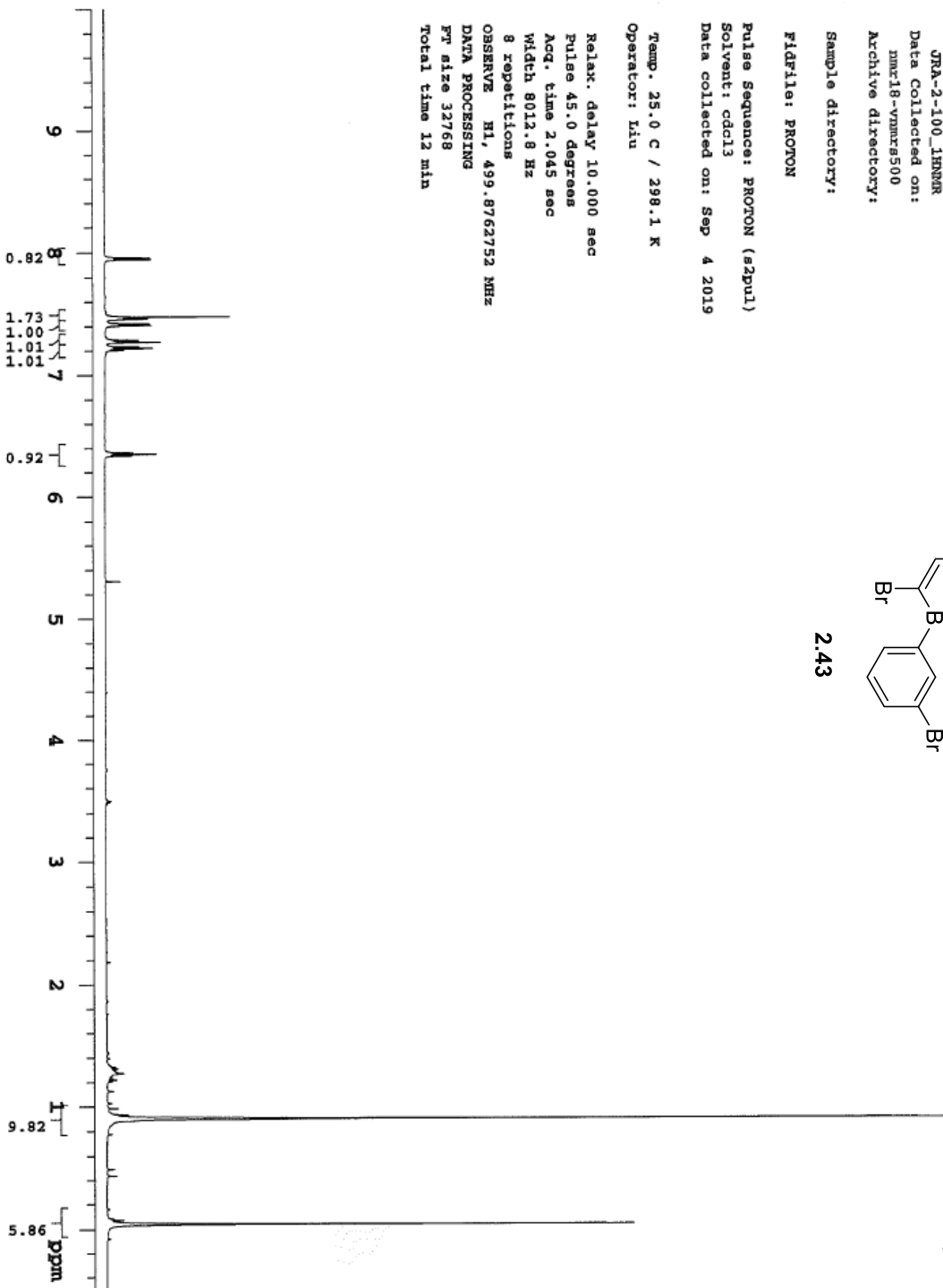
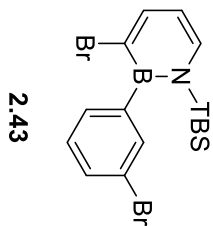
Sample directory:

FIDFile: PROTON

Pulse Sequence: PROTON (s2pul)
Solvent: cdcl3
Data collected on: Sep 4 2019

Temp. 25.0 C / 298.1 K
Operator: Liu

Relax. delay 10.000 sec
Pulse 45.0 degrees
Acq. time 2.045 sec
Width 8012.8 Hz
8 repetitions
OBSERVE H1, 499.8762752 MHz
DATA PROCESSING
PP size 32768
Total time 12 min



3-Br-N-TBS-B-(m-Br-Ph)-1,2-azaborine

Sample Name:

JRA-2-100_fr2_13CNMR

Data Collected on:

nmr18-vnmrs500

Archive directory:

Sample directory:

File: CARBON

Pulse Sequence: CARBON (s2pul)

Solvent: cdcl3

Data collected on: Sep 4 2019

Temp. 25.0 C / 298.1 K

Operator: ldu

Relax. delay 1.000 sec

Pulse 45.0 degrees

Acq. time 1.049 sec

Width 31250.0 Hz

200 repetitions

OBSERVE C13, 125.6939894 MHz

DECOUPLE H1, 499.8787746 MHz

Power 45 dB

continuously on

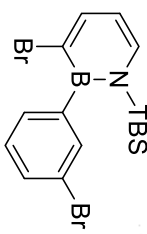
WALTZ-16 modulated

DATA PROCESSING

Line broadening 3.0 Hz

FT size 65536

Total time 34 min



2.43



3-Br-N-TBS-B-(m-Br-Ph)-1,2-azaborine

Sample Name:
JRA-2-100_11BMR
Data Collected on:
nmr11-inova500
Archive directory:

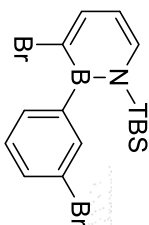
Sample directory:

F1dFile: B11

Pulse Sequence: s2pul
Solvent: cdcl3
Data collected on: Sep 4 2019

Temp. 25.0 C / 298.1 K
Operator: Lhu

Relax. delay 0.100 sec
Pulse 22.2 degrees
Acq. time 0.064 sec
Width 32064.1 Hz
295 repetitions
OBSERVE B11, 160.346887 MHz
DATA PROCESSING
Line broadening 3.0 Hz
F1 size 4096
Total time 23 min



2.43

37.412

